Earth-Science Reviews 279 (2026) 105528

Contents lists available at ScienceDirect

Earth-Science Reviews

journal homepage: www.elsevier.com/locate/earscirev

Geochemistry of CO_2-rich gas emissions in the Carpathians: Multiscale geological sources and implications for orogenic degassing

Boglárka Mercedesz Kis [a,b,h,*], Réka Szalay [a], Antonio Caracausi [c], Paolo Randazzo [c], Tivadar M. Tóth [d], László Palcsu [e], Judit Orsovszki [e,f], Alessandro Aiuppa [g], Fausto Grassa [c], Szabolcs Harangi [b,h]

[a] Babeș-Bolyai University, Faculty of Biology and Geology, Department of Geology, M. Kogălniceanu str., 1, 400084 Cluj-Napoca, Romania
[b] Eötvös University, Institute of Geography and Earth Sciences, Department of Petrology and Geochemistry, Pázmány P. stny., 1/C, 1117 Budapest, Hungary
[c] Istituto Nazionale di Geofisica e Vulcanologia, Sezione di Palermo, Via Ugo La Malfa, 153, 90146 Palermo, Italy
[d] University of Szeged, Department of Geology, Egyetem str., 2, 6722 Szeged, Hungary
[e] HUN-REN Institute for Nuclear Research, Bem square, 18/C, 4026 Debrecen, Hungary
[f] Isotoptech Zrt., Bem square, 18/C, 4026 Debrecen, Hungary
[g] Università di Palermo, DiSTeM, Via Archirafi, 36, 90123 Palermo, Italy
[h] MTA–HUN-REN CSFK Lendület "Momentum" Pannonian-Volcano Research Group, Institute for Geological and Geochemical Research, HUN-REN Research Centre for Astronomy and Earth Sciences, Budaörsi út 45, 1112 Budapest, Hungary

ARTICLE INFO

Keywords:
Carpathians
Fluid-geochemistry
Noble gases
CO_2
Magma degassing
Metamorphic reactions
Orogenic degassing

ABSTRACT

Degassing of deep-seated fluids is a key process occurring in orogenic systems, yet its sources and controlling mechanisms remain poorly constrained. The Carpathians represent a major degassing province in Europe, where CO_2 emissions are concentrated in the Neogene–Quaternary volcanic arc and carbonate-rich flysch nappes along tectonized suture zones (Magura, Pieniny and Ceahlău-Severin suture zone), while CH_4 of mostly thermogenic origin dominates in the Outer Flysch belt. We present the first regional geochemical dataset and map of CO_2 and CH_4 emissions in the Western and Eastern Carpathians, integrating chemical and isotopic analyses with lithological and structural constraints.

Helium isotopes reveal variable mantle–crustal mixing: elevated R/R_a values (>3) near long-dormant volcanic centres, especially Ciomadul, reflect persistent deep magmatic reservoirs with 60-70% mantle/magmatic ^3He input, whereas radiogenic ^4He signatures dominate non-volcanic flysch and metamorphic regions, producing low R/R_a values (~0.02). CO_2 acts as the primary carrier of mantle He, but metamorphic devolatilization of marls and carbonates at 5–20 km depth provides the principal crustal CO_2 source, consistent with "orogenic CO_2 degassing" described in other collisional belts. Degassing sites cluster along nappe boundaries and fault zones, where enhanced permeability enables rapid volatile ascent.

Carbon isotopes and $CO_2/^3He$ ratios confirm heterogeneous carbon sources of the CO_2 gases emitted at the surface, with mantle and crustal inputs at different proportions. In general, the biogenic CO_2 contributions are negligible, with the majority of samples plotting along a mantle-limestone mixing line, indicating significant crustal-derived CO_2 up to 80-95% for non-volcanic areas, and 40-70% for volcanic areas. The carbon isotopes and $CO_2/^3He$ ratios are variably modified by groundwater interaction (dissolution and precipitation processes). Mantle-derived He flux averages are 1.59×10^{-13} g m^{-2} s^{-1} for Ciomadul volcano, 8.64×10^{-14} g m^{-2} s^{-1} for the Eastern Carpathians volcanic area and 3.46×10^{-14} g m^{-2} s^{-1} for the Eastern Carpathians non-volcanic area. CO_2 fluxes show average values of 1.4×10^6 g km^{-2} y^{-1} for the Ciomadul volcanic area, 1.18×10^8 g km^{-2} y^{-1} for the volcanic area of the Eastern Carpathians and 5.1×10^7 g km^{-2} y^{-1} for the non-volcanic area of the Eastern Carpathians. Mantle-derived He fluxes coupled with $CO_2/^3He$ indicates a 4.66 Mt. year^{-1} mantle CO_2 flux for the Carpathians. These values match with other active orogens, highlighting the Carpathians as a key setting to investigate volatile transport, crust–mantle interactions, and their contribution to the global carbon cycle.

* Corresponding author at: Babeș-Bolyai University, Faculty of Biology and Geology, Department of Geology, M. Kogălniceanu str. 1, 400084 Cluj-Napoca, Romania.
E-mail address: boglarka.kis@ubbcluj.ro (B.M. Kis).

https://doi.org/10.1016/j.earscirev.2026.105528
Received 18 October 2025; Received in revised form 30 April 2026; Accepted 3 May 2026
Available online 5 May 2026

Contents

1. Introduction

There have been increasing efforts in the scientific community to estimate natural carbon emissions in both volcanic and non-volcanic regions, in order to better understand natural carbon fluxes into the atmosphere and reconstruct the evolution of the Earth's atmosphere over geological time (Tamburello et al., 2018; Werner et al., 2019; Fischer and Aiuppa, 2020; Zhang et al., 2024). Key priorities include identifying and mapping areas of volatile release, definition of sources as well as conducting flux measurements of volatile compounds to quantify carbon emissions from deep geological reservoirs. A state-of-art quantification on the total carbon flux, estimated to be between 75 and 112 Mt. CO_2 $year^{-1}$ from the Earth's most active volcanoes is given by Werner et al., 2019 and Fischer and Aiuppa, 2020, who calculated CO_2 fluxes by compiling measurements from active volcanic plumes, diffuse-degassing areas, hydrothermal systems and mid-ocean ridges, by using proxies such as SO_2 fluxes obtained through ground-based and satellite remote sensing, combined with CO_2/SO_2 ratios.

Significant progress has also been made in understanding the factors controlling gas emissions also in long-dormant volcanic areas (volcanoes that last erupted more than 10 ka ago, e.g. Chiodini and Frondini, 2001; Caracausi et al., 2015; Cardellini et al., 2017; Kis et al., 2017) and tectonically active regions (Tamburello et al., 2018; Zhang et al., 2024). Results indicate that diffuse degassing from non-erupting or dormant volcanic systems as well as from active tectonic areas can produce CO_2 emissions comparable to those released from actively erupting volcanoes. A well-known example is the Campi Flegrei Solfatara hydrothermal system, which, despite the absence of ongoing eruptions, emits up to 3000 t day^{-1} of CO_2, a flux similar to that of persistently degassing active volcanoes (Cardellini et al., 2017). Caracausi et al. (2015) further demonstrated a relationship between volcanic degassing and the time elapsed since the last eruption, indicating that deep magmatic degassing can persist for long periods after eruptive activity has ceased. Chiodini et al. (2004) highlighted that globally significant CO_2 are dissolved into and released by regional aquifer systems, emphasizing the importance of non-eruptive pathways of degassing.

Recent studies also indicate that carbon outflux from continental reworking, e.g. metamorphic decarbonation reactions in the Himalayas (Becker et al., 2008; Zhang et al., 2017b, 2024) and continental rifting, e.g. the Gulu-Yadong rift in the Lhasa terrane, South Tibet (Zhang et al., 2017a) or the East African rift system (Lee et al., 2016), and Main Ethiopian Rift (Hunt et al., 2017) could be surprisingly comparable with volcanic carbon outflux. Degassing in tectonically active areas reveals fault systems that may correlate with regional seismicity. Mapping these gas emissions, quantitatively evaluating fluxes and performing regular monitoring provides insights into mantle-crust tectonics and can be relevant to seismic hazard assessment (Bräuer et al., 2008, 2018; Chiodini et al., 2004, 2020; Caracausi et al., 2022).

The geochemistry of different gas species has been extensively studied within major orogenic units worldwide, e.g. in the Apennines (Parello et al., 2000; Chiodini et al., 2004), Alps (Marty et al., 1992), Caucasus (Polyak et al., 2000, 2011), Himalayas (Becker et al., 2008; Evans et al., 2008; Zhang et al., 2017b; Klemperer et al., 2013, 2022) Andes-Cordilleras (Barry et al., 2022) These studies reveal multiple processes contributing to the formation/genesis of fluids including both mantle and crustal sources, e.g. mantle-derived degassing transferred into the crust via active and fossil magmatic systems, prograde metamorphic processes, especially decarbonation of carbonate-bearing rocks, dehydration of hydrous minerals; pyrolysis of organic matter and biogenic fluid addition.

The Carpathians in eastern-central Europe, an arcuate-shaped mountain range spanning approximately ~1300-km (Fig. 1), represent one of the longest and largest continuous orogenic systems of Europe. The Carpathians are divided into Western, Eastern and Southern Carpathians based on their geographical position. They enclose the Pannonian and Transylvanian Basins and extend across Slovakia, Poland, Ukraine and Romania (Golonka et al., 2020). Despite being absent from the global degassing surveys (Kerrick, 2001; Mörner and Etiope, 2002; Zhang et al., 2024), this orogenic belt is characterized by intense fluid emissions of different chemical compositions (Cornides and Kecskés, 1987; Leśniak, 1998; Vaselli et al., 2002; Kotarba and Nagao, 2008; Polyak et al., 2018; Kis et al., 2019). In the volcanic and tectonically active regions of the Romanian sector of the Eastern Carpathians, magmatic/mantle-derived degassing is considered a major source of deep fluids, where volcanic systems release significant amounts of CO_2 and He from magmatic reservoirs, with $^3He/^4He$ ratios reaching up to 4.5 R/R_a (Vaselli et al., 2002; Kis et al., 2019). Deep CO_2 and H_2O emanations in the Southeastern part of the Carpathians were also linked to lithospheric-scale deformations and mantle processes, e.g. asthenospheric upwelling beneath the Vrancea slab (Lange et al., 2023). In the Ukrainian sector of the Eastern Carpathians, He isotope compositions further reflect the regional geodynamic setting, with higher $^3He/^4He$ ratios observed in areas of crustal thinning and elevated heat flow (Polyak et al., 2018). A minor mantle-derived He flux is also sustained in the Polish sector of the Western Carpathians, despite the presence of a thick continental lithosphere (Leśniak, 1998). Regarding the origin of

CO_2, several studies (Leśniak, 1998; Kotarba and Nagao, 2008; Polyak et al., 2018) consistently indicate that it is predominantly derived from crustal sources. A major crustal source of CO_2 is decarbonation of carbonate rocks. Secondary processes such as dissolution and mixing can alter the original isotopic signature of CO_2 as it migrates toward the surface.

We investigated the geochemical features of the free gas emissions of the Carpathian orogenic system, with emphasis on the Western and Eastern segments. Our objective is to constrain the origin and sources of fluids in the frame of the regional geotectonic setting, to identify potential geochemical processes occurring at depth and to constrain fluxes of deep gases. Our work represents the first comprehensive, orogen-scale assessment of gas geochemistry across the Carpathian orogenic system, integrating new measurements with an expanded regional dataset to overcome the limitations of earlier studies, which addressed the gas sources and geochemistry only locally. In fact, given the geological continuity of the Carpathian arc and the similarities in the gas composition and tectonic context, a broader regional perspective was required to evaluate regional scenario of deep CO_2 degassing. Our study reveals that the Carpathians are within the global context of actively degassing orogens, highlighting its significance as a global degassing site.

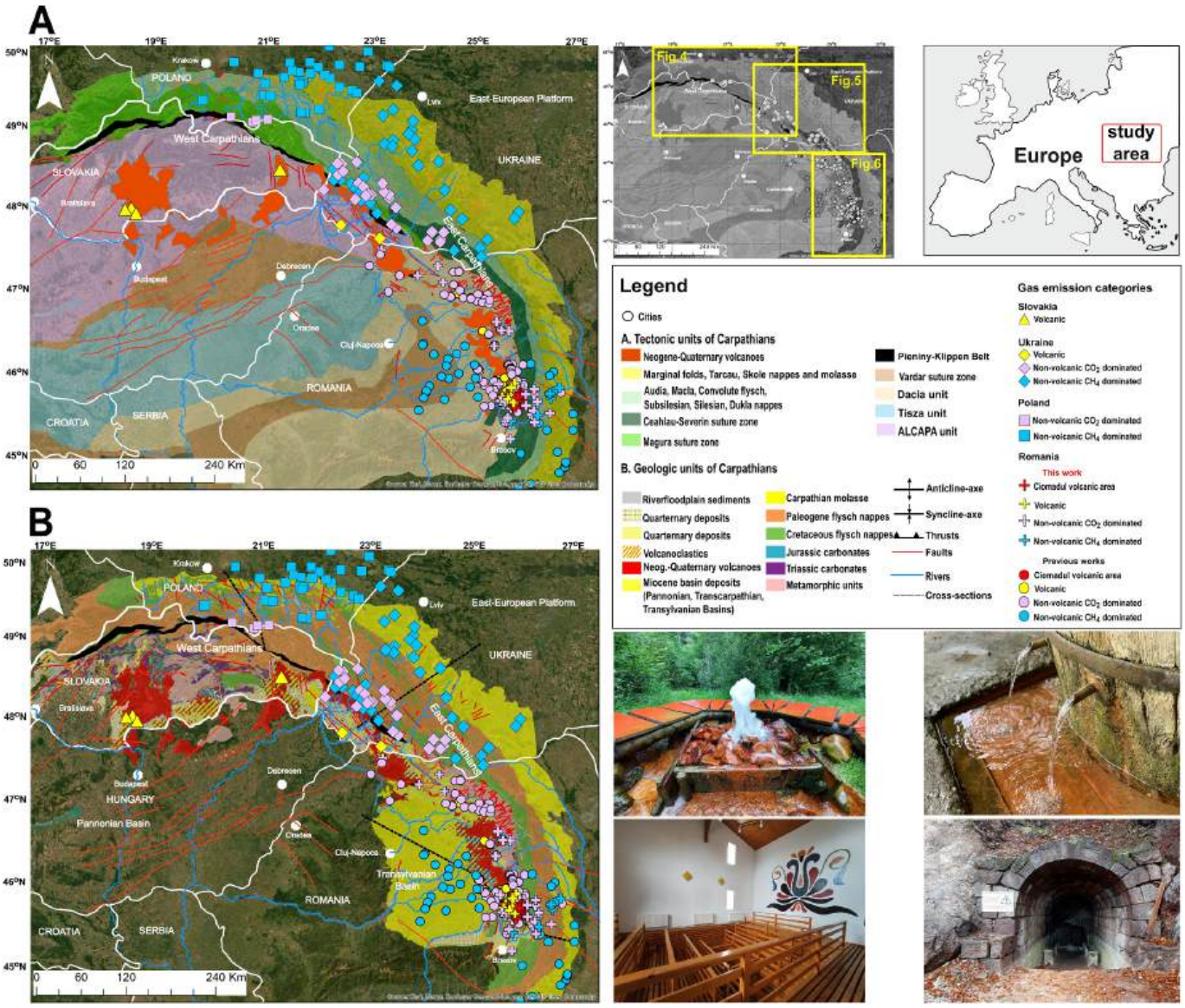

Fig. 1. Tectonic (A) and geologic (B) map of the Western and Eastern Carpathians with selected images of gas manifestations (Kis B.M. personal photography). Maps modified after (Giusca et al., 1967; Răileanu et al., 1967, 1968; Saulea et al., 1967, 1968; Ianovici and Rădulescu, 1968; Murgeanu et al., 1968, 1970; Patrulius et al., 1968; Csontos and Vörös, 2004; Horváth et al., 2006; Marks et al., 2006; Schmid et al., 2020) Geochemical data on gas emissions, for the Polish segment: Leśniak et al., 1997; Kotarba and Nagao, 2008; Palcsu et al., 2017, for the Slovakian segment: Michalko and Baková-Personal Communication, for the Ukrainian segment: Polyak et al., 2018; Pavlyuk et al., 2019a, 2019b, for Romanian segment: This Work, Mants, 1974; Péter and Makfalvi, 1977; Althaus et al., 2000; Vaselli et al., 2002; Baciu et al., 2007, 2017; Frunzeti, 2013; Fórizs and Makfalvi, 2014; Gyila et al., 2017; Italiano et al., 2017, Kis et al., 2019, 2022; Lange et al., 2023; Szalay and Kis, 2023. Symbols: red cross - This work Ciomadul; yellow cross - This work, Romania volcanic CO_2; Light purple cross - This work, Romania non-volcanic, CO_2 dominance; Neon blue cross - This work, Romania CH_4 dominance. Yellow diamond – Ukraine volcanic CO_2, light purple diamond – Ukraine, non-volcanic CO_2 dominance, neon blue diamond – Ukraine, non-volcanic CH_4 dominance; light purple square – Poland non volcanic, CO_2 dominance, neon blue square – Poland, non-volcanic CH_4 dominance; yellow triangle – Slovakia volcanic CO_2. (For interpretation of the references to colour in this figure legend, the reader is referred to the web version of this article.)

2. Geotectonic background

The Carpathian-Pannonian region is part of the Mediterranean orogenic system characterized by retreating subduction zones and back-arc basins (Horváth, 1993; Horváth et al., 2006). The Carpathian orogen was formed during the Cretaceous–Miocene through the progressive closure of several Alpine Tethys oceanic domains, including the Ceahlău–Severin, Pieniny, and Magura basins, followed by Miocene slab rollback and back-arc extension associated with the eastward migration of subduction, extrusion and rotation of the ALCAPA (=Alpine-Carpathian-Pannonian) and Tisza–Dacia microplates (Csontos and Vörös, 2004; Horváth et al., 2006, 2015; Schmid et al., 2020). Slab roll-back and trench retreat induced major back-arc extension and the formation of the Pannonian Basin (Royden et al., 1983; Ratschbacher et al., 1991a, 1991b; Csontos et al., 1992; Tari et al., 1992; Horváth, 1993). Progressive consumption of the downwelling oceanic lithosphere culminated in continent–continent collision at ~12 Ma between the ALCAPA–Tisza–Dacia system and the European Platform and its promontories at the Eastern Carpathians. The subduction and collision events are recorded by large-scale shortening and nappe stacking along the arcuate Carpathian flysch nappe system (Săndulescu, 1984; Matenco and Bertotti, 2000; Csontos and Vörös, 2004; Matenco et al., 2010; Oszczypko et al., 2007, 2018; Schmid et al., 2020). Active geodynamic situation still exists at the southeast Carpathians, where a descending steep, near-vertical slab beneath the Vrancea region generate intense intermediate-depth seismicity (60–180 km, Mw up to ~7; Wenzel et al., 1999; Ismail-Zadeh et al., 2012; Wortel and Spakman, 2000; Radulian et al., 2023).

The Pannonian Basin is underlain by thin lithosphere and crust (<60 km and <25 km, respectively; Horváth et al., 2006; Kalmár et al., 2023), whereas the surrounding Carpathian orogen is characterized by a thick lithosphere (≥120 km), reaching maximum thickness beneath the southern Eastern Carpathians and the Alps–Dinarides, with a steep east–northeastward gradient of the lithosphere–asthenosphere boundary from ~80 to ~200 km over short lateral distances (Dérerová et al., 2006; Horváth et al., 2006, 2015). The thickness of the continental crust beneath the Pieniny Klippen Belt and Polish Carpathians is 36–40 km (Oszczypko, 2004; Golonka et al., 2018), 40–45 km beneath the Ukrainian Carpathians (Polyak et al., 2018), 32–42 km beneath the Romanian segment of the Carpahians and reaches ~55 km beneath the Vrancea seismogenic zone (Dérerová et al., 2006). Seismic activity associated with fault systems has been recorded in the Western Carpathians, with earthquake hypocentres located in the crust at depths of 4-20 km where magnitudes are usually small (Hók et al., 2016). The Eastern Carpathians exhibit a concentrated seismic strain in the Vrancea area, characterized by earthquakes with hypocentres between 60 and 180 km, and magnitudes reaching even ~7 Mw (Wenzel et al., 1999; Ismail-Zadeh et al., 2012; Radulian et al., 2023). This seismic activity is closely linked to the presence of a steep, near-vertical slab in the Vrancea region, which descends into the asthenosphere (Sperner et al., 2004). Dehydration processes have been proposed as potential triggering mechanisms for these earthquakes (Ismail-Zadeh et al., 2012; Ferrand and Manea, 2021).

Heat flow in the Carpathians varies between the different tectonic domains. In the Slovakian segment, values are between 50 and 60 mW m^{-2}, increasing to 90–120 mW m^{-2} in the East Slovakian and Danube basins and in the volcanic areas (Zeyen et al., 2002; Horváth et al., 2015). The Polish Western Carpathians show comparable values of 50–70 mW m^{-2} (Majorowicz et al., 2019). In the Ukrainian Eastern Carpathians, heat flow is lowest on the East European Platform (30–35 mW m^{-2}), increases to 50–70 mW m^{-2} in the flysch belt, and reaches 80–90 mW m^{-2} in the Transcarpathian Basin at the western margin of the Neogene volcanic chain (Horváth et al., 2015; Majcin et al., 2016; Polyak et al., 2018; Gordienko et al., 2019). Within the Carpathian orogen and Neogene volcanic regions, heat flow generally ranges between 50 and 70 mW m^{-2} and locally reaches 90–120 mW m^{-2} (Horváth et al., 2015; Majcin et al., 2016; Gordienko et al., 2019). In Romania, Neogene volcanic units show values of 70–80 mW m^{-2}, with a maximum of 131 mW m^{-2} recorded at Tuşnad in the Ciomadul volcanic area (Demetrescu and Andreescu, 1994).

The evolution of the Carpathian–Pannonian region was accompanied by diverse magmatism over the last ~20 Myr (Szabó et al., 1992; Mason et al., 1998; Harangi, 2001; Harangi et al., 2006; Seghedi et al., 2004; Trua et al., 2006; Harangi and Lenkey, 2007; Lexa et al., 2010; Seghedi and Downes, 2011; Harangi et al., 2026). Explosive silicic volcanism during Pannonian Basin *syn*-rift extension (18.1–14.4 Ma) represents Europe's most voluminous volcanic event during the Neogene to Quaternary (Lukács et al., 2018). The subsequent 16–9 Ma widespread calc-alkaline volcanism in the interior and the northern part of the Pannonian Basin has been regarded as the response of lithospheric thinning rather than the ongoing subduction (Harangi et al., 2001, 2007; Konečný et al., 2002; Harangi and Lenkey, 2007), while the 11–0.1 Ma alkaline basalt volcanic fields were formed due to asthenospheric mantle flow beneath the anomalously thinned basin area (Harangi et al., 2015a). Contemporaneously with the basalt volcanism, calc-alkaline to adakitic volcanic activity occurred along the Eastern Carpathians forming the ~160 km long Călimani–Gurghiu–Harghita (CGH) volcanic chain (Szakács and Seghedi, 1995) parallel with the East Carpathian orogen. These eruptions postdated the active subduction and therefore, this volcanism is regarded as post-collisional (Seghedi et al., 2011, 2019, 2023). The latest eruptions (160–30 ka; Molnár et al., 2019) built the Ciomadul volcanic complex (Moriya et al., 1995; Moriya et al., 1996; Harangi et al., 2015a; Szakács et al., 2015; Lukács et al., 2021; Karátson et al., 2022) in the southern Harghita, close to the Vrancea seismogenic zone. Although last eruption occurred ~30 ka, zircon geochronology, geophysical and petrological data and intense CO_2 degassing indicate the persistence of a trans-crustal magma reservoirs beneath the volcano (Popa et al., 2012; Harangi et al., 2015b; Kis et al., 2017, 2019; Laumonier et al., 2019; Lukács et al., 2021; Cserép et al., 2023).

Widespread CO_2, and CH_4 emissions have been documented along the Western and Eastern Carpathian range and adjacent regions. The CO_2 emissions primarily appear as CO_2-rich mineral water springs/wells (locally referred to as burkut, borviz, cevice) as well as CO_2-rich dry emissions named mofettes (Ciężkowski et al., 2010; Michalko, 2016; Kis et al., 2020).

An expanded and more detailed version of the geological and petrological information on the Carpathians is provided in the Supplementary Material.

3. Gas geochemistry

In the Romanian segment of the Carpathians, a total of 158 sites were investigated (Fig. 1) of which in situ compositional measurements using Multi-GAS device were conducted at 143 locations. These sites include dry gas emissions (mofettes), bubbling gases, drillings and mineral water springs. The sampling and analysis methods are described in the Supplementary material and in the data article Kis et al., 2026, while the data are available directly accessing the repository, Kis et al., 2025 https://ecl.earthchem.org/view.php?id=4173

To evaluate gas compositions and geochemistry across the Eastern and Western Carpathian range, we integrated our dataset with available data from previous studies conducted by Leśniak et al., 1997; Leśniak, 1998; Kotarba and Nagao, 2008; Palcsu et al., 2017 in the Polish segment; Polyak et al., 2018; Pavlyuk et al., 2019a, 2019b in the Ukrainian segment; Mants, 1974; Péter and Makfalvi, 1977; Filipescu and Humă, 1979; Althaus et al., 2000; Vaselli et al., 2002; Baciu et al., 2007, 2017; Etiope et al., 2009 Fórizs and Makfalvi, 2014; Gyila et al., 2017; Italiano et al., 2017; Kis et al., 2019, 2022; Lange et al., 2023; Szalay and Kis, 2023 in the Romanian segment and Michalko and Baková-Personal Communication for the Slovakian segment.

The dataset, which integrates the newly acquired data with the large dataset from existing literature, constitutes a comprehensive database of

gas emissions across the Carpathians, covering a total of 749 different sites. The maximum, minimum and mean compositional and isotopic values ($\delta^{13}C_{CO2}$ of CO_2 and $^3He/^4He$ ratios and $^4He/^{20}Ne$) for each region, together with their histograms is available in Table 1, Fig. 1 in the Supplementary material).

The investigated sites were categorised based on geographical, geological locations as well as their dominant gas species:

- Based on their geological locations, we can differentiate sites that are 1. volcanic: located right in the vicinity or within a maximum of 10 km distance from volcanic centres. Ciomadul volcano is identified as a subgroup, being the youngest volcano in the Carpathians 2. non–volcanic: gas emissions sourced from non-volcanic geological units, such as the flysch sequences or metamorphic units.
- Based on their dominant gas species (concentration exceeding 50%), we distinguish between: CO_2-dominant gases and CH_4-dominant volatiles. N_2-dominated gases appear rarely and were considered part of the CO_2 or CH_4 – group respectively, based on the second most abundant component.
- Based on their geographical locations, sites are grouped according to their origin within the Slovakian, Ukrainian, Polish and Romanian segments of the Carpathians.

3.1. Chemical compositions of the samples

The Carpathian gases are dominated by CO_2 and CH_4, with N_2 being less frequently observed (Fig. 2). The Western and Eastern Carpathians exhibit similarities in the chemical composition of the gas emissions. Throughout the Carpathian range, CO_2, and CH_4 reach concentration values exceeding 90% in free gases (Kis et al., 2025-EarthChem Repository data-https://ecl.earthchem.org/view.php?id=4173, Figs. 1 and 2, Table 1-Supplementary Material, Kis et al., 2026), in both volcanic and non–volcanic (sedimentary and metamorphic) geological environments.

In volcanic regions, gas samples are predominantly CO_2-rich, with concentrations reaching as high as 100%. These samples typically plot along the CO_2/10-N_2 mixing line, indicating varying contributions from N_2. The presence of N_2 is assumed to be atmospheric, introduced in the feeding system of manifestations through fracture-permeability and interactions with the shallow hydrogeological circuit (Kis et al., 2020). N_2 in deep reservoirs can also be released from organically bound nitrogen (Palcsu et al., 2014) Some volcanic sites exhibit minor amounts of CH_4, with concentrations of up to 0.01% in the Ukrainian sector and as high as 7.65% in Romania. Elevated CH_4 concentrations are found in the Ciomadul volcanic system, which aligns with similar observations in other volcanic and hydrothermal regions in the Apennines, where high CH_4 concentrations arise from various geochemical processes, e.g. pyrolysis of organic-matter-bearing sediments that interact with the ascending magmatic fluids; reduction of CO_2 or CO under high temperatures (>300-350 °C) or CO_2 and H_2 synthesis at high temperatures (>200 °C) (Tassi et al., 2012a, 2012b).

The non–volcanic areas reveal a more complex and heterogeneous gas composition. Pure CO_2 (100%) and pure CH_4 (100%) gases can be detected throughout the Carpathians, alongside mixtures of CO_2, CH_4 and N_2. In CO_2-dominanted regions, maximum CH_4 concentrations vary between 4.1 and 33.29%, while maximum CO_2 concentrations in CH_4-dominated sites range between 37.7 and 42.9%. The gas samples frequently fall along mixing lines between CO_2/10 – N_2, CO_2 – CH_4 and also N_2 – CH_4 (Fig. 2).

Among the other components N_2 reaches values similar to the atmosphere (up to 78%), or even higher quantities, up to 96%, possibly suggesting the existence of deep N_2 sources. A detailed investigation of the origin of the N_2 is beyond the aims of this study. O_2 concentration is generally low or absent, with the highest concentrations up to 15%, observed in the Ukrainian segment of the Carpathians. Minor components like H_2S reach concentrations up to 560 ppm at Ciomadul volcano, Romanian segment of the Carpathians. He has generally concentrations, between 1.44 and 0.01%.

3.2. Isotopic composition of noble gases

The inert nature of helium makes it a powerful tool for differentiating between mantle-derived and crustal-derived volatiles. While ^3He is mainly regarded as primordial, having been entrapped into the Earth's mantle during its accretion, radiogenic helium (^4He) is the dominant form of helium found in stable continental areas, produced by the decay of crustal U and Th in the crust (Marty and Tolstikhin, 1998; Sano, 2018). The $^3He/^4He$ ratio, expressed as R/R_a, varies significantly across gas emissions from volcanic, non–volcanic CO_2-dominated and non–volcanic CH_4-dominated sites in the Carpathians (Fig. 3 A, B, C, E, F). Overall, the distribution of R/R_a, ranges between 0.01 and 4.48 indicating a complex origin of fluids in the region, deriving from the mantle and crustal sources.

Volcanic sites exhibit elevated R/R_a values. For instance, the Ukrainian volcanic locations have a maximum of 2.27 R_a (Polyak et al., 2018), while sites within the youngest volcano, Ciomadul, have the highest value of 4.48 R_a (Vaselli et al., 2002). At other Romanian volcanic sites in the Eastern Carpathians, the maximum measured value is 4.27 R_a (Vaselli et al., 2002). In contrast, non–volcanic CO_2-dominated sites present generally lower R/R_a values compared to volcanic sites (e.g. in the Polish sector, the maximum R/R_a is 0.97; in the Ukrainian sector the maximum is 1.12, and in the Romanian sector the maximum is 1.73 R/R_a). Minimum values reach the crustal end member of 0.02 R_a at CO_2-rich samples in the Carpathians.

The non–volcanic CH_4–dominated sites display the lowest values of R/R_a in the region, with a maximum of 1.01 R_a in the Romanian sector and a minimum value of 0.01 R_a in all the regions (Poland, Ukraine, Romania). The measured $^4He/^{20}Ne$ ratios across all investigated sites range from 0.12 to 10,000, suggesting atmospheric contamination at some sites. This contamination may result from gas transport, through shallow hydrogeological circuits, rapid gas exchange at the gas/water interface during low fluxes in bubbling pools, or contamination upon sampling. All the values with $^4He/^{20}Ne \leq 0.318$ (the $^4He/^{20}Ne$ ratio of the atmosphere, Sano and Wakita, 1985) were excluded from geochemical interpretations, and for a more rigorous analysis, only $^4He/^{20}Ne$ values greater than 1 were considered on the computed geological-geochemical maps and in the discussion.

The mantle end-member values in the Carpathian region were constrained from fluid inclusions in olivine, orthopyroxene and clinopyroxene found in ultramafic xenoliths from the monogenetic basaltic volcanoes of the Perşani, with R/R_a values reported between 6.5 and 7.3 (Althaus et al., 1998), 5.94 to 5.96 (Kis et al., 2019), and 5.8 (Faccini et al., 2020). Additionally, shoshonites from the Malnaș volcanic dome showed R/R_a values ranging from 3 to 3.8 (Molnár et al., 2021). These measurements are lower than the mean values for the European Subcontinental Lithospheric Mantle (SCLM), which is 6.1 (Gautheron and Moreira, 2002).

3.3. Isotopic composition of CO_2 ($^{13}C_{CO2}$)

The $\delta^{13}C_{CO2}$ values range between very light values of –27.2‰ to heavier compositions of –0.05‰ (V-PDB) (Figs. 2 and 3 Supplementary material). This broad variation indicates several potential sources for CO_2, including mantle-derived carbon, marine carbonates and biogenic processes, and their extensive mixing. Furthermore, secondary processes like dissolution into groundwater, exsolution, and precipitation reactions can also influence the final isotopic signature of the CO_2 (Hoefs, 2018). In volcanic regions, the $\delta^{13}C_{CO2}$ values mostly fall within a narrow range of –4.57 to –3.15‰ (V-PDB) and reach maximum values between –1.58 and –0.05‰ (V-PDB) (Figs. 2 and 3 Supplementary material). Exceptions are given by some particular sites that exhibit

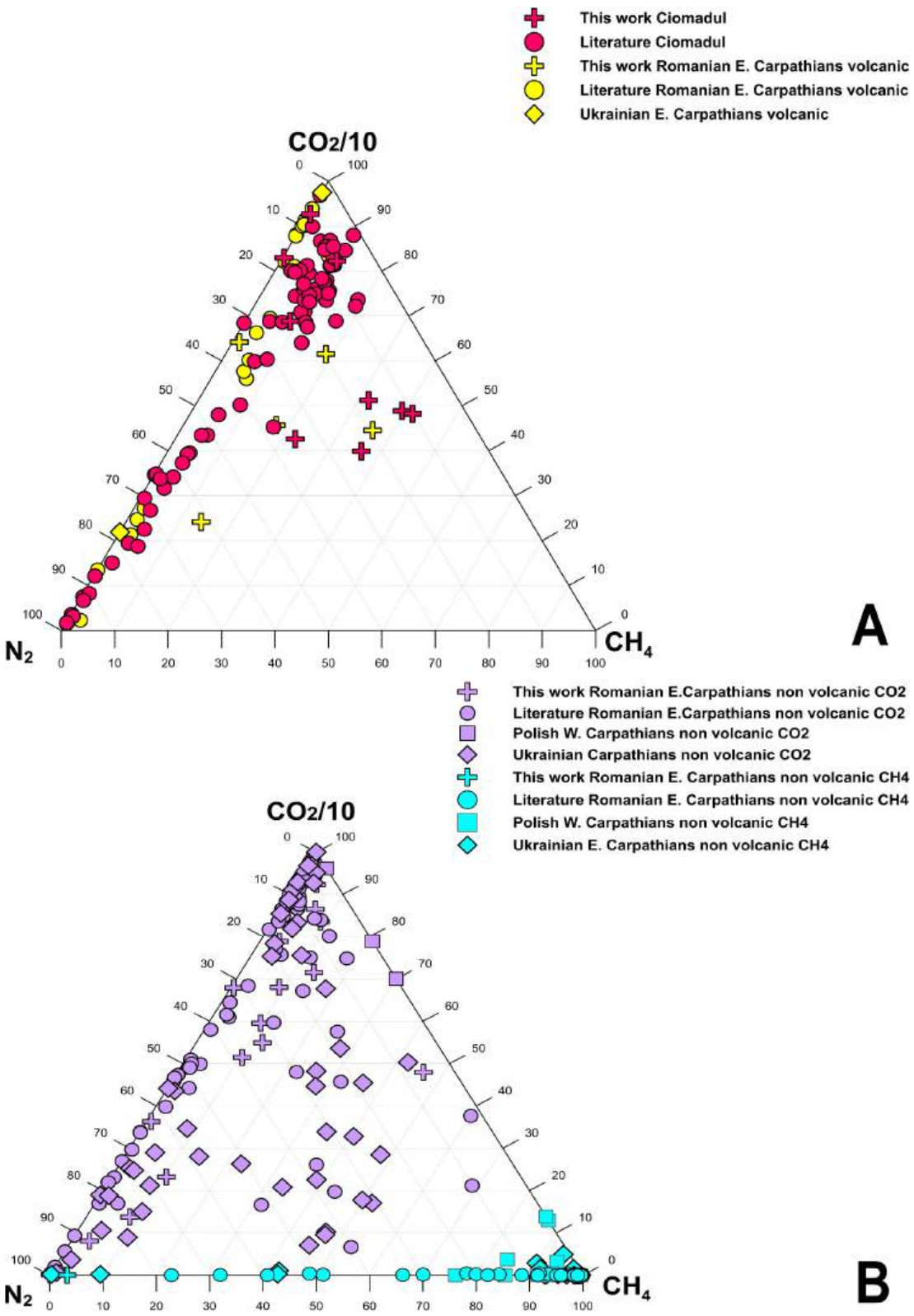

Fig. 2. Ternary diagram of $CO_2/10$-N_2-CH_4 showing the relative concentrations of the Carpathian gases (A) in volcanic areas and (B) in non-volcanic areas. The samples distribution denotes two mixing lines between a N_2 and CO_2 -dominated gas and a three-component mixing between the N_2-CO_2-CH_4. Data after This work, literature data as in Fig. 1. Symbols: red cross - This work Ciomadul; yellow cross - This work, Romania volcanic CO_2; Light purple cross - This work, Romania non-volcanic, CO_2 dominance; Neon blue cross - This work, Romania CH_4 dominance. Yellow diamond – Ukraine volcanic CO_2, light purple diamond – Ukraine, non-volcanic CO_2 dominance, neon blue diamond – Ukraine, non-volcanic CH_4 dominance; light purple square – Poland non-volcanic, CO_2 dominance, neon blue square – Poland, non-volcanic CH_4 dominance; yellow triangle – Slovakia volcanic CO_2. Literature data after Fig. 1. (For interpretation of the references to colour in this figure legend, the reader is referred to the web version of this article.)

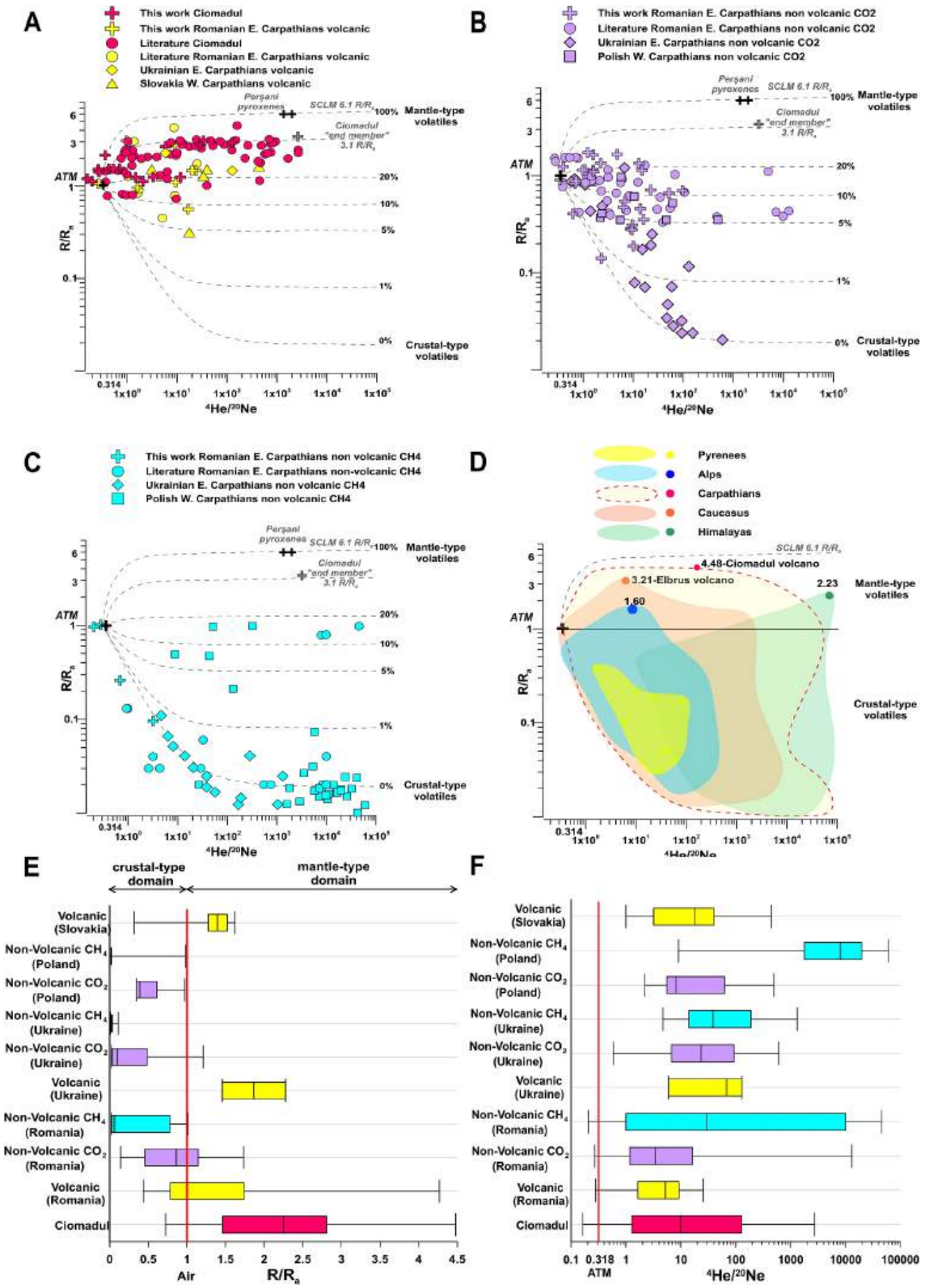

Fig. 3. He isotopic ratios (R/R_a) vs. $^4He/^{20}Ne$: A. for volcanic areas, B. for non-volcanic CO_2-dominated areas, C. for non-volcanic CH_4-dominated areas and D. for some major orogenic systems from the Tethyan realm. The theoretical lines represent mixings between atmospheric-mantle and atmospheric-crustal sources. The end members for the helium isotopic ratios are the following: ATM ($R/R_a = 1$, $^4He/^{20}Ne = 0.318$, (Sano and Wakita, 1985), subcontinental lithospheric mantle = SCLM (mean ratio of SCLM, $R/R_a = 6.1$, $^4He/^{20}Ne \geq 1000$, (Gautheron and Moreira, 2002), crustal end-member ($R/R_a = 0.02$, $^4He/^{20}Ne \geq 1000$, (Sano and Marty, 1995). Data for gas emissions from the Carpathians (Fig. 3A, B, C) as in Fig. 1. Data for comparisons (Fig. 3D) with the Alps after (Marty et al., 1992) with the Caucasus after (Polyak et al., 2000; Polyak et al., 2011) and with the Himalayas, after (Hoke et al., 2000; Klemperer et al., 2013; Zhang et al., 2017b; Klemperer et al., 2022), for the Pyrenees after (Milesi et al., 2025). E and F represent box-plots with the He isotopic ratios (R/R_a) and He^4/Ne^{20}. Box edges represent the lower and upper quartiles (25% and 75% of the data), the middle line the median values, whiskers the minimum and maximum values. Symbols as in Fig. 2.

values as low as –17.2‰ (V-PDB) suggesting contribution from shallow biogenic sources. Non–volcanic CO_2–dominated sites exhibit similar $\delta^{13}C_{CO2}$ ranges, with minimum values of –9.11 and maximum of –0.05‰ (V-PDB).

In contrast, non–volcanic CH_4–dominated sites are more homogeneous, with their minimum ranges from –27.2 to –13.9‰ (V-PDB) and maximum values falling between –20.8 and –2.1‰ (V-PDB) (Figs. 2 and 3 Supplementary material).

4. Discussion

The Tethyan orogenic systems including the Pyrenees, the Alps, the Caucasus and the Himalayas exhibit region-specific variations in CO_2 emissions and He isotopes. Across these systems, He isotopic signatures indicate crustal sources, with mantle-derived contributions occurring only in specific tectonic and magmatic settings (Fig. 3D).

In the Pyrenees, the He isotopic ratios (R/R_a between 0.03 and 0.37) indicate a purely crustal source for volatiles with some minor contribution from the mantle (~2%), associated with the thinning of the continental crust, fossil magma injections at the depth, possibly associated with the Miocene magmatism event and hydrothermal fluid circulation associated with the deep Tech fault, that facilitate the upwelling of mantle derived He components (Milesi et al., 2025) (Fig. 3D).

Similarly, the isotopic signature of helium in the Alps is also predominantly crustal, with the CO_2-dominated fluids derived from prograde metamorphism under relatively low-temperature conditions of calcareous and pelitic rocks (Wexsteen et al., 1988; Marty et al., 1992; Bissig et al., 2006). The R/R_a values range from very low 0.005 to 0.02, typically produced within the crust. Mantle-derived He is identified in regions where the crust has been thinned due to extension and magmatic activity, such as the Rhone Graben (France), characterized by crustal thinning, where R/R_a values reach 2.53 and at the boundaries with the Pannonian Basin, associated with extension with R/R_a values reaching 5.89 at Bad Radkersburg (Austria) (Marty et al., 1992; Bräuer et al., 2016) (Fig. 3D).

In the Caucasus, a similar pattern is observed, He isotope ratios suggest crustal origin, with mantle-derived helium (R/R_a values that have also $^4He/^{20}Ne$ pair ratios are up to 3.21) restricted to volcanic regions, such as Mount Elbrus and Kazbek, reflecting mantle-derived He from magmatic activity. The lateral variation of He isotopes is influenced by the tectonic-magmatic zoning of the orogen. The enhanced $CO_2/^3He$ ratios in the region suggest solubility-controlled shallow processes, coupled with contributions from a metamorphic CO_2-rich, He-free component (Kikvadze et al., 2010; Polyak et al., 2000; Polyak et al., 2011) (Fig. 3D).

The collision zone of the Himalayas provides the most comprehensive evidence of the importance of metamorphic reactions in CO_2 production. Prograde metamorphism of different rocks (dolomitic and calcareous rocks, calcareous pelites) and related decarbonation/devolatilization reactions in the Himalayas has been a significant source of CO_2, with paleoclimatic implications, as demonstrated by fluid-geochemical and petrological evidence (Kerrick and Caldeira, 1993; Evans et al., 2008; Pradhan and Sen, 2024). The localized mantle-derived He (R/R_a = 2.23) is associated with melts generated in the hot, incipiently molten Tibetan mantle wedge and the Yarlung-Zangbo Suture area (Klemperer et al., 2022), while other sites exhibit purely crustal-derived volatiles (Groppo et al., 2017; Rolfo et al., 2017; Zhang et al., 2017b; Klemperer et al., 2022; Liu et al., 2024) (Fig. 3D). While the active collision zone of the Himalayas exhibit, besides metamorphic volatiles, also mantle-derived fluids associated with active mantle wedge processes, older orogenic systems within the Tethyan realm are dominated by crustal volatiles, with mantle signatures associated either with the presence of volcanoes and related magmatic systems.

The suite of geochemical processes documented across several orogenic belts in the Tethyan realm, where CO_2 is released during present-day prograde metamorphism, associated with crustal He isotopic signatures, was denoted as "orogenic CO_2 degassing" or "degassing derived from continental reworking" (Drivenes et al., 2016; Rolfo et al., 2017; Groppo et al., 2022; Zhang et al., 2024), overwriting the canon that the orogenic systems represent only sinks for CO_2. Orogenic degassing along with "volcanic degassing" and "tectonic degassing", constitutes a fundamental component of the Earth's atmospheric evolution, emphasizing the need for advanced research to address the unresolved complexities of the global carbon cycle (Zhang et al., 2024).

The Carpathians exhibit similarities to other Tethyan orogenic systems, in both their geodynamic evolution and the geochemistry of their volatile emissions. The newly collected and the existing gas data, summarized here, enables a comprehensive synthesis of gas emissions across the Western and Eastern Carpathians and provides the first regional map of the distribution of the free CO_2 and CH_4 degassing sites throughout the entire area. These two gas species, CO_2 and CH_4, exhibit distinct spatial distributions, likely reflecting variations in the lithological and tectonic structures and evolution at local and regional scale (Fig. 1).

4.1. Geochemical zones of the gas emissions in the Carpathians

CO_2-dominated emissions are predominantly concentrated within a relatively narrow range in the inner part of the Carpathian arc (Fig. 1), closely associated with volcanic systems and the neighbouring flysch nappes (Airinei and Pricăjan, 1975; Leśniak et al., 1997; Polyak et al., 2018; Kis et al., 2020; Vaselli et al., 2002). In the Western Carpathians (Slovakian segment), CO_2 is prevalent near the Neogene volcanic units and in the Inner Carpathian nappes (Michalko, 2016). In the Polish sector, CO_2 emissions occur in the southern part of Magura Nappe and along its boundary with the Pieniny Klippen Belt, including areas such as Wysowa, Tylicz, Krynica and Muszyna (Ciężkowski et al., 2010; Dušan et al., 2010). In the Eastern Carpathians (Ukrainian segment), the CO_2 emissions and related mineral waters originate from the Cretaceous and the Paleogene sediments of the Skyba, Krosno, Rakhiv, Burkut, Magura, and Dukla flysch nappes, as well as near the Marmarosh massif, the Pieniny Klippen Belt and the Vihorlat-Gutin volcanic zone (Oszczypko, 2004; Oszczypko et al., 2015, 2018). Similarly, in the Romanian segment, CO_2 degassing aligns with the Late Miocene to Quaternary volcanic regions and the flysch units, particularly in the Cretaceous sequences of the Ceahlău, Teleajen and Macla nappes (Airinei and Pricăjan, 1975).

The suture areas such as the Pieniny Klippen Belt – Magura (West) and Ceahlău-Severin (East), are critical areas for CO_2-degassing. These extensively tectonized units are characterized by complex lithologies comprising both siliciclastic and calcareous sequences (Schmid et al., 2020), e.g. the Ceahlău-nappe is defined as being a "typical sandy-calcareous flysch with turbiditic limestone interlayers" with limestone fragments up to 60% (e.g the Sinaia beds; Ștefănescu et al., 2007, similarly, the Magura nappe is rich in carbonates (Gradziński et al., 2012). Together with the neighbouring nappes, they are characterized by complex lithostratigraphic structure, comprising carbonates and marls interbedded within siliciclastic sequences (Săndulescu, 1984; Matenco and Bertotti, 2000; Ślączka et al., 2006; Ștefănescu et al., 2007; Melinte-Dobrinescu and Jipa, 2007; Necea et al., 2021).

Beneath the flysch nappes, the Danubian metamorphic basement is also overlain by a carbonate-rich sedimentary sequence composed of continental to shallow-lacustrine Permian clastics, Lower Triassic clastic deposits, Middle to Upper Triassic carbonates, a Lower to Middle Jurassic clastic succession, Middle Jurassic to Early Cretaceous carbonates, and, locally, fine-grained Late Cretaceous sediments (Schmid et al., 2020; Krstekanić et al., 2022).

Distinct lithologies influences the gas distributions, for instance, hydrocarbons, sourced from bituminous shales and trapped in the flysch sandstones, dominate the marginal flysch nappes (Tarcău, Vrancea nappes) but are absent in the suture areas (e.g. Pieniny Klippen Belt, Ceahlău nappe). In contrast to CO_2, CH_4 emissions are primarily

associated with the nappe-stacks of the Outer Flysch belt, where CH_4 is of thermogenic origin (the type of natural gas formed through the thermal decomposition of organic matter, at high temperatures and pressures within the Earth's crust, as defined by Schoell, 1983) as evidenced by various studies (Baciu et al., 2017; Kotarba et al., 2020; Krézsek et al., 2023). Therefore, the geochemistry of CH_4 systems falls beyond the scope of the current study.

The proximity of young volcanic units and the simultaneous presence of silicates and carbonates in the flysch sedimentary sequences provide essential opportunities for reactions that can release fluids (Bucher and Frey, 2002). These fluid-releasing processes within the Carpathian orogen will be discussed in the next sections.

While extensive research has been conducted on the origin and generation of hydrocarbons in the Western and Eastern Carpathians, primarily due to their economic significance and exploration interests (Pawlewicz, 2006, 2007; Kotarba and Nagao, 2008; Pavlyuk et al., 2019a, 2019b), the origin, sources and geological/geochemical processes responsible for CO_2 generation remain still unclear. A variety of geological/geochemical processes have been proposed to explain the widespread CO_2-degassing across the Carpathians. These include "post-volcanic" phenomena associated with the Neogene to Quaternary volcanic chain (Airinei and Pricăjan, 1975), thermal metamorphism of carbonates (Vaselli et al., 2002), and metamorphic degassing of sedimentary sequences (Oszczypko et al., 2018). To contribute to overcoming uncertainties surrounding the origins of CO_2, we conducted a thorough investigation at a regional scale across the Western and Eastern Carpathians, focusing on the chemical and isotopic composition of gases including noble gases as conservative tracers and carbon isotopes. We also examined the lithostratigraphy and potential pressure-temperature (P/T) conditions of the geological sequences capable of generating carbonate fluids within the Carpathian range. Through this integrated approach, we aim at improving our understanding of the complex interplay of geological and geochemical factors contributing to CO_2 emissions in the region.

4.2. Mantle derived volatiles

The spatial distribution of noble gases ($^3He/^4He$ expressed as R/R_a, where Ra is the helium isotopic signature in air, 1.384×10^{-6}) along the Carpathian arc (Figs. 1 and 3) reveals two distinct sources for volatiles: mantle-derived and crustal-radiogenic, with variable mixing occurring between the two. Following the approach of Sano and Wakita (1985) we calculated the proportions of atmospheric, mantle/magmatic derived and crustal-radiogenic He for each site. The end-members considered were the atmosphere ($R/R_a = 1$), the subcontinental lithospheric mantle (SCLM; mean ratio $R/R_a = 6.1$, Gautheron and Moreira, 2002), and the crustal end-member ($R/R_a = 0.02$, Sano and Marty, 1995).

Across the Carpathians, a coherent relationship is observed between elevated heat flow and increasing mantle He proportions. Elevated R/R_a values (>2) occur predominantly within the Neogene to Quaternary volcanic belts (Fig. 1; regional maps Figs. 4–7), which are also characterized by relatively high conductive heat flow. In the Polish segment of the Western Carpathians, low heat-flow (40-60 mW/m^2, Horváth et al., 2006, 2015) coincides with crustal R/R_a signatures, with mantle contributions below 5%. This reflects a cold, thick lithosphere and fluids dominated by radiogenic ^4He (Fig. 4). Toward the Slovakian segment, heat flow rises to 70-100 mW/m^2, particularly near the Neogene volcanic areas and at the border with the Pannonian Basin (Horváth et al., 2006, 2015). R/R_a values rise accordingly, with slightly higher mantle inputs of 10-20%, consistent with the proximity of the hotter and thinner lithosphere of the Pannonian Basin and/or the alkali basalt volcanism in the past few hundred thousand years (Fig. 4). A similar pattern is observed in the Ukrainian sector of the Eastern Carpathians. Here, high heat-flow values (80-110 mW/m^2, Horváth et al., 2006, 2015) near the Transcarpathian Basin correspond to localized increases in the mantle He input, reaching 50% at the basin transition zone, as also documented by Polyak et al. (2018) (Fig. 5C). Northeastward, toward the flysch units, both heat flow (~40 mW/m^2, Horváth et al., 2006, 2015) and mantle input (<1%) decrease, indicating thickened lithosphere and dominantly CH_4-bearing systems.

The most pronounced expression of the heat-flow and mantle input relationship occur in the Romanian segment of the Eastern Carpathians. The Ciomadul volcanic area exhibits high geothermal gradient (Demetrescu and Andreescu, 1994), high regional heat flow, reaching 100 mW/m^2 (Horváth et al., 2006, 2015) and R/R_a values peak at ~2.5-4.5 (This work, Althaus et al., 2000; Vaselli et al., 2002, Kis et al., 2019). The calculated mantle/magmatic He fractions exceed 60-70%, indicating persistent magmatic input. Such high mantle contributions suggest possible magma accumulation at the crust/mantle boundary zone and ascent of CO_2 along fracture zones (Fig. 7). Ciomadul represents the only part of the Carpathians where ongoing magmatic degassing is the dominant present-day process. Away from the Ciomadul volcanic area, both heat flow (60-70 mW/m^2, toward the Transylvanian Basin; 40-50 mW/m^2, toward the flysch belt and Carpathian molasse) and mantle/magmatic He contributions decrease (<1%), returning to crustal dominance (Figs. 6 and 7).

To contextualize the observations in the Carpathians, it is necessary to consider the principal mechanisms for transporting primordial He to the surface. The most effective mechanisms to transport primordial helium and thermal energy to the Earth's surface include partial melting and magma mobility (Torgersen, 1993; Sano and Marty, 1995; Marty and Tolstikhin, 1998; Zhang et al., 2024). Due to its incompatible geochemical behaviour, He is expected to be incorporated into the melt that is formed during magma generation (Bianchi et al., 2010; Olson and Sharp, 2022). Mantle-derived He outgassing therefore corresponds to areas where magma is emplaced in the crust, leading occasionally to volcanic activity (Zhang et al., 2024). This occurs in various tectonic settings from oceanic and continental extensional regions and subducting zones. The mantle-derived He is commonly transported to the surface by CO_2-rich fluids. CO_2 has low solubility in silicate melts (Marty and Jambon, 1987; Hilton et al., 2002) and may enter the mantle through recycling/remobilisation of crustal carbon (Whitley et al., 2019; Stewart and Ague, 2020). CO_2 release from a subducting slab is controlled by processes such as the alteration of oceanic crust, metamorphic decarbonation, carbonate dissolution and slab-melting (Mason et al., 2017; Arzilli et al., 2023). Carbon released from slab dehydration enters the mantle wedge, form a diapir and is incorporated to the generated magmas (Chen et al., 2021; Ducea et al., 2022). Exsolution of CO_2 from basaltic magma starts even in the upper mantle depth (Allison et al., 2021). This can contribute to the fast ascent of basaltic magmas and ultimately volcanic eruptions, but CO_2 gas can also escape from the magma body and migrate to the surface along tectonic fracture zones.

Mantle He transport is, however, not restricted to volcanic arcs. There are many examples of mantle-He transport even along strike-slip tectonic regimes. Kennedy et al. (1997) observed indications of mantle fluid influx along the San Andreas Fault, whereas Kulongoski et al., 2013 explained the elevated R/R_a values with the continuous transport of mantle He from incipient upper mantle melts through the San Andreas Fault. Similarly, in the East Anatolian Fault Zone region, mantle-derived fluids reach the surface through lithospheric discontinuities and related increased vertical permeability of the fault zone. Although the East Anatolian Fault Zone lacks volcanic activity, it is believed that magma bodies may have intruded at the fault zone and they are facilitating the release of mantle-derived fluids. This assumption is also supported by the presence of geothermal anomalies and thermal waters (Italiano et al., 2013). CO_2 emissions are reported in continental extensional areas with no current volcanic activity, such as in the Rhine Graben, Germany (Griesshaber et al., 1992) and in the Eger Rift area, Germany-Czech Republic (Bräuer et al., 2018). In these cases, increases in CO_2 flux and mantle He were observed associating to tectonic events. In both cases, however, magma accumulation in the mantle-crust boundary zone is assumed. CO_2 emissions were also observed in volcanologically

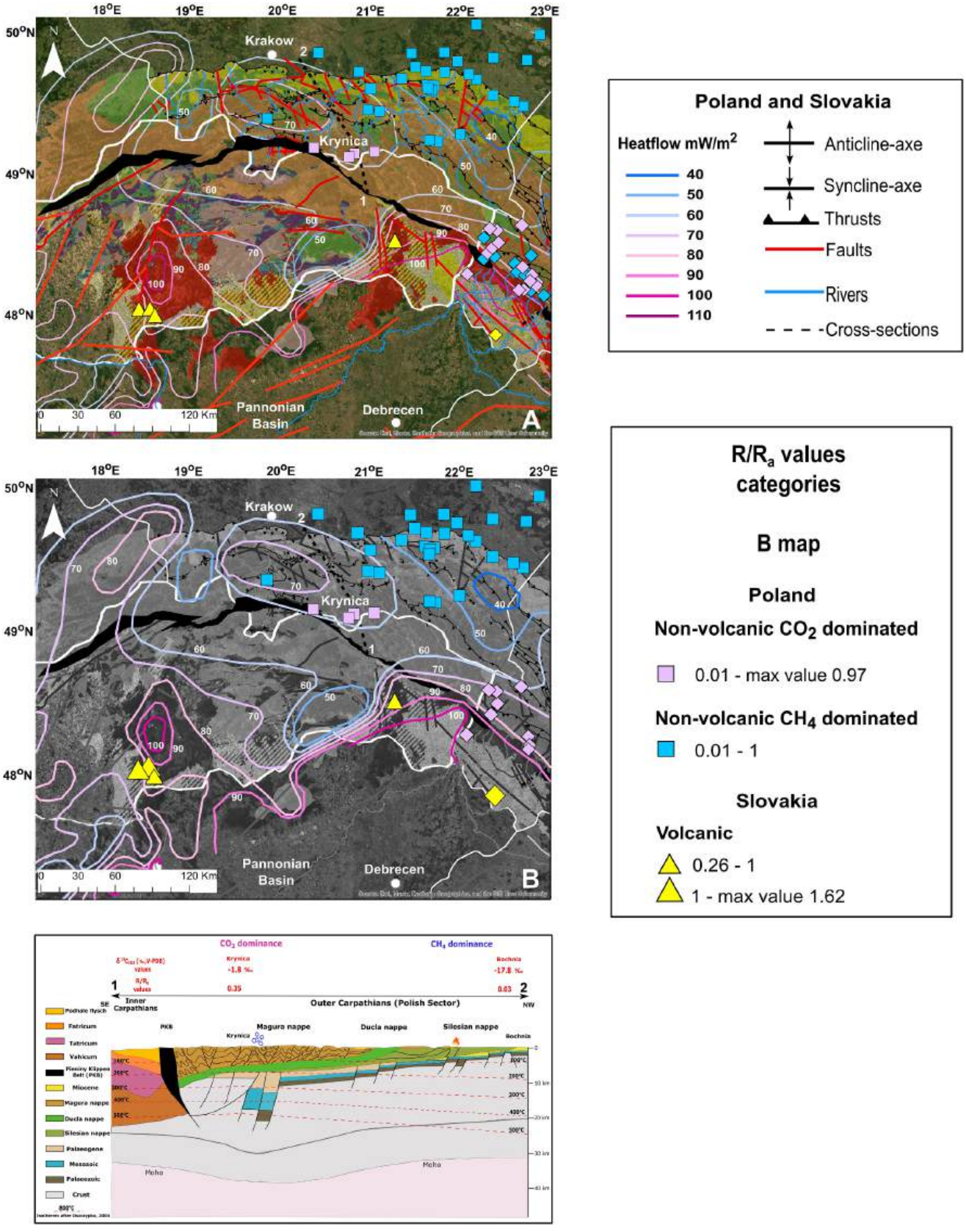

Fig. 4. Slovakian and Polish segment of the Western Carpathians. A. Geology and chemical zoning of the gas emissions, geological data references after Fig. 1, heat flow data after (Horváth et al., 2006, 2015). B. Non-contaminated ($^4He/^{20}Ne > 1$) He isotopic ratios vs. thermal heat flow. Geological map and data references after Fig. 1, geological cross section modified after (Oszczypko, 2004). Symbols as in Fig. 1.

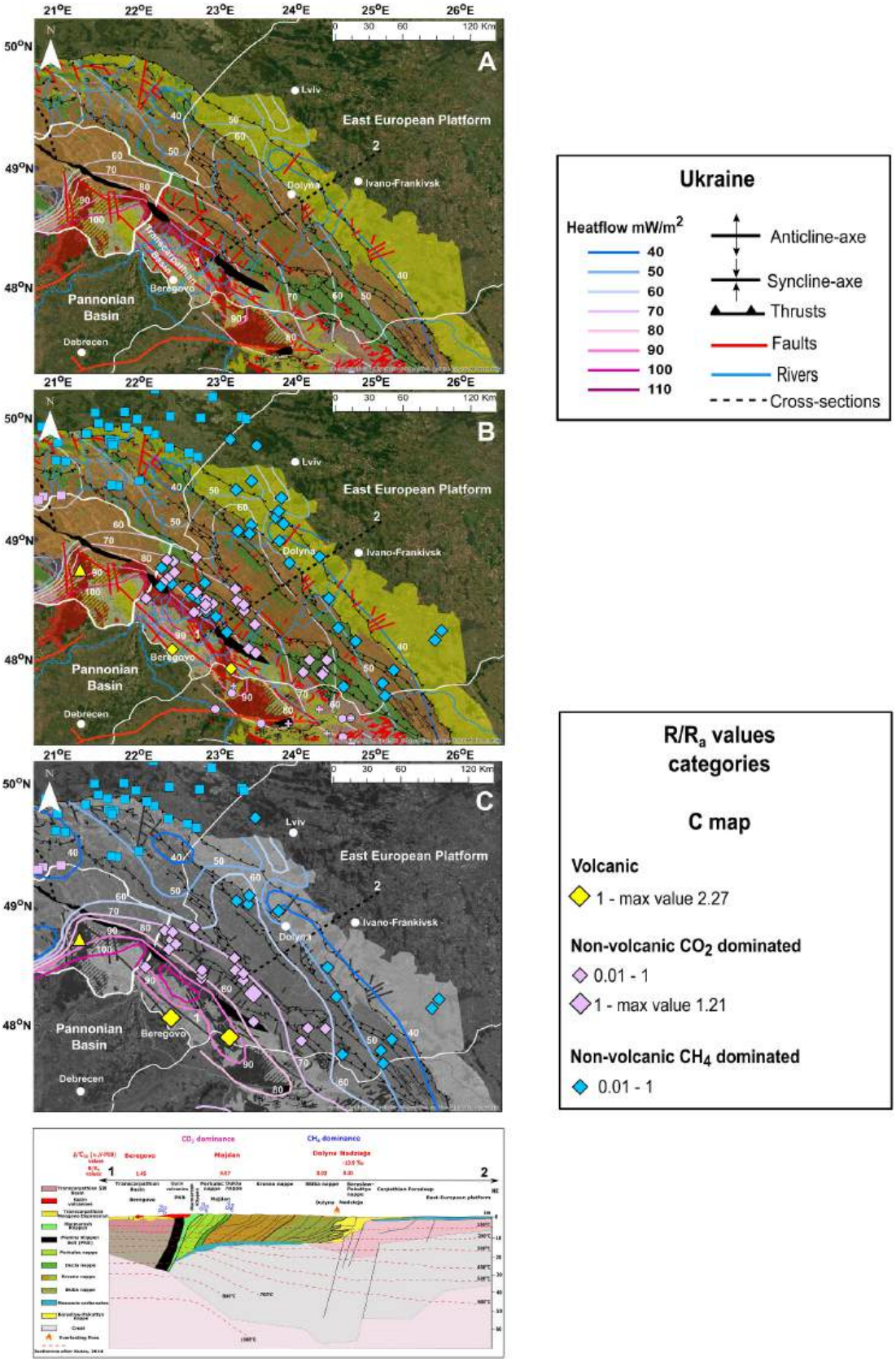

Fig. 5. Ukrainian segment of the Eastern Carpathians. A. Geology and heat flow data, references after Fig. 1 and after (Horváth et al., 2006, 2015). B Geology and chemical zoning of the gas emissions. C. Non-contaminated ($^4He/^{20}Ne > 1$) He isotopic ratios vs. thermal heat flow. Geological map references after Fig. 1. Geological cross section modified after Oszczypko et al., 2007 and Kutas, 2014. Symbols as in Fig. 1.

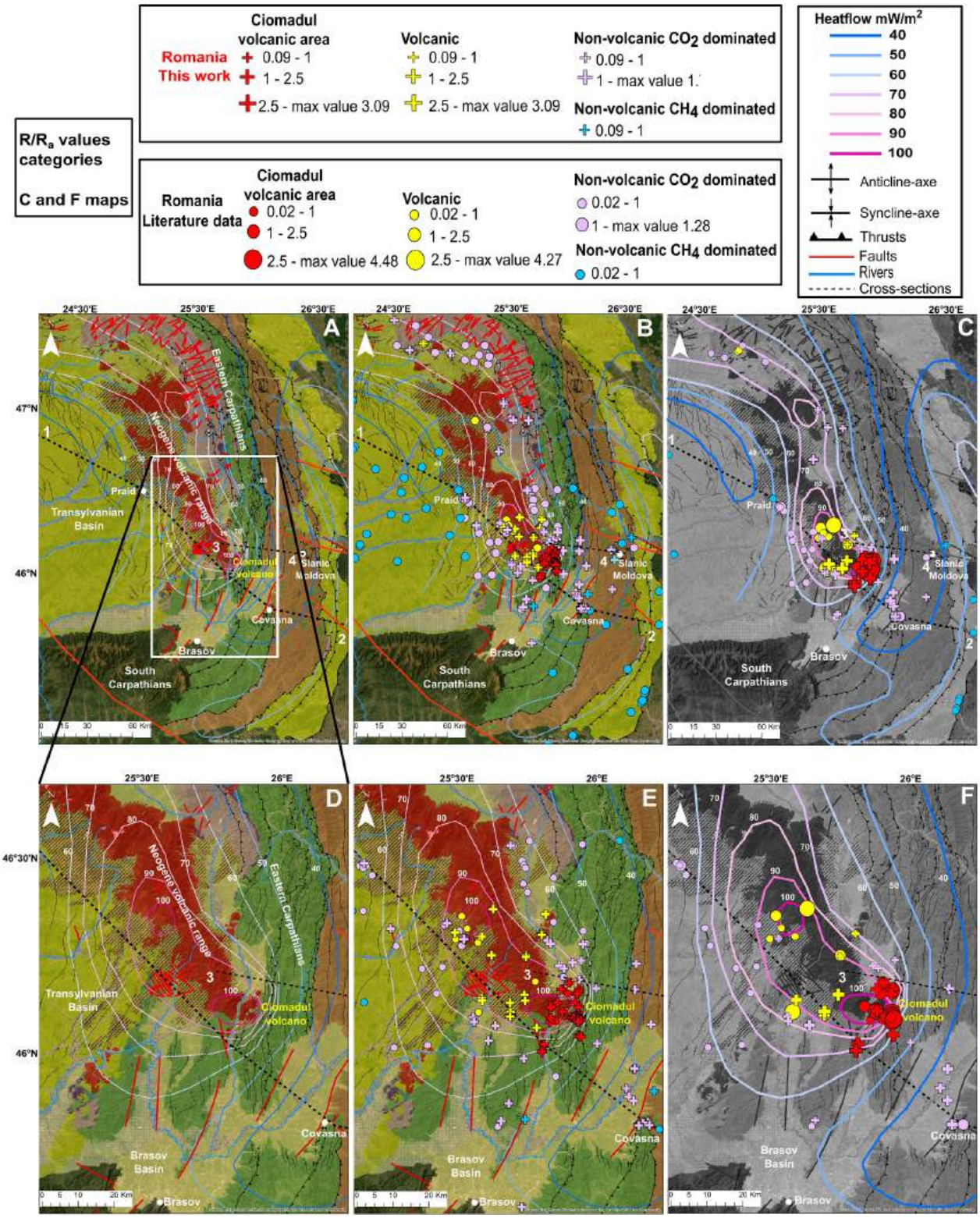

Fig. 6. Romanian segment of the Eastern Carpathians. A. Geology with heat flow data, references after Fig. 1 and (Horváth et al., 2006, 2015). B Geology and chemical zoning of the gas emissions, references after Fig.1. C. Non-contaminated ($^4He/^{20}Ne > 1$) He isotopic ratios vs. thermal heat flow. Zoomed versions: geology (D), chemical (E), non-contaminated ($^4He/^{20}Ne > 1$) He isotopic ratios vs. thermal heat flow (Horváth et al., 2006, 2015) (F). Symbols as in Fig. 1.

inactive areas, such as in Sicily and Vulture Line in Southern Apennines (Caracausi et al., 2013; Caracausi and Sulli, 2019), but, again, the CO_2 transport was thought to be related to deep magma accumulation/intrusions at depth. Mantle He isotopic ratios are also observed in modern flat-slab subduction settings, e.g. Kii Peninsula in Japan or the Peruvian flat slab in South America. In these specific tectonic settings, mantle-derived He is thought to be transported to the surface by high-temperature supercritical aqueous fluids derived from the underlying flat slab. These transport processes are particularly effective in flat slab subduction environments with shallow subduction angles (Gutscher

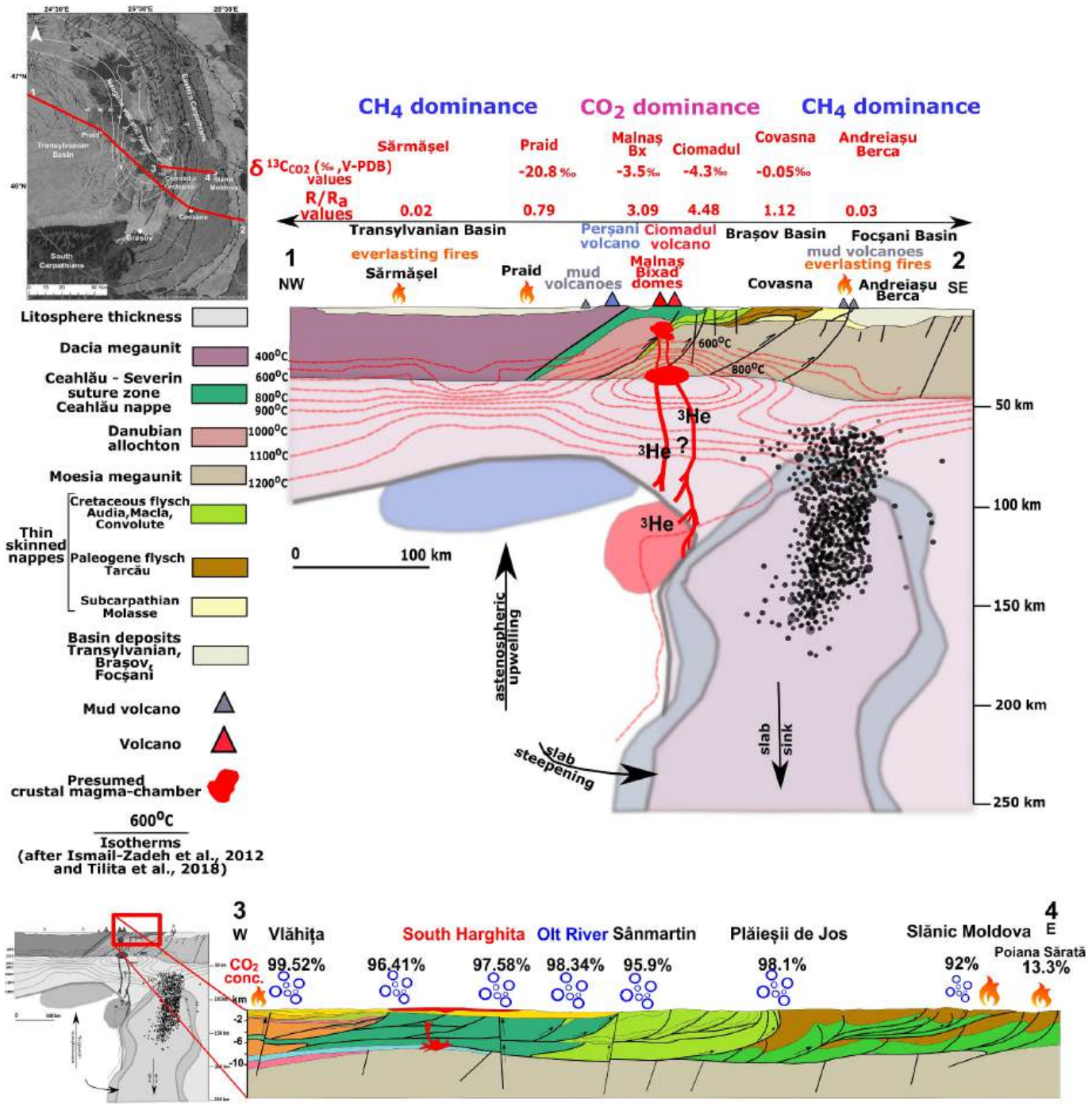

Fig. 7. Geological cross sections of the south-eastern part of Romanian sector of the Carpathians, modified after (Murgeanu et al., 1962; Săndulescu et al., 1972; Ismail-Zadeh et al., 2012; Schmid et al., 2020; Seghedi et al., 2011; Tiliță et al., 2018). The most effective ^{3}He transport occurs through the volcanic system of Ciomadul, whereas CO_2 degassing – originating from both the mantle and the crust as a result of metamorphism – takes place along the nappe structures of the Eastern Carpathians (indicated with blue bubbles and the measured CO_2 concentrations of the surface manifestations. (For interpretation of the references to colour in this figure legend, the reader is referred to the web version of this article.)

et al., 2000; Hiett et al., 2021; Matsumoto et al., 2003; Newell et al., 2015; Umeda et al., 2006). A similar situation has been described in the suture zone of the Himalaya-Tibet collision, where a sharp He boundary separates the Himalayan domain dominated by crustal He from the Tibetian domain enriched in mantle fluids attributed to the melts in the hot mantle wedge (Klemperer et al., 2022).

These examples demonstrate that mantle He transport may occur through 1. active magmatism/volcanism, 2. remobilisation from intruded magma bodies and enhanced circulation through deep faults, or 3. deep fluid circulation in flat slab settings of continental collision zones. Degassing processes along the Carpathians is evaluated therefore within this broader framework.

Although there is no current volcanic activity and even Quaternary volcanism was sporadic, there has been long-lasting volcanism (over 16 Myr; Harangi et al., 2026; Pécskay et al., 2006, 2015) along the Carpathian orogenic belt. Volcanic activity seems to have been related to subduction of oceanic lithosphere, but there are multiple observations discussed in several papers (Konečný et al., 2002; Lexa et al., 2010;

Seghedi et al., 2011, 2019; Harangi et al., 2026 and references therein) suggesting a distinct origin. Magmas are considered to have been generated by partial melting of lithospheric mantle metasomatized previously by subduction-related fluids. In the Western segment, magma generation was related to lithospheric extension (Harangi et al., 2007). In the Eastern segment, volcanism was partly post-collisional when slab detachment and hot asthenospheric mantle flow could cause partial melting (Seghedi et al., 2011). In the Western Carpathians, the most recent volcanic activity formed a monogenetic alkaline basalt volcanic field by scattered eruptions from 8 Ma up to a few hundred thousand years ago (Konečný et al., 1999). In the Eastern Carpathians, even younger volcanism occurred in the southernmost Harghita, where repeated eruptions built up the dacitic Ciomadul volcano from 160 ka to 30 ka (Harangi et al., 2010, 2015b; Szakács et al., 2015; Molnár et al., 2019). During this volcanism, only a portion of the accumulated magma erupted, whereas much more remained in the crustal levels. Zircon geochronology and thermal modelling suggest long, several 100's thousands of years existence of magmas in the crust (Lukács et al., 2021). Geophysical studies indicate that magma could still reside in the crust beneath Ciomadul (Popa et al., 2012; Harangi et al., 2015b). This is also consistent with the high heat flow associated with high geothermal gradient (Demetrescu and Andreescu, 1994).

CO_2 and CH_4 emissions are widespread along the Carpathian orogenic area and gas emissions show variable He isotopic signatures. As we show, elevated R/R_a values (>2) are observed only in areas where volcanic activity occurred in the past and where there is still high heat-flow. Similar situation is observed in the case of the Caucasus, where the elevated R/Ra values are concentrated along the Mount Elbrus and Kazbeh volcanic areas (R/R_a values 3.21, Kikvadze et al., 2010; Polyak et al., 2000, 2011). In the Carpathians, the Ciomadul volcano is characterized by intense CO_2 gas emissions, in the form of bubbling pools, bubbling peat bogs and low-temperature dry mofettes as well as CO_2-rich mineral water springs. The total CO_2 flux was estimated at minimum 8000 t y^{-1}, comparable with dormant volcanic areas worldwide (Kis et al., 2017). He isotopic composition of these gases (>2 R/Ra, the highest R/R_a values are 4.48 reported by Vaselli et al., 2002 and 3.09 reported by Althaus et al., 2000; Kis et al., 2019) suggests a significant magmatic input, exceeding 60-70% presumably related to a degassing magma body at the crust-mantle boundary zone (Fig. 7).

Similarly to the elevated He isotopic ratios, the $\delta^{13}C_{CO2}$ values show SCLM mantle-like values ($\delta^{13}C_{CO2}$ − 3.5‰ representative of the mantle below the Carpathians; Bräuer et al., 2016; Rizzo et al., 2018) between −4.5 to −4.7‰ V-PDB at Ciomadul (This Work; Vaselli et al., 2002; Kis et al., 2019); away from volcanic areas, $\delta^{13}C_{CO2}$ values increase systematically to limestone-like values ($\delta^{13}C_{CO2} = 0$; (Sano and Marty, 1995) of $\delta^{13}C_{CO2}$ − 0.5-0.05 e.g. at Covasna (This work and Lange et al., 2023).

During the prolonged periods of volcanism (eruption of Ciomadul-type magmas commenced 950 kyr, whereas the main volcanic edifice was developed for the last 160 kyr; Molnár et al., 2018, 2019), magma bodies continuously degassed either during magma ascent or during crystallization. Gases escaped from the magma body and migrated upwards or remained in the melt and were transferred to the surface during eruptive phases. However, during quiescence periods, some volatiles may have been trapped and accumulated at crustal levels and contaminated by crustal fluids (e.g., Christopher et al., 2015). Such magmatic gas-traps may have been reactivated during faulting and associated seismic events. The emitted CO_2 gases and those trapped in clinopyroxene crystals (Malnaș dome; Molnár et al., 2021) exhibit lower R/R_a values (3.2-4.5) compared to those obtained from the ultramafic xenoliths in the alkali basalts of the Perșani volcanic field (Althaus et al., 1998; Kis et al., 2019; Faccini et al., 2020; Molnár et al., 2021). The ultramafic xenoliths are characterized by 5.5-6.5 Ra, which is typical of the subcontinental lithospheric mantle (SCLM). This discrepancy within 50 km distance can be explained by small-scale heterogeneity of the lower lithosphere (Kis et al., 2019; Molnár et al., 2021). The Ciomadul primary magmas may have been derived from a lithospheric mantle source metasomatized by subduction-related fluids (Bracco Gartner et al., 2020) and therefore it is characterized by relatively low R/R_a He isotope values (Kis et al., 2019), similarly to the magmatic CO_2 gases in Central Italy (Martelli et al., 2004). Nevertheless, the CO_2 gases at the Ciomadul volcanic area have elevated R/R_a values, that exhibit a marked decline with increasing distance from the volcano (Vaselli et al., 2002; Kis et al., 2019). This corroborates the magmatic origin of the CO_2 at Ciomadul, whereas He isotopes show predominantly crustal component in the surroundings.

The volcanism of Ciomadul took place within the flysch belt, which represents a thin-skinned fold-and-thrust zone of the accretionary prism. Magma generation in such a tectonic setting could be attributed to the final stage of slab detachment, when slab verticalization induced suction in the overlying lithosphere and mantle flow around the retreating slab (Chalot-Prat and Girbacea, 2000; Bracco Gartner et al., 2020; Ducea et al., 2020; Seghedi et al., 2023; Harangi et al., 2026). Such post-collisional volcanism characterized the entire Calimani-Gughiu-Harghita chain (from 11 Ma; Pécskay et al., 2006) northwest from Ciomadul. There are several CO_2 emission sites along these already inactive volcanic areas, that show elevated R/R_a values (Vaselli et al., 2002) suggesting involvement of magmatic gas components. These may have been derived from the magmatic gases trapped in various crustal levels during the long-lasting volcanism and variably contaminated by crustal fluids since that time. These trapped CO_2 gases with elevated R/R_a values are emitted at other parts of the Neogene to Quaternary volcanic belt. In the Polish segment of the Carpathians, CO_2 gases have R/R_a values up to 0.97 with He/Ne ratio of 5.8 (Leśniak et al., 1997), which could be related to the Late Miocene intrusive magmatic bodies. The trapped gases could be intermittently transported to the surface along the deep-seated fault system of the Pieniny Klippen Belt. In central and southern Slovakia, close to the Miocene andesitic volcanoes of the Visegrád-Börzsöny and Central Slovakian Volcanic Field (Krupivská-Štiavnička) the R/R_a values of the CO_2 gases are up 1.62 (Bakova-Michalko personal communication), whereas in Ukraine, near to the Beregovo and Gutin volcanic units, R/R_a values up to 2.27 have been reported (Polyak et al., 2018).

In summary, the relatively high, mantle-like He transport in the Carpathians is primarily related to Neogene to Quaternary volcanism. The most marked area for mantle-He emission is the Ciomadul, the youngest volcano of the Carpathian-Pannonian Region, where the most recent eruption occurred 30 ka and there are signs for a still active magma body in the continental crust. All other areas show lower R/R_a values, where crustal He has an increasing role. Nevertheless, the 1–2.5 R/R_a values indicate still significant mantle origin of the gases. We argue that considerable amount of magmatic CO_2 gas was trapped in different crustal level during past volcanism where they mixed with crustal gases. Seismic activity can occasionally deliberate portions of gas, which transport to the surface along tectonic lines. In the Outer flysch belt, CH_4 becomes more common, and CO_2 gas shows dominant crustal origin along these zones (Figs. 4–7).

4.3. Crustal-derived components

He isotopic composition indicates significant mixing between mantle-derived and crustal sources, with R/R_a values ranging from 0.01 to 1.73 R/R_a. ^4He is produced by the radioactive decay of U and Th in the rocks. It is termed as “radiogenic” or “crustal” helium, suggesting its crustal origin, whereas ^3He is an unambiguously mantle-derived in natural fluids (Sano, 2018). Hence, it results that the ratio between the two isotopes is a useful tool to figure out the origin of He in natural fluids, because the He isotopic signature in its possible source is well distinguished (Air: 1 R_a, Crust: <0.05 R_a, SCLM 6.1 ± 0.9 R_a, (Gautheron and Moreira, 2002; Sano, 2018).

In the non-volcanic regions of the Carpathians, such as the flysch belt and metamorphic sequences, the contribution of mantle-derived He is

much lower or even absent in the gas emissions (Fig. 3). The leading carrier gases for the radiogenic He is CO_2 and CH_4 similar to mantle derived He. In gas emissions dominated by CH_4, the He isotopic ratios cluster within the radiogenic values, suggesting a pure crustal origin of these gases throughout all sectors of the Carpathians. Exceptions arise in specific areas from Polish and Romanian segments, such as Homorod Brasov and Praid, where 7.5 and 20% respectively of mantle contributions are detected. In the CH_4-hosted gas samples, He is predominantly derived from radiogenic sources, with a minor admixture of mantle-derived components.

Many CO_2-rich samples across the Carpathians reveal a significant crustal-derived He, reaching up to 98.9% at several sites ($R/R_a = 0.18$, in the Romanian segment, meaning 93% radiogenic input, $R/R_a = 0.028$ in the Ukrainian segment, meaning 98.9% radiogenic input and $R/R_a = 0.35$ in the Polish segment, meaning 92% radiogenic input) (Fig. 3), indicating that CO_2 in the Carpathians is primarily crustal-derived, resembling trends observed in other major orogenic systems, such as the Alps, Caucasus or Himalayas (Kerrick and Caldeira, 1998; Polyak et al., 2000, 2011; Becker et al., 2008; Evans et al., 2008; Kikvadze et al., 2010; Groppo et al., 2017; Rolfo et al., 2017; Klemperer et al., 2022).

Collision orogenic (mountain building) systems are generally considered complex geodynamic environments where the interplay of magmatic and metamorphic processes, together with the tectonic forces govern volatile emissions and significantly contribute to global carbon cycling (Kerrick and Caldeira, 1998; Liu et al., 2024; Skelton, 2013; Zhang et al., 2024). Research on the remobilisation of crustal carbon has emphasised the role of active subduction zones, particularly those associated with magmatism and volcanism, as key sites for the recycling and release of carbon (Kelemen and Manning, 2015; Lee et al., 2016; Mason et al., 2017; Chen et al., 2021; Ducea et al., 2022; Arzilli et al., 2023; Liu et al., 2024).

However, CO_2 in the crust can be generated by a variety of geochemical processes such as regional metamorphism (Kerrick and Caldeira, 1998; Kerrick, 2001; Evans et al., 2008; Groppo et al., 2017; Rolfo et al., 2017), contact metamorphism (Aarnes et al., 2010; Svensen and Jamtveit, 2010), biogenic decay and even breakdown of kerogen (Schoell, 1983; Clayton et al., 1990; Wycherley et al., 1999). These studies have emphasised the critical importance of metamorphic processes within collision orogenic environments in producing CO_2, reshaping our understanding of volatile dynamics in orogenic systems, by involving decarbonation reactions within carbonate (dolomitic, magnesitic) rocks and carbonate-bearing pelitic sediments/marls under conditions of prograde metamorphism ($T > 150$ °C, the limit between diagenesis and metamorphism). For instance, the interaction of dolomite with quartz at relatively low temperatures ($T < 500$ °C) can produce talc and calcite while releasing CO_2. Metamorphism of the protoliths proceeds with the increase of temperature and pressure conditions to further decarbonation, devolatilization reactions releasing CO_2 and H_2O (Bucher and Frey, 2002; Groppo et al., 2017; Groppo et al., 2020; Tamang et al., 2024). These metamorphic reactions are now recognised as a significant source of CO_2 emissions in collision orogens (Kerrick and Caldeira, 1999; Barry et al., 2013; Skelton, 2013; Groppo et al., 2017, 2020; Rolfo et al., 2017; Tamang et al., 2024).

It has long been believed that collision orogenic areas represent mainly a sink for CO_2 due to chemical weathering reactions that consume CO_2 and contribute to its drawdown from the atmosphere, also having a strong paleoclimatic influence (Raymo et al., 1988). However, recent studies indicate that the fluxes of metamorphic/orogenic CO_2, even though their quantification is challenging, surpass the influence of weathering processes and the drawdown of CO_2 (Skelton, 2013; Zhang et al., 2024). This imbalance highlights those metamorphic reactions, that may occur on millennial timescales contribute substantially to the global CO_2 budget and influence the shaping of the Earth's atmospheric evolution (Becker et al., 2008; Evans et al., 2008; Skelton, 2013; Hilton and West, 2020; Clift et al., 2024; Pradhan and Sen, 2024).

According to Polyak et al. (2018) and Vaselli et al. (2002), the CO_2 emissions in the Ukrainian and Romanian segments of the Carpathians originate from both mantle processes and the thermal decomposition of carbonates linked to magmatic activity. The crustal sources of gases could only be understood through the lithological and mineralogical characteristics, as well as the deposition and burial history of the Carpathians. The flysch nappes represent heterogeneous sequences, primarily composed of sandy-shaly deposits, containing carbonates and marls (Săndulescu, 1984; Mason et al., 1996; Melinte-Dobrinescu and Jipa, 2007; Briceag et al., 2009; Solcanu, 2015; Schmid et al., 2020). Beneath the flysch nappes, the Danubian metamorphic basement contains a sedimentary cover consisting of continental to shallow-water lacustrine Permian clasts, Lower Triassic clasts, Middle to Upper Triassic carbonates, Lower to Middle Jurassic succession of clasts, Middle Jurassic to Early Cretaceous carbonates, and locally Late Cretaceous fine-grained sediments (Schmid et al., 2020; Krstekanić et al., 2022).

Given the average geothermal gradient of 20-25 °C/km for the Romanian segment of the Carpathian nappe systems and 70 °C/km for Ciomadul (Băile Tușnad) (Demetrescu and Andreescu, 1994), at a depth of 10 km (~ 3 kbar) we can predict a low-temperature scenario of around 200 °C in the flysch areas and a high-temperature scenario of 700 °C near the Ciomadul volcano. Under these temperature and pressure conditions, various metamorphic reactions occur, leading to the release of CO_2 (Bucher and Frey, 2002). We model the CO_2 production in the Carpathians based on the available petrographic data (Săndulescu, 1984; Melinte-Dobrinescu and Jipa, 2007; Solcanu, 2015).

Two models were developed using the Domino/Theriak code (De Capitani and Petrakakis, 2010) under physical conditions of P = 2000–4000 bar and T = 200–500 °C, with excess water (Fig. 8). The thick lines in the figures of both models represent the primary reactions, while the thin lines show the partial pressure of the CO_2 in the CO_2-H_2O solution.

In the first scenario, the reactions involve simple siliceous carbonates, in which the protolith consists of calcite-dolomite and quartz (20Cc + 10Do + 5Qz molar). These minerals react to form talc (Tc) or tremolite (Tr), depending mainly on the temperature, while releasing CO_2, e.g.

$$3\,Do + 4\,Qz + H_2O = Tc + 3\,Cc + 3\,CO_2$$

$$Tc + 2\,Do + 4\,Qz = Tr + 2\,Cc + 2\,CO_2$$

In the second case, the more reliable protolith model for normal marls contains kaolinite as the most common clay mineral beyond Cc (calcite), Do (dolomite) and Qz (quartz) (20Cc + 10Do + 5Qz + 5Kln molar). The corresponding CMASH (Ca-Mg-Al-Si-H) system allows Ca—Al silicates to form as products of subsequent metamorphic reactions. The appearance of all essential newly forming minerals (chlorite, margarite, anorthite and hornblende) coincides with CO_2 release. Both simplified models demonstrate that the release of CO_2 increases proportionally with rising temperatures.

The observations in Romania correspond with those proposed by Oszczypko et al. (2018) for the Polish segment of the Carpathians. It has been suggested that the CO_2 in the Polish segment, specifically in the Magura nappe near the Krynica, Wysowa and Muszyna area is generated through metamorphic processes occurring at the basal part of the nappe system, which is underlain by the Mesozoic-Paleozoic platform. The geothermal gradient of 29 °C/km in this area leads to a temperature of ~580 °C at a depth of 20 km with pressure conditions of 5.5–6 kbar. Such conditions are favourable to develop subsequent metamorphic zones, where dehydration and decarbonation processes may occur at temperatures above ~190 °C, leading to the formation of minerals like talc. In Krynica the metamorphic reactions can take place at temperatures of 240-300 °C at a depth of about 10 km (Figs. 4, 5, 7). Additionally, the presence of the "Zuber" type of waters with particular chemical and isotopic compositions (with extremely enriched $\delta^{18}O_{H2O}$

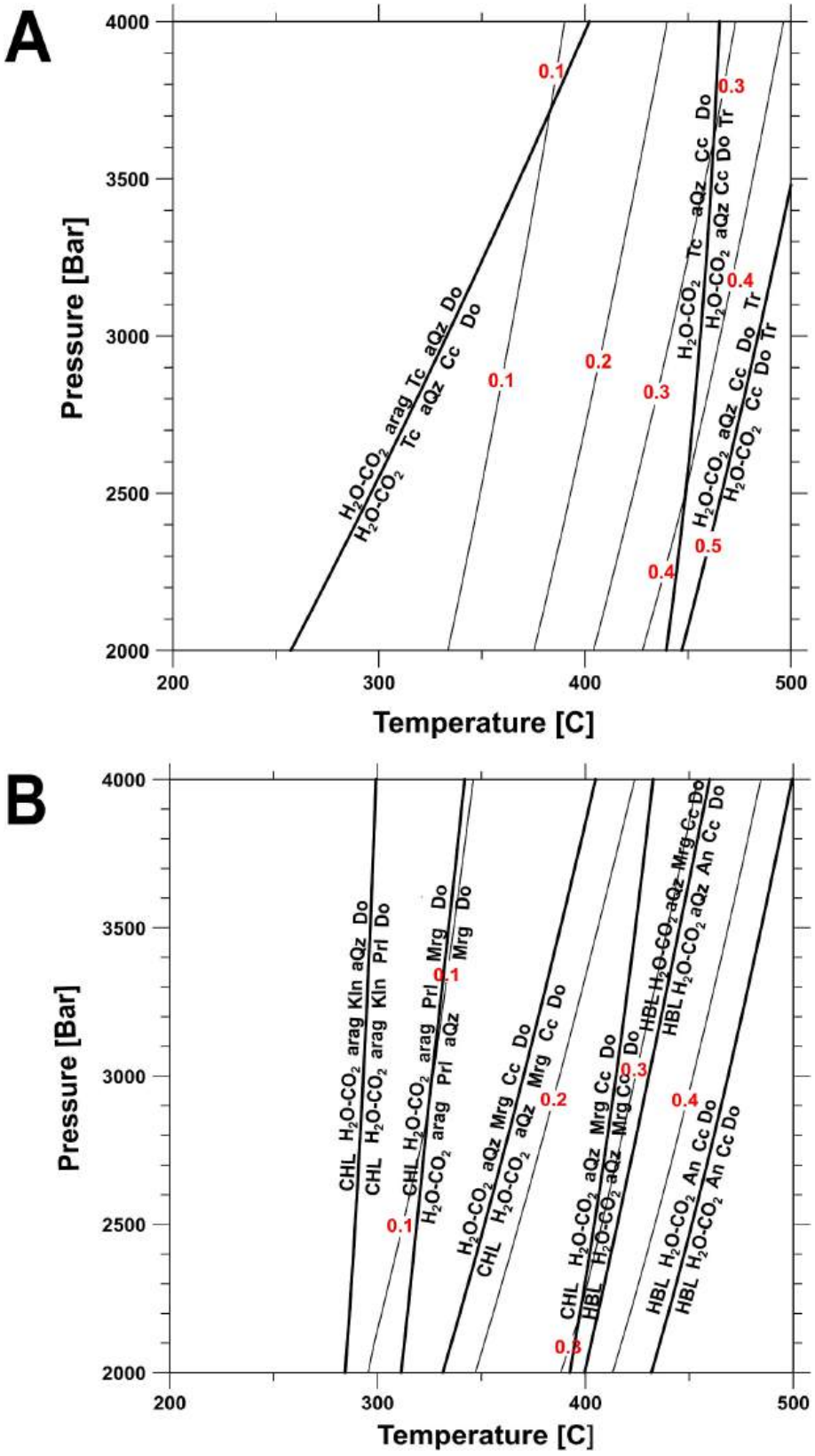

Fig. 8. Metamorphic processes generating CO_2 fluids computed by the Domino/Theriak code (De Capitani and Petrakakis, 2010) under physical conditions of P = 2000–4000 bar and T = 200–500 °C, with excess water. The thick lines in the figures of both models represent the primary reactions, while the thin lines show the partial pressure of the CO_2 in the CO_2-H_2O solution. Mineral abbreviations as follows: A. Cc-calcite, Do-dolomite, Tc-talc, arag-aragonite, aQz-alpha quartz, Tr-tremolite, B. Marl and kaolinite protolith Kln-kaolinite, Chl-chlorite, Prl-pyrophyllite, Mrg-margarite, Hbl-hornblende, An-anorthite minerals.

V-SMOW ratios up to positive values), noted as "dehydration or diagenetic waters", serves as further evidence for these processes (Oszczypko and Zuber, 2002). Similar dehydration waters have also been identified in the Romanian segment of the Carpathians (Kis et al., 2020).

The metamorphic production of CO_2 within the Carpathians corresponds with the presence of crustal-derived He in CO_2-dominated gases, as also supported by geophysical evidence of an electrical conductivity anomaly at approximately 10 km depth along the collision suture zones of the Western and Eastern Carpathians (Pinna et al., 1992; Stănică and Stănică, 1993; Żytko, 1997), which aligns with the CO_2-rich zones identified in the Polish, Ukrainian and Romanian segments. This phenomenon was attributed to metamorphic devolatilization processes (Rokityansky and Ingerov, 1999; Neska, 2016) Additional evidence for the metamorphism of marly limestones under depth conditions exceeding 5 km is provided by crustal xenoliths discovered within the Neogene volcanic products of eastern Slovakia (Marcinčáková and Košuth, 2015). Furthermore, contact-metamorphic processes at the interface between volcanic rocks and flysch sequences may also contribute to fluid generation and cannot be ruled out.

4.4. $\delta^{13}C_{CO2}$ vs. $CO_2/^3He$ relationships

The amount of CO_2 and its carbon isotopic composition ($\delta^{13}C_{CO2}$) in geogenic fluids can be influenced by secondary processes at shallow levels (dissolution, precipitation, mixing) that complicate the distinction between different CO_2 sources simply by using mixing between the different potential deep sources (e.g. Sano and Marty, 1995). In this context, the C—He systematics are helpful in evaluating enrichments or depletions relative to their sources (e.g., the mantle-like signature) and how the carbon isotopic signature of CO_2 is modified by these processes (Holland and Gilfillan, 2013; Barry et al., 2020; Randazzo et al., 2022, 2025). Mixing is a first-order process that could affect the amounts and isotopic composition of the different gaseous species emitted in the atmosphere. In fact, during the transfer through the crust, mantle-derived gases can mix with crustal fluids originating from different sources, with the resulting fluids that take memory of this process (Randazzo et al., 2021, 2025).

Sano and Marty (1995) proposed an approach for the magmatic systems based on three-component mixing equations, which allows for the deconvolution of mantle and crustal carbon fractions due to their distinct $CO_2/^3He$ ratios and $\delta^{13}C$ values (Fig. 9). Usually, values higher than mantle $CO_2/^3He$ ratios can be interpreted as due to the addition of crustal-derived CO_2, produced by decarbonation reactions and/or biological processes, as suggested from previous large-scale geochemical investigations (e.g. Sano and Marty, 1995; Sherwood Lollar et al., 1997). Here, we assume a $CO_2/^3He$ ratio of 2–7 × 10^9 and $\delta^{13}C_{CO2} = -3.5‰$ as representative of the mantle below the Carpathians (Bräuer et al., 2016; Rizzo et al., 2018) a value slightly different from the typical MORB

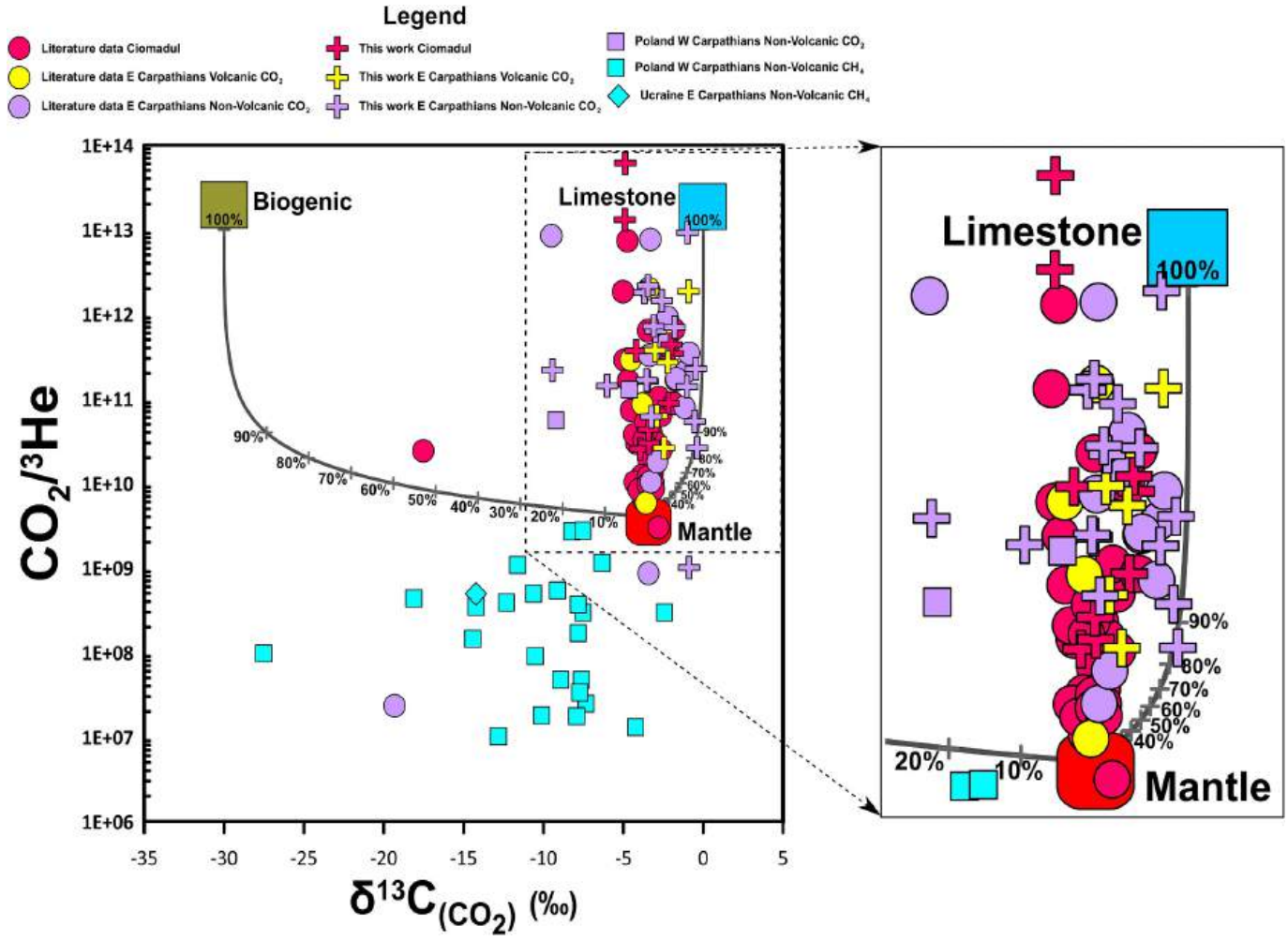

Fig. 9. $CO_2/^3He$ vs. ^{13}C-CO_2 plot of the investigated gas emissions. Lines show the theoretical binary mixing between a mantle end member ($CO_2/^3He$ = 2–7 × 10^9 and $\delta^{13}C$ = –3.5‰, Bräuer et al., 2016; Rizzo et al., 2018) and the crustal end members represented by marine limestones ($CO_2/^3He$ = 10^{13}, $\delta^{13}C$ = 0‰) and organic sediments ($CO_2/^3He$ = 1 × 10^{13}, $\delta^{13}C$ = –30‰) (Sano and Marty, 1995). Curves labelled as 100–10% represent binary mixing trajectories between mantle and the crustal end-members, allowing the crustal and mantle contributions to be estimated directly from the position of each sample. Symbols as in Fig. 2.

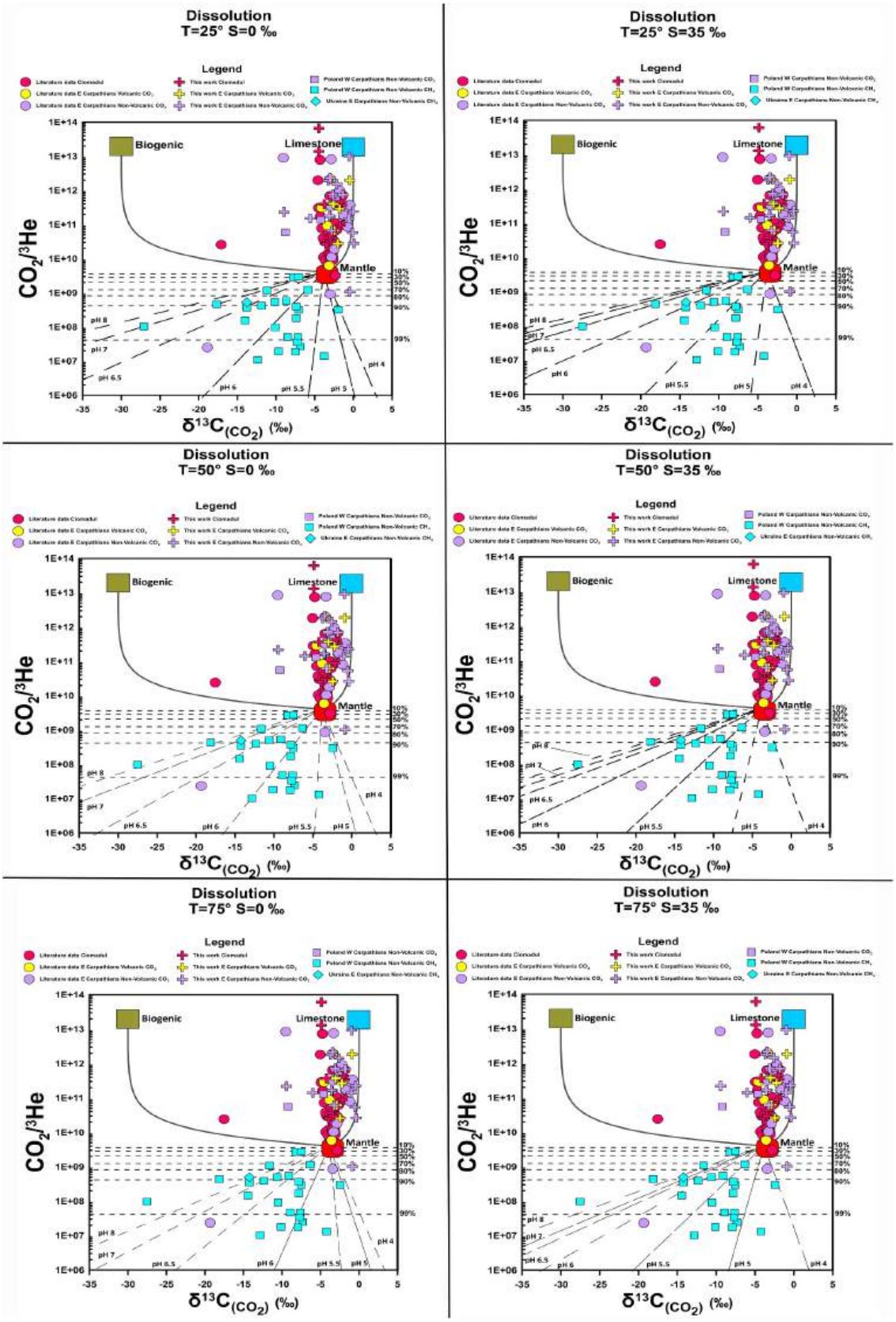

Fig. 10. $CO_2/^3He$ vs. ^{13}C-CO_2 of the investigated gas emissions. Lines show the theoretical binary mixing between a mantle end member (Bräuer et al., 2016; Rizzo et al., 2018) and crustal end members represented by marine limestones and organic sediments (Sano and Marty, 1995). Dashed lines represent the predicted model for a Rayleigh-type carbonate dissolution at different temperatures (25 °C, 50 °C and 75 °C) and salinity (S = 0‰ or S = 35‰), with the fractions (%) of CO_2 lost from the gas phase due to dissolution into groundwater. Equations from Buttitta et al. (2023), Gilfillan et al. (2009) and Randazzo et al. (2025). Symbols as in Fig. 2.

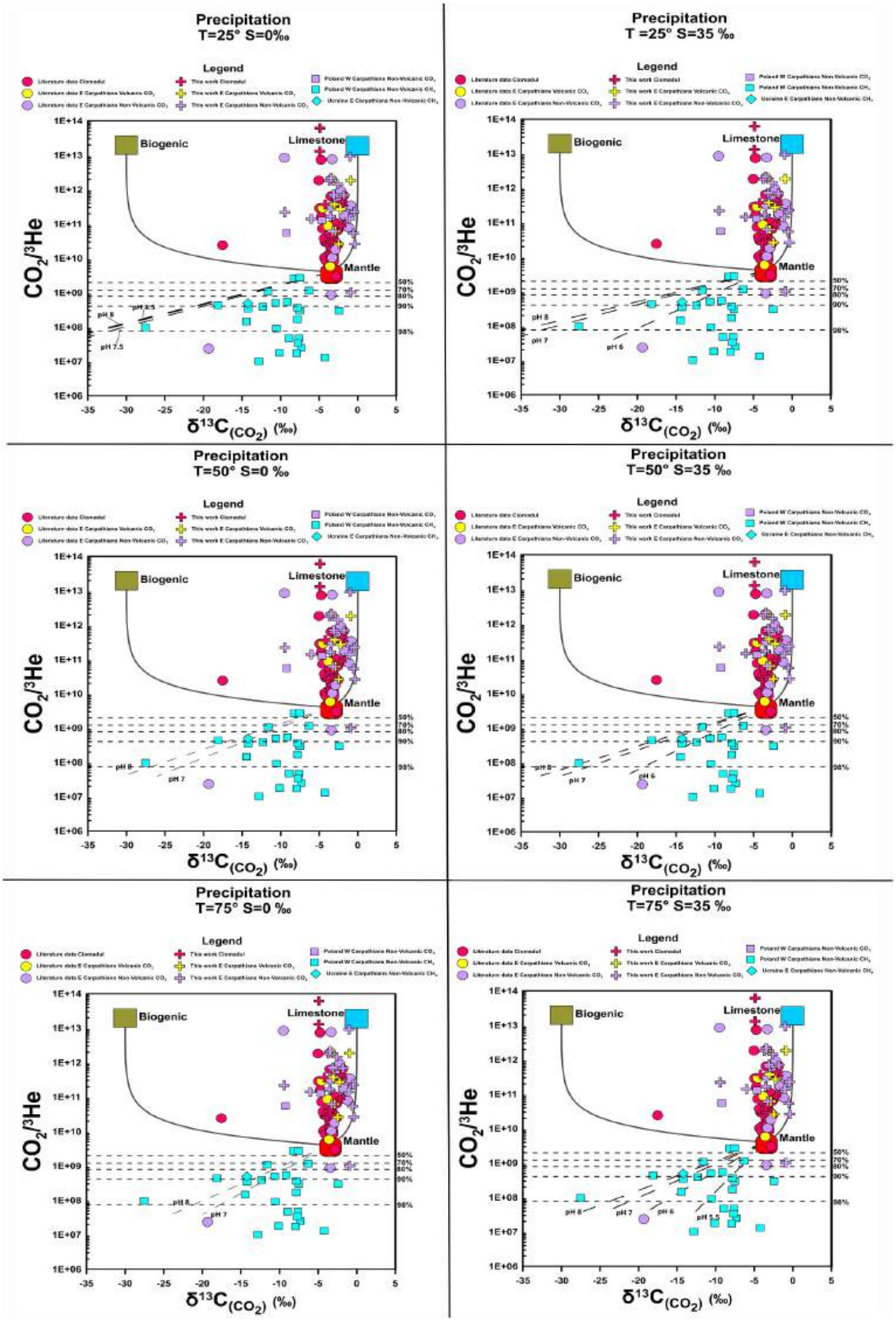

Fig. 11. $CO_2/^3He$ vs. ^{13}C-CO_2 of the investigated gas emissions. Lines show the theoretical mixing between a mantle end member (Bräuer et al., 2016; Rizzo et al., 2018) and crustal end members represented by marine limestones and organic sediments (Sano and Marty, 1995). Dashed lines represent the predicted trends for carbonate precipitation at different temperatures (25 °C, 50 °C and 75 °C) and salinity (S = 0‰ or S = 35‰), with the fractions of CO_2 removed from the fluid phase due to precipitation. Equations from Buttitta et al., (2023), Gilfillan et al. (2009) and Randazzo et al. (2025). Symbols as in Fig. 2.

mantle (e.g., $CO_2/^3He$ = 1.5-2 × 10^9, Marty et al., 2020) because, in continental setting, the lithospheric mantle often brings record of heterogeneities caused by deep processes such as subduction and/or metasomatism that can lead to carbon enrichment or, in general, a modification of its chemical composition (e.g., Rizzo et al., 2018).

We find that the $CO_2/^3He$ ratios in the sample dataset are either higher (up to 6.1× 10^{13}) or lower (as low as 3.1 × 10^7) than the inferred mantle range (Fig. 9). In addition to the mantle end member, we assume two crustal-sourced end-members with $CO_2/^3He$ ratio of 10^{13} and $\delta^{13}C$ of 0‰, −30‰ for limestone and biogenic, respectively (Sano and Marty, 1995). With these, we can solve the contribution of the different CO_2 sources ($CO_2/^3He$ vs $\delta^{13}C_{CO2}$ diagrams, Figs. 9, 10 and 11). The data distribution indicates a heterogeneous carbon source, primarily reflecting a mixture between mantle and crustal-derived (limestone end member) gases, along with a low contribution from biogenic sources (Fig. 9). By assuming mixing processes in controlling the CO2 and He in the Carpathian natural fluids, the $CO_2/^3He$ vs $\delta^{13}C_{CO2}$ relationship (Fig. 9) shows that biogenic CO_2 contribution is minimal, the majority of samples align along the mantle-limestone mixing line, where the percentage curves quantify the proportion of limestone-derived CO_2 relative to the mantle component. Volcanic samples from Ciomadul (red symbols, Fig. 9) cluster predominantly within the intermediate to mantle-like fields of 40-70% limestone range (corresponding 30-60 mantle %, respectively), indicating that the crustal limestone source is a significant contributor even in magmatically influenced systems. It is worth noting that $\delta^{13}C_{CO2}$ values closer to those of mantle-derived carbon coincide with the highest He isotopic ratios observed in volcanic areas ($\delta^{13}C_{CO2}$ at Ciomadul; −4.5 to −4.7‰ V-PDB; Vaselli et al., 2002; Kis et al., 2019).

Non-volcanic samples from the Eastern Carpathians (purple symbols, Fig. 9) plot even closer to the limestone end-member, corresponding to a 80-95% limestone-derived CO_2, consistent with shallow crustal CO_2 degassing unrelated to magmatism.

Carbon isotope composition and $CO_2/^3He$ ratios are likewise severely modified by secondary processes during gas–water interactions, as suggested by samples plotting below the mantle $CO_2/^3He$ ratios. Such values cannot be explained by binary mixing, instead suggest secondary processes. CO_2 can be retained either in form of carbonate minerals (mineral trapping) or dissolved in solution (solubility trapping) (e.g., Gilfillan et al., 2009; Randazzo et al., 2022) leading to decreased $CO_2/^3He$ ratios and more negative $\delta^{13}C$ in the residual gases.

Recent studies about CO_2-rich mineral water springs scattered across the Carpathians (Ciężkowski et al., 2010; Bodiš et al., 2017; Italiano et al., 2017) indicate the dissolution of the rising CO_2 in groundwater systems as a regional phenomenon impacting the fluids; while evidence for carbonate precipitation reactions, forming calcite and dawsonite minerals, linked to CO_2 emissions include the observations from the Magura nappe in the Polish Carpathians (Dulinski et al., 1995; Gradziński et al., 2012) and in Romanian segments (Italiano et al., 2017; Cseresznyés et al., 2024).

To model CO_2 dissolution and carbonate precipitation processes in the shallow crustal layers of the study area, we consider two end member conditions as representative of the possible scenarios at depth: 1) a low salinity (S) water reservoir (S = 0‰), and 2) a salt-rich water reservoir (S = 35‰). Assuming a mantle-like composition typical of the SCLM for the initial gas ($CO_2/^3He$ = 2–7 × 10^9, $\delta^{13}C$ = −3.5‰; (Bräuer et al., 2016; Rizzo et al., 2018; Marty et al., 2020) we model the progressive variation of the $CO_2/^3He$ ratio and $\delta^{13}C_{CO2}$ in the residual gas as an open-system (Rayleigh type) (for methods and equations see Randazzo et al. (2025) and reference therein,) under different temperature (25 °C–75 °C) and pH (4–8) conditions (Figs. 10 and 11 - dissolution and precipitation models for different temperature and salinity with the fractions of CO_2 lost from the gas phase due to dissolution into groundwater or fraction of CO_2 removed from the fluid phase due to precipitation). Our model of partial CO_2 dissolution in water at pH between 4 and 8, T = 25C° and S = 0‰ fits the data that are characterized by $CO_2/^3He$ ratios lower than the mantle values, highlighting that part of the gases emitted in the studied region can be representative of different degrees of CO_2 loss by dissolution in water (up to 90%). Therefore, the water-gas interactions can reasonably explain the $CO_2/^3He$ vs. $\delta^{13}C$ relationships at the regional scale over a large range of T (25–75 °C), S (0–35‰), and pH (4 to 8). On the other hand, the precipitation modelled curves only partially fit the composition of the natural fluids (Fig. 11), but even though a significant number of data points are not consistent with carbonate precipitation, we cannot rule out the possibility that this process locally affects the chemical and isotopic composition ($\delta^{13}C$) of gases in the Carpathians. It is important to emphasize that here we consider the case of the SCLM ($CO_2/^3He$ = 2–7 × 10^9, $\delta^{13}C$ = −3.5‰; Bräuer et al., 2016; Rizzo et al., 2018; Marty et al., 2020) as the mantle end-member, which can be modified by gas-water interactions under different conditions (25 °C < T < 100 °C, 5 < pH < 8 and 0‰ < S < 35‰). These processes should be evaluated independently and constrained with isotopic data from waters and rocks, enabling a more precise characterization of the secondary processes affecting these degassing systems.

4.5. Degassing and flux of mantle-derived fluids

The different sectors of the Carpathians exhibit a complex geochemical and geodynamic framework, with mantle-derived volatiles providing evidence of deep mantle contributions. A quantitative He flux estimate can provide insights into the transfer of volatiles through the crust (e.g., Randazzo et al., 2025). During the transfer of mantle-derived fluids through the crust, the addition of crustal radiogenic ^4He decreases the mantle He isotopic ratio. Using the approach proposed by (O'Nions and Oxburgh, 1988), it is possible to assess the flux of mantle-derived He. This method is based on the progressive addition of a crustal He component under steady-state degassing (O'Nions and Oxburgh, 1988), that dilutes the mantle He component, resulting in a decrease of the He isotopic signature from the typical SCLM -derived value (6.1 Ra ±0.9; Gautheron and Moreira, 2002) to the radiogenic signature (0.02 Ra; Ballentine and Burnard, 2002). The limitation of this approach consists in the fact that only the mantle derived He and CO_2 flux can be quantified, whereas constraining the crustal CO_2 fluxes require direct CO_2-flux measurements at each site together with groundwater analyses to determine the dissolved fraction, so that total emissions can be established and the crustal component derived as the difference between the total and the mantle-derived flux inferrer from He systematics.

Considering the complete dataset available (this work +literature data) we compute the mantle He flux by using an average R/R_a value for each area (i.e., the Ciomadul, Eastern Carpathians volcanic and Eastern Carpathians non-volcanic). Our estimates of the mantle He fluxes range from 10^{10} to 10^{12} atoms m^{-2} s^{-1} for the Ciomadul and for the Eastern Carpathians volcanic area, meaning a He flux of 1.59 × 10^{-13} and 8.64 × 10^{-14} g m^{-2} s^{-1} respectively, while for the Eastern Carpathians non-volcanic area the values range from 10^9 to 10^{11} atoms m^{-2} s^{-1}, meaning a He flux of 3.46 × 10^{-14} g m^{-2} s^{-1} (Table 2-Supplementary Material, Fig. 12). These values are up to three orders of magnitude higher than those typically observed in stable continental areas (~10^7 atoms m^{-2} s^{-1}; O'Nions and Oxburgh, 1988). We then calculated the mantle-derived ^3He flux (Fig. 12 and Table 2-data-Supplementary Material, with flux values and data that we used to compute the fluxes). These values range from 4.94 × 10^{-19} to 10^{-17} g m^{-2} s^{-1} for Ciomadul volcano, 1.69 × 10^{-19} to 10^{-17} g m^{-2} s^{-1} for the Eastern Carpathians volcanic area, and 3.22 × 10^{-20} to 10^{-18} g m^{-2} s^{-1} for the Eastern Carpathians non-volcanic area (Table 2-Supplementary Material).

Following Randazzo et al. (2025) we can use the combination of available $CO_2/^3He$ ratios, R/R_a values, and mantle He fluxes to estimate mantle CO_2 fluxes. Our average values are 1.4 × 10^6 g km^{-2} y^{-1} for the Ciomadul volcanic area, 1.18 × 10^8 g km^{-2} y^{-1} for the volcanic area of the Eastern Carpathians and 5.1 × 10^7 g km^{-2} y^{-1} for the non-volcanic area of the Eastern Carpathians. The total mantle-derived carbon flux estimated

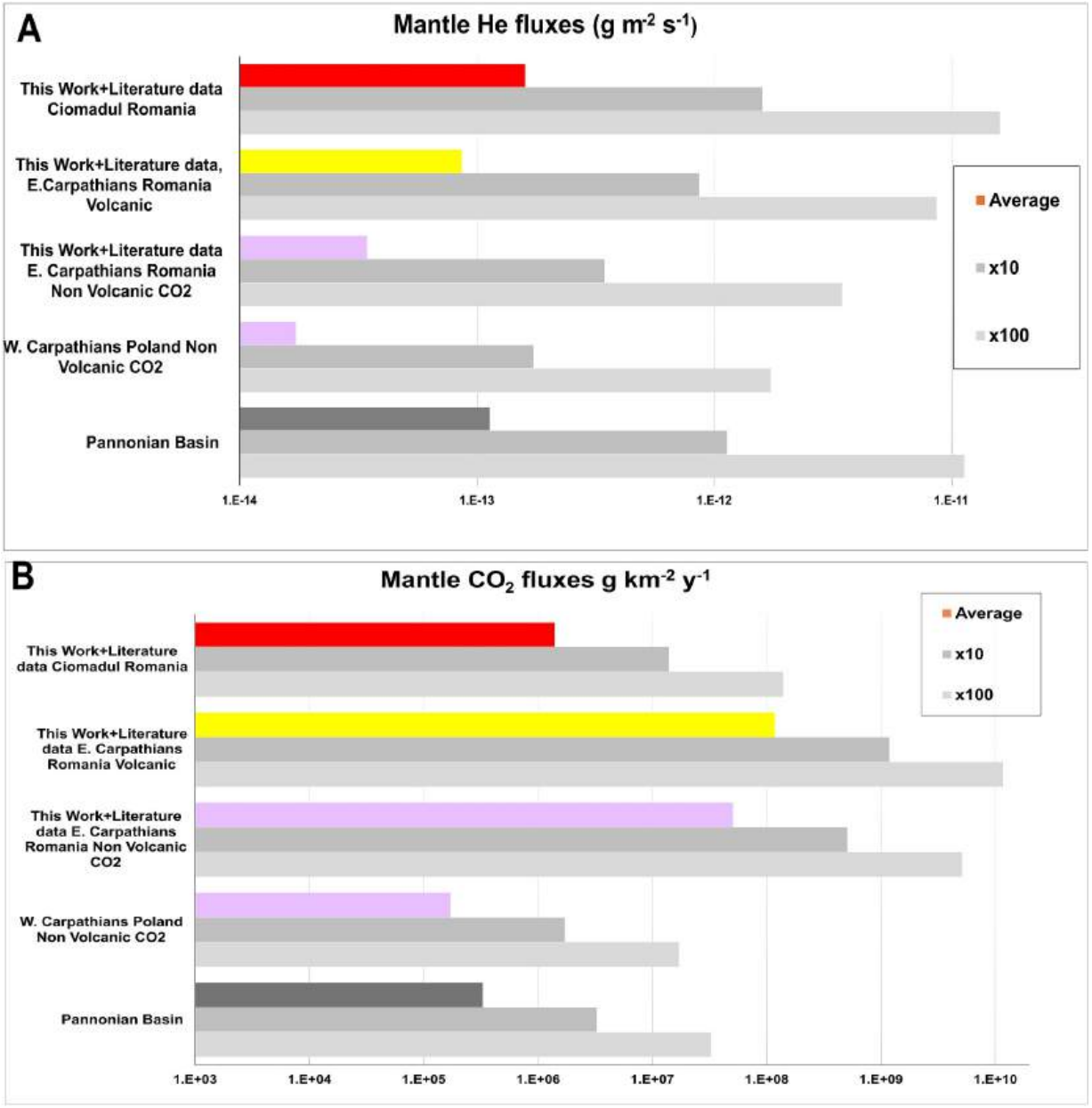

Fig. 12. A. Mantle He fluxes in g m^{-2} s^{-1}estimated for each region (data in Table 2, Supplementary Material): red representing This Work and Literature data from the Ciomadul volcanic area; yellow, representing This Work and Literature data from the Eastern Carpathians volcanic area; light purple, representing This Work and Literature data for the Eastern Carpathians, non-volcanic, CO_2 dominated area; light purple representing available data from the Polish sector of the Western Carpathians; and dark grey for the Pannonian Basin area for reference (after Randazzo et al., 2025). B. Mantle CO_2 fluxes in g km^{-2} y^{-1} estimate for each region and the Pannonian Basin for reference (after Randazzo et al., 2025); symbols as in the A figure. (For interpretation of the references to colour in this figure legend, the reader is referred to the web version of this article.)

for the Carpathians, considering both volcanic and non-volcanic areas, calculated to an area of 100,000 km^2 is 4.66 Mt. $year^{-1}$ (Fig. 13). This average for the Carpathians is lower than that of volcanic arcs and continental rift systems, that exhibit one order of magnitude higher values, but similar to other collision zones worldwide (Fig. 13).

The Carpathians represent a major orogenic system previously missing from global CO_2 inventories, yet, their estimated mantle-carbon fluxes are comparable to those of arc volcanoes and continental rifts. This shows that global natural carbon fluxes still remain insufficiently constrained, especially for collisional tectonic settings, as noted in our work and in recent studies. Many segments of the Tethyan belt still lack CO_2 flux estimates, further emphasizing the need for broader regional assessments. In this context, the Carpathians provide an important piece to the larger puzzle of the natural carbon emissions in such tectonic environments).

4.6. *Pathways and migration channels*

Degassing of CO_2 in the Carpathians occurs only at specific locations, possibly linked to pathways and migrations channels provided by folded nappe structures of the Carpathians and related fault-systems, as seen from the cross-sections in Figs. 4, 5 and 7. The thrusted and folded build-up of the flysch nappes together with some deep-seated faults, e.g., the Transcarpathian Fault (Nakapelyukh et al., 2018), Krynicza Fault (Oszczypko and Zuchiewicz, 2007), Dragoș-Vodă Fault, the Olt-River fault-zone (Bala et al., 2015), may have created favourable channels

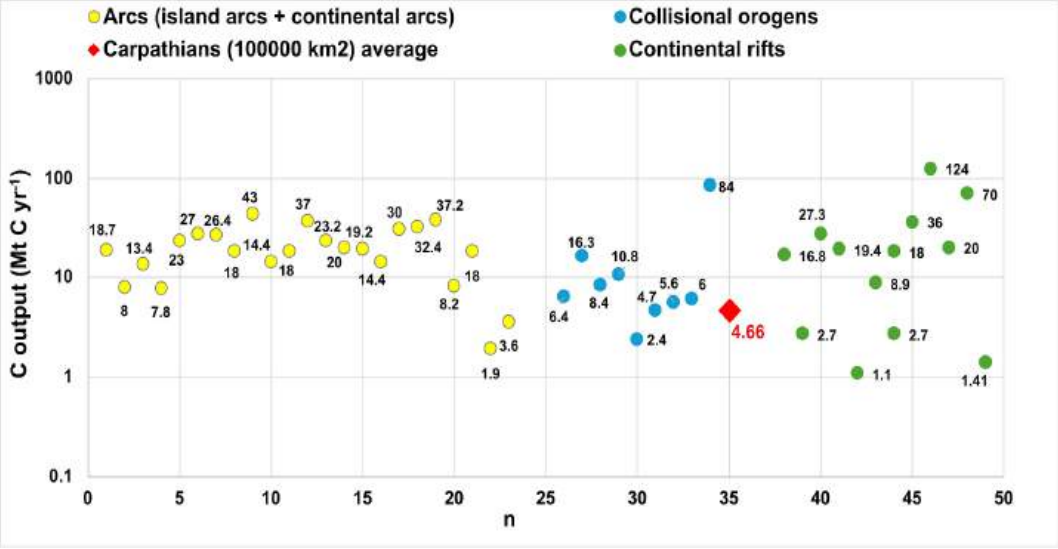

Fig. 13. Diagram showing carbon outfluxes (Mt C yr $^{-1}$) for different tectonic settings: volcanic arcs (yellow dots), collisional orogens (blue dots), continental rifts (green dots), data derived from the compilation of Zhang et al., 2024 (including the work of: Marty et al., 1989; Peacock, 1990; Allard, 1992; Varekamp et al., 1992; Bebout, 1996; Sano and Williams, 1996; Marty and Tolstikhin, 1998; Sleep and Zahnle, 2001; Hilton et al., 2002; Chiodini et al., 2004; Coltice et al., 2004; Becker et al., 2008; Evans et al., 2008; Fischer, 2008; Newell et al., 2008; Dasgupta and Hirschmann, 2010; Shinohara, 2013; Kelemen and Manning, 2015; Lee et al., 2016; Brune et al., 2017; Hunt et al., 2017; Aiuppa et al., 2019; Kagoshima et al., 2015; Fischer et al., 2019; Plank and Manning, 2019; Ratschbacher et al., 2019; Wong et al., 2019; Stewart et al., 2019; Muirhead et al., 2020; Bekaert et al., 2021; Guo et al., 2021; Zhao et al., 2022; Hirschmann, 2023; Zhang et al., 2024; Randazzo et al., 2025) and red diamond for the Carpathians. Values for the Carpathians considering a total area 100,000 km^2 and summing all contributions from volcanic and non-volcanic areas. (For interpretation of the references to colour in this figure legend, the reader is referred to the web version of this article.)

for fluid flow. These areas could be characterized with increased porosity-permeability conditions, that provide rapid fluid flow (Kleine et al., 2016). The presence of immiscible fluids as modelled by Groppo et al. (2022) enhances CO_2 release through permeable structures of the crust. We propose an open system where CO_2 migration is fast and continuous, driven by migration channels that are likely influenced by the tectonic features of the Carpathians. CO_2 degassing and elevated concentration (>90%) was measured at certain nappe borders and faults (Figs. 4–7), suggesting the tight spatial relationship between degassing localities and structural characteristics. CO_2 degassing along the Carpathian range suggest a firm tectonic control over fluid movement.

The area of Ciomadul stands out for having the highest mantle contribution in their gas emissions alongside the highest heat flow within the Carpathians. The elevated mantle contribution at the Ciomadul dome field can be attributed to factors such as the permeability of the young volcanic conduits and faults, that can facilitate the upwelling of mantle-derived fluids through the magmatic system. A well pronounced lateral variation of He isotopic ratios (R/R_a) is evident across the Carpathians, marked by elevated R/R_a values near the volcanic regions and a systematic decrease moving away from these areas toward the flysch belt and basin regions, eventually reaching crustal end-member values.

The lateral transport of mantle-derived fluids is facilitated by the folded-thrusted sheet structure of the flysch nappes and related post-thrust fault systems that characterize the area (Oszczypko and Zuchiewicz, 2007; Bala et al., 2015; Nakapelyukh et al., 2018; Polyak et al., 2018).

5. Summary and conclusions

Understanding degassing, geochemical characteristics, and sources of deep fluids is a global concern. Much like other extensively studied orogenic systems worldwide, such as the Apennines (Chiodini et al., 1999), the Alps (Marty et al., 1992), the Himalayas (Kerrick and Caldeira, 1998; Evans et al., 2008; Groppo et al., 2017; Zhang et al., 2017b; Klemperer et al., 2022), the Carpathians is also a significant degassing area, as resulted from the abundance of available sites and related data.

CO_2 emissions in the Carpathians are concentrated in the inner arc, mainly linked to Neogene–Quaternary volcanic range and carbonate-rich flysch nappes, particularly at the extensively tectonized suture zones such as the Pieniny Klippen Belt–Magura and Ceahlău–nappes. These lithological and structural settings together with their carbonate-rich basements provide favourable conditions for fluid release, contrasting with CH_4 emissions of thermogenic origin in the Outer Flysch belt. While hydrocarbons have been extensively studied, the mechanisms driving CO_2 degassing remain less constrained. To resolve these uncertainties, we conducted a regional investigation combining chemical and isotopic analyses with lithostratigraphic and pressure–temperature constraints, offering new insights into the geological and geochemical processes controlling CO_2 emissions across the Carpathians. Combining our recent data with previous investigations, we computed a dataset that presents the first regional map of free CO_2 and CH_4 degassing sites in the Western and Eastern Carpathians, along with the first comprehensive geochemical investigation of gases in the region.

The spatial distribution of He isotopes across the Carpathian arc indicates a variable contribution of mantle- and crustal-derived volatiles, with significant mixing between the two. Elevated R/R_a values mark regions where mantle He is efficiently transported to the surface, often associated with magmatic processes. In the Carpathians, mantle-derived components ($R/R_a > 2$) are most prominent near long dormant volcanic regions, particularly at Ciomadul, where anomalously high values reflect the persistence of deep magmatic reservoirs and active degassing long after volcanism ceased. CO_2 plays a central role in transporting mantle He, and its widespread degassing across both volcanic and non-volcanic areas highlights the complex interplay of mantle input, crustal fluid generation and volatile-migration pathways.

Radiogenic He, carried mainly by CO_2 and CH_4, dominates in non-volcanic regions such as the thick flysch belt and metamorphic sequences, where CO_2 and CH_4-rich gases show crustal signatures. CO_2 emissions are largely crustal in origin, produced through metamorphic decarbonation reactions of marls and carbonates under prograde metamorphic conditions, resembling trends in other orogenic belts like

the Alps, Caucasus and Himalayas. Thermodynamic modelling supports that regional metamorphism and burial-related processes at depths of 5–20 km that generate significant CO_2, consistent with geophysical anomalies and geochemical evidence across the Carpathians. These findings highlight the importance of metamorphic devolatilization as a major source of crustal volatiles in collisional orogens, defined as "orogenic CO_2 degassing," contributing substantially to regional gas emissions and the global carbon cycle emphasised also by recent global surveys (Zhang et al., 2024). The Carpathians share these traits, and with new geochemical data providing the first regional mapping of CO_2 and CH_4 emissions, reflecting local lithological and tectonic controls.

CO_2 degassing in the Carpathians occurs at structurally controlled sites, closely linked to folded nappe systems and major fault zones such as the Transcarpathian, Krynicza, Dragoș-Vodă, and Olt-River faults. These tectonic features enhance porosity and permeability, creating preferential pathways for rapid fluid migration. Field observations show CO_2 concentrations exceeding 90% along nappe borders and fault zones, highlighting the spatial correlation between degassing localities and structural architecture. At Ciomadul, the highest mantle contribution coincides with young volcanic conduits and high heat flow, enabling efficient ascent of mantle-derived volatiles. Helium isotope ratios (R/R_a) display systematic lateral variations, with elevated mantle signatures near volcanic centres and progressive decrease toward the flysch belt and basin regions. We propose an open system where tectonic structures and post-thrust faults facilitate both vertical and lateral transport of mantle-derived fluids across the Carpathians.

The combined use of $\delta^{13}C$ of CO_2 and $CO_2/^3He$ ratios provides insights into the origin and evolution of geogenic CO_2 in the Carpathians. Our data reveal heterogeneous carbon sources, with most samples representing mixtures of mantle-derived and crustal (limestone) end-members, and only minor biogenic contributions. $\delta^{13}C$ values close to mantle compositions coincide with high $^3He/^4He$ ratios in volcanic areas, whereas higher $CO_2/^3He$ ratios indicate additional crustal inputs. Secondary processes, particularly CO_2 dissolution in groundwater and carbonate precipitation, further modify both isotopic signatures and C—He systematics.

The Carpathians display a heterogeneous geochemical framework, with mantle-derived volatiles providing evidence for deep contributions to crustal fluid systems. Using helium isotope systematics and the (O'Nions and Oxburgh, 1988) approach, we estimated mantle He fluxes across different Carpathian sectors.

He fluxes reach 1.59×10^{-13} to 8.64×10^{-14} g m^{-2} s^{-1} in volcanic areas such as Ciomadul and the Eastern Carpathians, up to three orders of magnitude higher than stable continental regions, while non-volcanic areas show lower but still elevated values, with He flux of 3.46×10^{-14} g m^{-2} s^{-1}. Corresponding mantle-derived ^3He fluxes range from 10^{-19} to 10^{-17} g m^{-2} s^{-1} in volcanic zones and are an order of magnitude lower in non-volcanic settings, ranging from 10^{-20} to 10^{-18} g m^{-2} s^{-1}.

Combining He fluxes with $CO_2/^3He$ ratios, we estimated mantle CO_2 fluxes of 1.4×10^6 g km^{-2} y^{-1} for the Ciomadul volcanic area, 1.18×10^8 g km^{-2} y^{-1} for the volcanic area of the Eastern Carpathians and 5.1×10^7 g km^{-2} y^{-1} for the non-volcanic area of the Eastern Carpathians. The total mantle-derived carbon flux estimated for the Carpathians, considering both volcanic and non-volcanic areas, calculated to an area of 100,000 km^2 is 4.66 Mt. year^{-1}, consistent with values reported for other volcanic and tectonically active regions worldwide.

The Carpathians display similarities with the other Tethyan orogenic systems such as the Pyrenees, Alps, Caucasus and Himalayas in both geodynamic evolution and volatile geochemistry. In all these orogens, CO_2 degassing is linked to prograde metamorphism and devolatilization, generating crustal-derived fluids, while mantle/magmatic derived ^3He is related to suture areas, volcanic and extensional domains. The spatial association of degassing with major suture zones, volcanic areas and tectonized nappe systems further emphasizes the similarities, placing the Carpathians in the broader fluid-geochemical pattern of the Tethyan collision orogens.

Declaration of competing interest

The authors declare that they have no known competing financial interests or personal relationships that could have appeared to influence the work reported in this paper.

Acknowledgements

This work was supported by a grant from the Ministry of Research, Innovation and Digitization, CNCS/CCCDI – UEFISCDI, project number TE63/2020. B.M. K also acknowledges funding from the János Bolyai Research Scholarship of the Hungarian Academy of Sciences. Sz.H. acknowledges funding from the Hungarian National Research, Development and Innovation Fund (NKFIH) via the research grant No. K116528 and from the research project of the MTA–HUN-REN CSFK Lendület "Momentum" PannonianVolcano Research Group, supported by the Hungarian Academy of Sciences (grant nr. LP2024-9/2024). A.A acknowledges funding from MUR (PRIN2017LMNLAW and PRIN2022HA8XCS).

We are grateful to the two anonymous reviewers for their helpful comments, which improved the manuscript.

Appendix A. Supplementary data

Supplementary data to this article can be found online at https://doi.org/10.1016/j.earscirev.2026.105528.

Data availability

Data is available at Kis, B. M., Szalay, R., Caracausi, A., Aiuppa, A., Palcsu, L., Orsovszki, J., Grassa, F., Harangi, S., 2025. Location, chemical and isotopic composition of free bubbling gases collected in the Eastern Carpathians, Romania., Version 1.0. EarthChem Repository Interdisciplinary Earth Data Alliance (IEDA). https://doi.org/10.60520/IEDA/114173.

References

Aarnes, I., Svensen, H., Connolly, J.A.D., Podladchikov, Y.Y., 2010. How contact metamorphism can trigger global climate changes: modeling gas generation around igneous sills in sedimentary basins. Geochim. Cosmochim. Acta 74, 7179–7195. https://doi.org/10.1016/j.gca.2010.09.011.

Airinei, Ștefan, Pricăjan, A., 1975. Some geological connections between the mineral carbonic and thermal waters and the post-volcanic manifestations correlated with the deep geological structure of the East Carpathians territory-Romania. Tech. Econ. Stud. E 12, 7–19.

Aiuppa, A., Fischer, T.P., Plank, T., Bani, P., 2019. CO_2 flux emissions from the Earth's most actively degassing volcanoes, 2005–2015. Sci. Rep. 9, 5442. https://doi.org/10.1038/s41598-019-41901-y.

Allard, P., 1992. Global emissions of 3helium by subaerial volcanism. Geophys. Res. Lett. 19, 1479–1481. https://doi.org/10.1029/92GL00974.

Allison, C.M., Roggensach, K., Clarke, A.B., 2021. Highly explosive basaltic eruptions driven CO_2 exsolution. Nat. Comm. 12, 217. https://doi.org/10.1038/s41467-020-20354-2.

Althaus, T., Niedermann, S., Erzinger, J., 1998. Noble gases in Ultramafic Mantle Xenoliths of the Persani Mountains, Transylvanian Basin, Romania. Mineral. Mag. 62A, 43–44. https://doi.org/10.1180/minmag.1998.62a.1.23.

Althaus, T., Niedermann, S., Erzinger, J., 2000. Noble gas studies of fluids and gas exhalations in the East Carpathians. Romania 60, 189–207.

Arzilli, F., Burton, M., La, G., Macpherson, C.G., Van Keken, P.E., Mccann, J., 2023. Decarbonation of subducting carbonate-bearing sediments and basalts of altered oceanic crust: Insights into recycling of CO_2 through volcanic arcs. Earth Planet. Sci. Lett. 602. https://doi.org/10.1016/j.epsl.2022.117945.

Baciu, C., Caracausi, A., Etiope, G., Italiano, F., 2007. Mud volcanoes and methane seeps in Romania: main features and gas flux. Ann. Geophys. 50, 4. https://doi.org/10.4401/ag-4435.

Baciu, C., Ionescu, A., Etiope, G., 2017. Hydrocarbon seeps in Romania: gas origin and release to the atmosphere. Mar. Pet. Geol. 89, 130–143. https://doi.org/10.1016/j.marpetgeo.2017.06.015.

Bala, A., Răileanu, V., Dinu, C., Diaconescu, M., 2015. Crustal seismicity and active fault systems in Romania. Rom. Rep. Phys. 67, 1176–1191.

Ballentine, C.J., Burnard, P.G., 2002. Production, release and transport of noble gases in the continental crust. Rev. Mineral. Geochem. 47, 481–538. https://doi.org/10.2138/rmg.2002.47.12.

Barry, P.H., Hilton, D.R., Fischer, T.P., De Moor, J.M., Mangasini, F., Ramirez, C., 2013. Helium and carbon isotope systematics of cold "mazuku" CO_2 vents and hydrothermal gases and fluids from Rungwe Volcanic Province, southern Tanzania. Chem. Geol. 339, 141–156. https://doi.org/10.1016/j.chemgeo.2012.07.003.

Barry, P.H., Negrete-Aranda, R., Spelz, R.M., Seltzer, A.M., Bekaert, D.V., Virrueta, C., Kulongoski, J.T., 2020. Volatile sources, sinks and pathways: a helium-carbon isotope study of Baja California fluids and gases. Chem. Geol. 7, 653. https://doi.org/10.1016/j.chemgeo.2020.119722.

Barry, P.H., De Moor, J.M., Chiodi, A., Aguilera, F., Hudak, M.R., Bekaert, D.V., Turner, S.J., Curtice, J., Seltzer, A.M., Jessen, G.L., Osses, E., Blamey, J.M., Amenábar, M.J., Selci, M., Cascone, M., Bastianoni, A., Nakagawa, M., Filipovich, R., Bustos, E., Schrenk, M.O., Buongiorno, J., Ramírez, C.J., Rogers, T.J., Lloyd, K.G., Giovannelli, D., 2022. The helium and carbon isotope characteristics of the Andean convergent margin. Front. Earth Sci. (Lausanne) 10. https://doi.org/10.3389/feart.2022.897267.

Bebout, G.E., 1996. Volatile transfer and recycling at convergent margins: Mass-balance and insights from high-P/T metamorphic rocks. In: Bebout, G.E., Scholl, D.W., Kirby, S.H., et al. (Eds.), Subduction Top to Bottom. American Geophysical Union, Washington, D. C, pp. 179–193. https://doi.org/10.1029/GM096p0179.

Becker, J.A., Bickle, M.J., Galy, A., Holland, T.J.B., 2008. Himalayan metamorphic CO_2 fluxes: quantitative constraints from hydrothermal springs. Earth Planet. Sci. Lett. 265, 616–629. https://doi.org/10.1016/j.epsl.2007.10.046.

Bekaert, D.V., Turner, S.J., Broadley, M.W., Barnes, J.D., Halldorsson, S.A., Labidi, J., Wade, J., Walowski, K.J., Barry, P.H., 2021. Subduction-driven volatile recycling: a global mass balance. Annu. Rev. Earth Planet. Sci. 49, 37–70. https://doi.org/10.1146/annurev-earth-071620-055024.

Bianchi, D., Sarmiento, J.L., Gnanadesikan, A., Key, R.M., Schlosser, P., Newton, R., 2010. Low helium flux from the mantle inferred from simulations of oceanic helium isotope data. Earth Planet. Sci. Lett. 297, 379–386. https://doi.org/10.1016/j.epsl.2010.06.037.

Bissig, P., Goldscheider, N., Mayoraz, J., Surbeck, H., Vuataz, F.D., 2006. Carbogaseous spring waters, coldwater geysers and dry CO_2 exhalations in the tectonic window of the lower Engadine Valley, Switzerland. Eclogae Geol. Helv. 99, 143–155. https://doi.org/10.1007/s00015-006-1184-y.

Bodiš, D., Bottlik, F., Černák, R., Kordík, J., Malík, P., Michalko, J., Vandrová, G., 2017. Origin of Mineral Water Fatra, Slovakia. Procedia Earth Planet. Sci. 17, 472–475. https://doi.org/10.1016/j.proeps.2016.12.119.

Bracco Gartner, A.J.J., Seghedi, I., Nikogosian, I.K., Mason, P.R.D., 2020. Asthenosphere-induced melting of diverse source regions for East Carpathian post-collisional volcanism. Contrib. Mineral. Petrol. 175. https://doi.org/10.1007/s00410-020-01690-4.

Bräuer, K., Kämpf, H., Niedermann, S., Strauch, G., Tesař, J., 2008. Natural laboratory NW Bohemia: Comprehensive fluid studies between 1992 and 2005 used to trace geodynamic processes. Geochem. Geophys. Geosyst. 9. https://doi.org/10.1029/2007GC001921.

Bräuer, K., Geissler, W.H., Kämpf, H., Niedermannn, S., Rman, N., 2016. Helium and carbon isotope signatures of gas exhalations in the westernmost part of the Pannonian Basin (SE Austria/NE Slovenia): evidence for active lithospheric mantle degassing. Chem. Geol. 422, 60–70. https://doi.org/10.1016/j.chemgeo.2015.12.016.

Bräuer, K., Kämpf, H., Niedermann, S., Strauch, G., 2018. Monitoring of helium and carbon isotopes in the western Eger Rift area (Czech Republic): relationships with the 2014 seismic activity and indications for recent (2000–2016) magmatic unrest. Chem. Geol. 482, 131–145. https://doi.org/10.1016/j.chemgeo.2018.02.017.

Briceag, A., Jipa, D., Melinte, M.C., 2009. Early cretaceous deposits of the Ceahlau Nappe (Romanian Carpathian Bend Region). Geoecomarina 15, 177–185. https://doi.org/10.5281/zenodo.57309.

Brune, S., Williams, S.E., Müller, R.D., 2017. Potential links between continental rifting, CO_2 degassing and climate change through time. Nat. Geosci. 10, 941–946. https://doi.org/10.1038/s41561-017-0003-6.

Bucher, K., Frey, M., 2002. Petrogenesis of Metamorphic Rocks, Petrogenesis of Metamorphic Rocks. Springer Berlin Heidelberg. https://doi.org/10.1007/978-3-662-04914-3.

Caracausi, A., Sulli, A., 2019. Outgassing of mantle volatiles in compressional tectonic regime away from volcanism: the role of continental delamination. Geochem. Geophys. Geosyst. 20, 2007–2020. https://doi.org/10.1029/2018GC008046.

Caracausi, A., Martelli, M., Nuccio, P.M., Paternoster, M., Stuart, F.M., 2013. Active degassing of mantle-derived fluid: a geochemical study along the Vulture line, southern Apennines (Italy). J. Volcanol. Geotherm. Res. 253, 65–74. https://doi.org/10.1016/j.jvolgeores.2012.12.005.

Caracausi, A., Paternoster, M., Nuccio, P.M., 2015. Mantle CO_2 degassing at Mt. Vulture volcano (Italy): relationship between CO_2 outgassing of volcanoes and the time of their last eruption. Earth Planet. Sci. Lett. 411, 268–280. https://doi.org/10.1016/j.epsl.2014.11.049.

Buttitta, D., Capasso, G., Paternoster, M., Barberio, M.D., Gori, F., Petitta, M., Picozzi, M., Caracausi, A., 2023. Regulation of deep carbon degassing by gas-rock-water interactions in a seismic region of Southern Italy. Science of the Total Environment 897, 165367. https://doi.org/10.1016/j.scitotenv.2023.165367.

Caracausi, A., Buttitta, D., Picozzi, M., Paternoster, M., Stabile, T.A., 2022. Earthquakes control the impulsive nature of crustal helium degassing to the atmosphere. Commun. Earth Environ. 3, 1–8. https://doi.org/10.1038/s43247-022-00549-9.

Cardellini, C., Chiodini, G., Frondini, F., Avino, R., Bagnato, E., Caliro, S., Lelli, M., Rosiello, A., 2017. Monitoring diffuse volcanic degassing during volcanic unrests: the case of Campi Flegrei (Italy). Sci. Rep. 7, 1–15. https://doi.org/10.1038/s41598-017-06941-2.

Chalot-Prat, F., Girbacea, R., 2000. Partial delamination of continental mantle lithosphere, uplift-related crust±mantle decoupling, volcanism and basin formation: a new model for the Pliocene±Quaternary evolution of the southern East-Carpathians, Romania. Tectonophysics 327, 83–107. https://doi.org/10.1016/S0040-1951(00)00155-4.

Chen, C., Förster, M.W., Foley, S.F., Liu, Y., 2021. Massive carbon storage in convergent margins initiated by subduction of limestone. Nat. Commun. 12. https://doi.org/10.1038/s41467-021-24750-0.

Chiodini, G., Frondini, F., 2001. Carbon dioxide degassing from the Albani Hills volcanic regions, Central Italy. Chem. Geol. 177, 67–83. https://doi.org/10.1016/S0009-2541(00)00382-X.

Chiodini, G., Frondini, F., Kerrick, D.M., Rogie, J., Parello, F., Peruzzi, L., Zanzari, A.R., 1999. Quantification of deep CO_2 fluxes from Central Italy. Examples of carbon balance for regional aquifers and of soil diffuse degassing. Chem. Geol. 159, 205–222. https://doi.org/10.1016/S0009-2541(99)00030-3.

Chiodini, G., Cardellini, C., Amato, A., Boschi, E., Caliro, S., Frondini, F., Ventura, G., 2004. Carbon dioxide Earth degassing and seismogenesis in central and southern Italy. Geophys. Res. Lett. 31, 2–5. https://doi.org/10.1029/2004GL019480.

Chiodini, G., Cardellini, C., Di Luccio, F., Selva, J., Frondini, F., Caliro, S., Rosiello, A., Beddini, G., Ventura, G., 2020. Correlation between tectonic CO_2 Earth degassing and seismicity is revealed by a 10-year record in the Apennines, Italy. Sci. Adv. 6, 1–8. https://doi.org/10.1126/sciadv.abc2938.

Christopher, T.E., Blundy, J., Cashman, K.V., Cole, P.D., Edmonds, M., Smith, P.J., Sparks, R.S.J., Stinton, A., 2015. Crustal-scale degassing due to magma system destabilisation and magma-gas decoupling at Soufriere Hills Volcano, Montserrat. Geochem. Geophys. Geosyst. 16. https://doi.org/10.1002/2015GC005791.

Ciężkowski, W., Chowaniec, J., Gorecki, W., Krawiec, A., Rajchel, L., Zuber, A., 2010. Mineral and thermal waters of Poland. Przeglad Geologiczny 58.

Clayton, J.L., Spencer, C.W., Koncz, I., Szalay, A., 1990. Origin and migration of hydrocarbon gases and carbon dioxide, Békés Basin, southeastern Hungary. Org. Geochem. 15 (3), 233–247.

Clift, P.D., Jonell, T.N., Du, Y., Bornholdt, T., 2024. The impact of Himalayan-Tibetan erosion on silicate weathering and organic carbon burial. Chem. Geol. https://doi.org/10.1016/j.chemgeo.2024.122106.

Coltice, N., Simon, L., Lécuyer, C., 2004. Carbon isotope cycle and mantle structure. Geophys. Res. Lett. 31, 5. https://doi.org/10.1029/2003GL018873.

Cornides, I., Kecskés, A., 1987. Deep-seated carbon dioxide in Slovakia: additional comments on the problem of its origin. Geologicky Zbornik. Geologica Carpathica (Bratislava) 38, 429–435.

Cserép, B., Szemerédi, M., Harangi, S., Erdmann, S., Bachmann, O., Dunkl, I., Seghedi, I., Mészáros, K., Kovács, Z., Virág, A., Ntaflos, T., Schiller, D., Molnár, K., Lukács, R., 2023. Constraints on the pre-eruptive magma storage conditions and magma evolution of the 56–30 ka explosive volcanism of Ciomadul (East Carpathians, Romania). Contrib. Mineral. Petrol. 178. https://doi.org/10.1007/s00410-023-02075-z.

Cseresznyés, D., Király, C., Gál, Á., Papucs, A., Kónya, P., Lakos, I., Kovács, I., Rinyu, L., Szamosfalvi, Á., Szabó, C., Falus, G., Czuppon, G., 2024. Surface occurrence of dawsonite and natural CO2 emanation in Covasna, in the Eastern Carpathians: a stable isotope study. Chem. Geol. 645. https://doi.org/10.1016/j.chemgeo.2023.121883.

Csontos, L., Vörös, A., 2004. Mesozoic plate tectonic reconstruction of the Carpathian region. Palaeogeogr. Palaeoclimatol. Palaeoecol. 210, 1–56. https://doi.org/10.1016/j.palaeo.2004.02.033.

Csontos, F., Nagymarosy, A., Horváth, F., Kovac, M., 1992. Tertiary evolution of the Intra-Carpathian arc: a model. Tectonophysics 208, 221–241. https://doi.org/10.1016/0040-1951(92)90346-8.

Dasgupta, R., Hirschmann, M.M., 2010. The deep carbon cycle and melting in Earth's interior. Earth Planet. Sci. Lett. 298, 1–13. https://doi.org/10.1016/j.epsl.2010.06.039.

De Capitani, C., Petrakakis, K., 2010. The computation of equilibrium assemblage diagrams with Theriak/Domino software. Am. Mineral. 95, 1006–1016. https://doi.org/10.2138/am.2010.3354.

Demetrescu, C., Andreescu, M., 1994. On the thermal regime of some tectonic units in a continental collision environment in Romania. Tectonophysics 230, 265–276. https://doi.org/10.1016/0040-1951(94)90140-6.

Dérerová, J., Zeyen, H., Bielik, M., Salman, K., 2006. Application if integrated geophysical modeling for determination of the continental litospheric thermal structure in the Eastern Carpathians. Tectonics 25. https://doi.org/10.1029/2005TC001883.

Drivenes, K., Sørensen, B.E., Larsen, R.B., 2016. Orogenic degassing, scapolitization and k-metasomatism during caledonian exhumation, Helgeland, Norway. Nor. J. Geol. 96. https://doi.org/10.17850/njg96-3-04.

Ducea, M.N., Barla, A., Stoica, A.M., Panaiotu, C., Petrescu, L., 2020. Temporal-geochemical evolution of the Persani volcanic field, Eastern Transylvanian Basin (Romania): implications for slab rollback beneath the SE Carpathians. Tectonics 39. https://doi.org/10.1029/2019TC005802.

Ducea, M.N., Currie, C.A., Balica, C., Lazar, I., Mallik, A., Petrescu, L., Vlasceanu, M., 2022. Diapirism of carbonate platforms subducted into the upper mantle. Geology 50, 929–933. https://doi.org/10.1130/G50000.1.

Dulinski, M., Grabczak, J., Kostecka, A., Weclawik, S., 1995. Stable isotope composition of spelean calcites and gaseous CO_2 from Tylicz (Polish Carpathians). Chem. Geol. 125, 271–280.

Dušan, B., Jozef, K., Igor, S., Peter, M., Pavel, L., Daniel, P., Jarmila, B., Daniel, M., 2010. Mineral waters in Slovakia - evaluation of chemical composition stability using both historical records and the most recent data. J. Geochem. Explor. 107, 382–390. https://doi.org/10.1016/j.gexplo.2010.06.009.

Etiope, G., Feyzullayev, A., Baciu, C.L., 2009. Terrestrial Methane Seeps and Mud Volcanoes: A Global Perspective of Gas Origin, 26, pp. 333–344. https://doi.org/10.1016/j.marpetgeo.2008.03.001.

Evans, M.J., Derry, L.A., France-Lanord, C., 2008. Degassing of metamorphic carbon dioxide from the Nepal Himalaya. Geochem. Geophys. Geosyst. 9. https://doi.org/10.1029/2007GC001796.

Faccini, B., Rizzo, A.L., Bonadiman, C., Ntaflos, T., Seghedi, I., Grégoire, M., Ferretti, G., Coltorti, M., 2020. Subduction-related melt refertilisation and alkaline metasomatism in the Eastern Transylvanian Basin lithospheric mantle: evidence from mineral chemistry and noble gases in fluid inclusions. Lithos 364–365. https://doi.org/10.1016/j.lithos.2020.105516.

Filipescu, M., Humă, I., 1979. Geochemistry of natural gases, Publishing House of the Academy of the Socialist Republic of Romania, Bucharest, In Romanian.

Fischer, T.P., 2008. Fluxes of volatiles (H_2O, CO_2, N_2, Cl, F) from arc volcanoes. Geochem. J. 42, 21–38. https://doi.org/10.2343/geochemj.42.21.

Fischer, T.P., Aiuppa, A., 2020. AGU centennial grand challenge: volcanoes and deep carbon global CO_2 emissions from subaerial volcanism-recent progress and future challenges. Geophys. Geochem. Geosys. 21, e2019GC008690. https://doi.org/10.1029/2019GC008690.

Fischer, T.P., Arellano, S., Carn, S., Aiuppa, Al, Galle, B., Allard, P., Lopez, T., Schinohara, H., Kelly, P., Werner, C., Cardellini, C., Chiodini, G., 2019. The emissions of CO2 and other volatiles from the world's subaerial volcanoes. Sci. Rep. 9, 18716. https://doi.org/10.1038/s41598-019-54682-1.

Fórizs, I., Makfalvi, Z., 2014. A Csíki-medence mofettái széndioxidjának eredete stabil C-izotópos mérések alapján. In: Mineral waters in the Carpathian Basin 10th International Scientific Conference. In: Miercurea Ciuc. In Hungarian, pp. 75–79.

Frunzeti, N., 2013. Geogenic Emissions of Greenhouse Gases in the Southern Part of the Eastern Carpathians/ Emisii Geogene de Gaze Cu Efect de seră în Sectorul Sudic al Carpaţilor Orientali. Babes-Bolyai University, Faculty of Environmental Science and Engineering, Cluj-Napoca. In Romanian.

Gautheron, Cécile, Moreira, M., 2002. Helium signature of the subcontinental lithospheric mantle. Earth Planet. Sci. Lett. 199, 39–47. https://doi.org/10.1016/S0012-821X(02)00563-0.

Gilfillan, S.M.V., Lollar, B.S., Holland, G., Blagburn, D., Stevens, S., Schoell, M., Cassidy, M., Ding, Z., Zhou, Z., Lacrampe-Couloume, G., Ballentine, C.J., 2009. Solubility trapping in formation water as dominant CO_2 sink in natural gas fields. Nature 458, 614–618. https://doi.org/10.1038/nature07852.

Giusca, D., Radulescu, D., Gherasi, N., Bombita, G., Vasilescu, A., Krau, 1967. Geological map 1:200 000, no.03 Baia Mare.pdf. Geological Institute of Romania.

Golonka, J., Krobicki, M., Waśkowska, A., 2018. The pieniny klippen belt in Poland. Geol. Geophys. Environ. 44, 111. https://doi.org/10.7494/geol.2018.44.1.111.

Golonka, J., Gawęda, A., Waśkowska, A., 2020. Carpathians. In: Encyclopedia of Geology: Volume 1-6, Second edition 4, pp. 372–381. https://doi.org/10.1016/B978-0-12-409548-9.12384-X.

Gordienko, V.V., Gordienko, I.V., Zavgorodnyaya, O.V., 2019. Geothermal resourses of Ukraine. In: IOP Conference Series: Earth and Environmental Science. Institute of Physics Publishing. https://doi.org/10.1088/1755-1315/249/1/012008.

Gradziński, M., Duliński, M., Hercman, H., Górny, A., Przybyszowski, S., 2012. Peculiar calcite speleothems filling fissures in calcareous sandstones and their palaeohydrological and palaeoclimatic significance: an example from the Polish Carpathians. Geol. Q. 56, 711–732. https://doi.org/10.7306/gq.1051.

Griesshaber, E., O'Nions, R.J., Oxburgh, E.R., 1992. Helium and carbon isotope systematics in crustal fluids from the Eifel, the Rhine Graben and Black Forest, F.R.G. Chem. Geol. 99, 213–235. https://doi.org/10.1016/0009-2541(92)90178-8.

Groppo, Chiara, Rolfo, F., Castelli, D., Mosca, P., 2017. Metamorphic CO_2 production in collisional orogens: Petrological constraints from phase diagram modeling of Himalayan, scapolite-bearing, calc-silicate rocks in the NKC(F)MAS(T)-HC system. J. Petrol. 58, 53–84. https://doi.org/10.1093/petrology/egx005.

Groppo, C., Rapa, G., Frezzotti, M.L., Rolfo, F., 2020. The fate of calcareous pelites in collisional orogens. J. Metam. Geol. 39, 181–207. https://doi.org/10.1111/jmg.12568.

Groppo, Chiara, Rolfo, F., Frezzotti, M.L., 2022. CO_2 outgassing during collisional orogeny is facilitated by the generation of immiscible fluids. Commun. Earth Environ. 3, 1–11. https://doi.org/10.1038/s43247-022-00340-w.

Guo, Z., Wilson, M., Dingwell, D.B., Liu, J., 2021. India-Asia collision as a driver of atmospheric CO2 in the Cenozoic. Nat. Commun. 12, 3891. https://doi.org/10.1038/s41467-021-23772-y.

Gutscher, M.A., Maury, R., Eissen, J.P., Bourdon, E., 2000. Can slab melting be caused by flat subduction? Geology 28 (6), 535–538. https://doi.org/10.1130/0091-7613(2000)28.

Gyila, S., Csige, I., Sóki, E., 2017. In: Recent seismo-tectonical imprints observed in the geophysical parameters of mineral waters and CO2 emanations in Covasna spa-town, Romania. In Hungarian, pp. 65–77.

Harangi, S., 2001. Neogene to Quaternary volcanism of the Carpathian-Pannonian Region - a review. Acta Geol. Hung. 44, 223–258.

Harangi, S., Lenkey, L., 2007. Genesis of the neogene to quaternary volcanism in the Carpathian-Pannonian region: role of subduction, extension, and mantle plume. Spec. Pap. Geol. Soc. Amer. 418, 67–92. https://doi.org/10.1130/2007.2418(04).

Harangi, S., Downes, H., Kósa, L., Szabo, Cs, Thirlwall, M.F., Mason, P.R.D., Mattey, D., 2001. Almandine garnet in Calc-alkaline volcanic rocks of the Northern Pannonian Basin (Eastern–Central Europe): geochemistry, petrogenesis and geodynamic implications. J. Petrol. 42, 1813–1843. https://doi.org/10.1093/petrology/42.10.1813.

Harangi, S., Downes, H., Seghedi, I., 2006. Tertiary-Quarternary subduction processes and related magmatism in the Alpine-Mediterranean region. Geol. Soc. Mem. 32, 167–190. https://doi.org/10.1144/GSL.MEM.2006.032.01.10.

Harangi, S., Downes, H., Thirlwall, M., Gméling, K., 2007. Geochemistry, petrogenesis and geodynamic relationships of miocene calc-alkaline volcanic rocks in the western Carpathian arc, Eastern Central Europe. J. Petrol. 48, 2261–2287. https://doi.org/10.1093/petrology/egm059.

Harangi, S., Molnár, M., Vinkler, A.P., Kiss, B., Jull, A.J., Leonard, A.G., 2010. Radiocarbon dating of the last volcanic eruptions of Ciomadul volcano, southeast Carpathians, Eastern-Central Europe. Radiocarbon 52, 1498–1507.

Harangi, S., Lukács, R., Schmitt, A.K., Dunkl, I., Molnár, K., Kiss, B., Seghedi, I., Novothny, Molnár, M., 2015a. Constraints on the timing of Quaternary volcanism and duration of magma residence at Ciomadul volcano, east-central Europe, from combined U-Th/He and U-Th zircon geochronology. J. Volcanol. Geotherm. Res. 301, 66–80. https://doi.org/10.1016/j.jvolgeores.2015.05.002.

Harangi, S., Novák, A., Kiss, B., Seghedi, I., Lukács, R., Szarka, L., Wesztergom, V., Metwaly, M., Gribovszki, K., 2015b. Combined magnetotelluric and petrologic constrains for the nature of the magma storage system beneath the Late Pleistocene Ciomadul volcano (SE Carpathians). J. Volcanol. Geotherm. Res. 290, 82–96. https://doi.org/10.1016/j.jvolgeores.2014.12.006.

Harangi, S., Seghedi, I., Lukács, R., 2026. The Neogene – Quaternary volcanism of the Carpathian – Pannonian region: from initial plate tectonic models to quantitative petrogenetic explanations. In: Tari, G.C., Kitchka, A., Krézsek, C., Lučić, D., Markič, M., Radivojević, D., Sachsenhofer, R.F., Šujan, M. (Eds.), The Miocene Extensional Pannonian Superbasin. The Geological Society of London, London. https://doi.org/10.1144/sp554-2024-84.

Hiett, C.D., Newell, D.L., Jessup, M.J., 2021. 3He evidence for fluid transfer and continental hydration above a flat slab. Earth Planet. Sci. Lett. 556, 116722. https://doi.org/10.1016/j.epsl.2020.116722.

Hilton, R.G., West, A.J., 2020. Mountains, erosion and the carbon cycle. Nat. Rev. Earth Environ. 1, 284–299. https://doi.org/10.1038/s43017-020-0058-6.

Hilton, D.R., Fischer, T.P., Marty, B., 2002. Noble gases and volatile recycling at subduction zones. Rev. Mineral. Geochem. 47, 319–370. https://doi.org/10.2138/rmg.2002.47.9.

Hirschmann, M.M., 2023. The deep Earth oxygen cycle: Mass balance considerations on the origin and evolution of mantle and surface oxidative reservoirs. Earth Planet. Sci. Lett. 619, 118311. https://doi.org/10.1016/j.epsl.2023.118311.

Hoefs, J., 2018. Stable Isotope Geochemistry, 8th ed. Springer International Publishing AG, Cham, Switzerland. https://doi.org/10.1007/987-3-319-78527-1.

Hók, J., Kysel, R., Kováč, M., Moczo, P., Kristek, J., Kristeková, M., Šujan, M., 2016. A seismic source zone model for the seismic hazard assessment of Slovakia. Geol. Carpath. 67, 273–288. https://doi.org/10.1515/geoca-2016-0018.

Hoke, L., Lamb, S., Hilton, D.R., Poreda, R.J., 2000. Southern limit of mantle-derived geothermal helium emissions in Tibet: implications for lithospheric structure. Earth Planet. Sci. Lett. 180, 297–308. https://doi.org/10.1016/S0012-821X(00)00174-6.

Holland, G., Gilfillan, S., 2013. Application of noble gases to the viability of CO_2 storage. In: Burnard, P. (Ed.), The Noble Gases as Geochemical Tracers. Advances in Isotope Geochemistry. Springer, Berlin, Heidelberg, pp. 177–223. https://doi.org/10.1007/978-3-642-28836-4_8.

Horváth, F., 1993. Towards a mechanical model for the formation of the Pannonian basin. Tectonophysics 226 (1–4), 333–357. https://doi.org/10.1016/0040-1951(93)90126-5.

Horváth, F., Bada, G., Szafián, P., Tari, G., Ádám, A., Cloetingh, S., 2006. Formation and deformation of the Pannonian Basin: constraints from observational data. Geol. Soc. Memoir. https://doi.org/10.1144/GSL.MEM.2006.032.01.11.

Horváth, F., Musitz, B., Balázs, A., Végh, A., Uhrin, A., Nádor, A., Koroknai, B., Pap, N., Tóth, T., Wórum, G., 2015. Evolution of the Pannonian basin and its geothermal resources. Geothermics 53, 328–352. https://doi.org/10.1016/j.geothermics.2014.07.009.

Hunt, J.A., Zafu, A., Mather, T.A., Pyle, D.M., Barry, P.H., 2017. Spatially variable CO2 degassing in the Main Ethiopian Rift: implications for magma storage, volatile transport, and rift-related emissions. Geochem. Geophys. Geosyst. 18, 3714–3737. https://doi.org/10.1002/2017GC006975.

Ianovici, V., Rădulescu, D., 1968. Geological map 1:200 000, no.20 Odorhei. Geological Institute of Romania, Bucharest. In Romanian.

Ismail-Zadeh, A., Matenco, L., Radulian, M., Cloetingh, S., Panza, G., 2012. Geodynamics and intermediate-depth seismicity in Vrancea (the south-eastern Carpathians): current state-of-the art. Tectonophysics 530–531, 50–79. https://doi.org/10.1016/j.tecto.2012.01.016.

Italiano, F., Sasmaz, A., Yuce, G., Okan, O.O., 2013. Thermal fluids along the East Anatolian Fault Zone (EAFZ): geochemical features and relationships with the tectonic setting. Chem. Geol. 339, 103–114. https://doi.org/10.1016/j.chemgeo.2012.07.027.

Italiano, F., Kis, B.M., Baciu, C., Ionescu, A., Harangi, S., Palcsu, L., 2017. Geochemistry of dissolved gases from the Eastern Carpathians - Transylvanian Basin boundary. Chem. Geol. 469, 117–128. https://doi.org/10.1016/j.chemgeo.2016.12.019.

Kagoshima, T., Sano, Y., Takahata, N., Maruoka, T., Fischer, T.P., Hattori, K., 2015. Sulphur geodynamic cycle. Sci. Rep. 5, 8330. https://doi.org/10.1038/srep08330.

Kalmár, D., Petrescu, L., Stipcevic, J., Balázs, A., Kovács, I.J., AlpArray and PACASE Working Groups, 2023. Lithospheric Structure of the Circum-Pannonian Region Imaged by S-To-P Receiver Functions. Geochem. Geophys. Geosyst. 24. https://doi.org/10.1029/2023GC010937.

Karátson, D., Veres, D., Gertisser, R., Magyari, K.E., Jánosi, Cs., Hambach, U., 2022. Ciomadul (Csomád), the youngest volcano in the Carpathians, Volcanism, Palaeoenvironment, Human Impact. Springer Nature, Switzerland, p. 268. https://doi.org/10.1007/978-3-030-89140-4.

Kelemen, P.B., Manning, C.E., 2015. Reevaluating carbon fluxes in subduction zones, what goes down, mostly comes up. Proc. Natl. Acad. Sci. U. S. A. 112, E3997–E4006. https://doi.org/10.1073/pnas.1507889112.

Kennedy, B.M., Kharaka, Y.K., Evans, W.C., Ellwood, A., DePaolo, D.J., Thordsen, J., Ambats, G., Mariner, R.H., 1997. Mantle Fluids in the San Andreas Fault System, California. Science (1979) 278, 1278–1281.

Kerrick, D.M., 2001. Present and past nonanthropogenic CO_2 degassing from the solid earth. Rev. Geophys. 39, 565–585. https://doi.org/10.1029/2001RG000105.

Kerrick, D.M., Caldeira, K., 1993. Paleoatmospheric consequences of CO_2 released during early Cenozoic regional metamorphism in the Tethyan orogen. Chem. Geol. 108, 201–230. https://doi.org/10.1016/0009-2541(93)90325-D.

Kerrick, D.M., Caldeira, K., 1998. Metamorphic CO_2 degassing from orogenic belts. Chem. Geol. 145 (3–4), 213–232. https://doi.org/10.1016/S0009-2541(97)00144-7.

Kerrick, D.M., Caldeira, K., 1999. Was the Himalayan orogen a climatically significant coupled source and sink for atmospheric CO_2 during the Cenozoic? Earth Planet. Sci. Lett. 173 (3), 195–203. https://doi.org/10.1016/S0012-821X(99)00229-0.

Kikvadze, O., Lavrushin, V., Pokrovskii, B., Polyak, B., 2010. Gases from mud volcanoes of western and Central Caucasus. Geofluids 10, 486–496. https://doi.org/10.1111/j.1468-8123.2010.00309.x.

Kis, B.M., Ionescu, A., Cardellini, C., Harangi, S., Baciu, C., Caracausi, A., Viveiros, F., 2017. Quantification of carbon dioxide emissions of Ciomadul, the youngest volcano of the Carpathian-Pannonian Region (Eastern-Central Europe, Romania). J. Volcanol. Geotherm. Res. 341. https://doi.org/10.1016/j.jvolgeores.2017.05.025.

Kis, B.M., Caracausi, A., Palcsu, L., Baciu, C., Ionescu, A., Futó, I., Sciarra, A., Harangi, S., 2019. Noble gas and carbon isotope systematics at the seemingly inactive ciomadul volcano (Eastern-Central Europe, Romania): evidence for volcanic degassing. Geochem. Geophys. Geosyst. 20, 3019–3043. https://doi.org/10.1029/2018GC008153.

Kis, B.M., Baciu, C., Zsigmond, A.R., Kékedy-Nagy, L., Kármán, K., Palcsu, L., Máthé, I., Harangi, S., 2020. Constraints on the hydrogeochemistry and origin of the CO2-rich mineral waters from the Eastern Carpathians – Transylvanian Basin boundary (Romania). J. Hydrol. (Amst). 591, 125311. https://doi.org/10.1016/j.jhydrol.2020.125311.

Kis, B.M., Szalay, R., Aiuppa, A., Bitetto, M., Palcsu, L., Harangi, S., 2022. Compositional measurement of gas emissions in the Eastern Carpathians (Romania) using the Multi-GAS instrument: approach for in situ data gathering at non-volcanic areas. J. Geochem. Explor. 240. https://doi.org/10.1016/j.gexplo.2022.107051.

Kis, B.M., Szalay, R., Caracausi, A., Aiuppa, A., Palcsu, L., Orsovszki, J., Grassa, F., Harangi, Sz, 2025. Location, chemical and isotopic composition of free bubbling gases collected in the Eastern Carpathians, Romania. In: EarthChem Repository. Interdisciplinary Earth Data Alliance (IEDA).. https://doi.org/10.60520/IEDA/114173.

Kis, B.M., Szalay, R., Caracausi, A., Randazzo, P., Tóth, M.T., Palcsu, L., Orsovszki, J., Aiuppa, A., Grassa, F., Harangi, Sz, 2026. Dataset of the CO_2-rich gas emissions in the Eastern Carpathians, Romania. Data Brief 64, 112376. https://doi.org/10.1016/j.dib.2025.112376.

Kleine, B.I., Zhao, Z., Skelton, A.D.L., 2016. Rapid fluid flow along fractures at greenschist facies conditions on Syros, Greece. Am. J. Sci. 316, 169–201. https://doi.org/10.2475/02.2016.03.

Klemperer, S.L., Kennedy, B.M., Sastry, S.R., Makovsky, Y., Harinarayana, T., Leech, M. L., 2013. Mantle fluids in the Karakoram fault: Helium isotope evidence. Earth Planet. Sci. Lett. 366, 59–70. https://doi.org/10.1016/j.epsl.2013.01.013.

Klemperer, S.L., Zhao, P., Whyte, C.J., Darrah, T.H., Crossey, L.J., Karlstrom, K.E., Liu, T., Winn, C., Hilton, D.R., Ding, L., 2022. Limited underthrusting of India below Tibet: $^3He/^4He$ analysis of thermal springs locates the mantle suture in continental collision. PNAS 119 (12), e2113877119. https://doi.org/10.1073/pnas.2113877119.

Konečný, V., Lexa, J., Hojstričová, V., 1999. The Central Slovakia Neogene volcanic field. In: Molnár, F., Lexa, J., Hedenquist, J.W., Thompson, T.B. (Eds.), Epithermal Mineralization of the Western Carpathians. Society of Economic Geologists, pp. 181–196. https://doi.org/10.5382/GB.31.06.

Konečný, V., Kováč, M., Lexa, J., Šefara, J., 2002. Neogene evolution of the Carpatho-Pannonian region: an interplay of subduction and back-arc diapiric uprise in the mantle. In: Stephan Mueller Special Publication Series, 1, pp. 105–123. https://doi.org/10.5194/smsps-1-105-2002.

Kotarba, M.J., Nagao, K., 2008. Composition and origin of natural gases accumulated in the Polish and Ukrainian parts of the Carpathian region: gaseous hydrocarbons, noble gases, carbon dioxide and nitrogen. Chem. Geol. 255, 426–438. https://doi.org/10.1016/j.chemgeo.2008.07.011.

Kotarba, M.J., Więcław, D., Bilkiewicz, E., Lillis, P.G., Dziadzio, P., Kmiecik, N., Romanowski, T., Kowalski, A., 2020. Origin, secondary processes and migration of oil and natural gas in the central part of the Polish Outer Carpathians. Mar. Pet. Geol. 121. https://doi.org/10.1016/j.marpetgeo.2020.104617.

Krézsek, C., Schléder, Z., Olaru-Florea, R., Tamas, A., Oteleanu, A., Stoicescu, A., Ungureanu, C., Dudus, R., Tari, G., 2023. Structure and petroleum systems of the Eastern Carpathians, Romania. Mar. Pet. Geol. 151. https://doi.org/10.1016/j.marpetgeo.2023.106179.

Krstekanić, N., Matenco, L., Stojadinovic, U., Willingshofer, E., Toljić, M., Tamminga, D., 2022. Strain partitioning in a large intracontinental strike-slip system accommodating backarc-convex orocline formation: the Circum-Moesian Fault System of the Carpatho-Balkanides. Glob. Planet. Change 208. https://doi.org/10.1016/j.gloplacha.2021.103714.

Kulongoski, J.T., Hilton, D.R., Barry, P.H., Esser, B.K., Hillegonds, D., Belitz, K., 2013. Volatile fluxes through the Big Bend section of the San Andreas Fault, California: helium and carbon-dioxide systematics. Chem. Geol. 339, 92–102. https://doi.org/10.1016/j.chemgeo.2012.09.007.

Kutas, R.I., 2014. Heat flow and geothermal models of the Earth's crust in the Ukrainian Carpathians. Geophys. J. 6, 36. In Ukrainian.

Lange, T.P., Palcsu, L., Szakács, A., Kővágó, Á., Gelencsér, O., Gál, Á., Gyila, S., Tóth, T., Maţenco, L., Krézsek, C.S., Lenkey, L., Szabó, C.S., Kovács, I.J., 2023. The link between lithospheric scale deformations and deep fluid emanations: inferences from the Southeastern Carpathians, Romania. Evol. Earth 1, 100013. https://doi.org/10.1016/j.eve.2023.100013.

Laumonier, M., Karakas, O., Bachmann, O., Gaillard, F., Lukács, R., Seghedi, I., Menand, T., Harangi, S., 2019. Evidence for a persistent magma reservoir with large melt content beneath an apparently extinct volcano. Earth Planet. Sci. Lett. 521, 79–90. https://doi.org/10.1016/j.epsl.2019.06.004.

Lee, H., Muirhead, J.D., Fischer, T.P., Ebinger, C.J., Kattenhorn, S.A., Sharp, Z.D., Kianji, G., 2016. Massive and prolonged deep carbon emissions associated with continental rifting. Nat. Geosci. 9, 145–149. https://doi.org/10.1038/ngeo2622.

Leśniak, P.M., 1998. Origin of carbon dioxide and evolution of CO_2-rich waters in the West Carpathians, Poland. Acta Geol. Pol. 48, 343–366.

Leśniak, P.M., Sakai, H., Ishibashi, J.I., Wakita, H., 1997. Mantle helium signal in the West Carpathians, Poland. Geochem. J. 31, 383–394. https://doi.org/10.2343/geochemj.31.383.

Lexa, J., Seghedi, I., Németh, K., Szakács, A., Konečný, V., Pécskay, Z., Fülöp, A., Kovacs, M., 2010. Neogene-quaternary volcanic forms in the Carpathian-Pannonian region: a review. Cent. Eur. J. Geosci. 2, 207–270. https://doi.org/10.2478/v10085-010-0024-5.

Liu, W., Zhang, M., Liu, Y., Cui, L., Sano, Y., Zhou, X., Li, Y., Zhang, L., Lang, Y.C., Liu, C. Q., Xu, S., 2024. Massive crustal carbon mobilization and emission driven by India underthrusting Asia. Commun. Earth Environ. 5. https://doi.org/10.1038/s43247-024-01438-z.

Lukács, R., Guillong, M., Schmitt, A.K., Molnár, K., Bachmann, O., Harangi, S., 2018. LA-ICP-MS and SIMS U-Pb and U-Th zircon geochronological data of Late Pleistocene lava domes of the Ciomadul Volcanic Dome Complex (Eastern Carpathians). Data Brief 18, 808–813. https://doi.org/10.1016/j.dib.2018.03.100.

Lukács, R., Caricchi, L., Schmitt, A.K., Bachmann, O., Karakas, O., Guillong, M., Molnár, K., Seghedi, I., Harangi, S., 2021. Zircon geochronology suggests a long-living and active magmatic system beneath the Ciomadul volcanic dome field (eastern-central Europe). Earth Planet. Sci. Lett. 565. https://doi.org/10.1016/j.epsl.2021.116965.

Majcin, D., Kutas, R., Bilčík, D., Bezák, V., Korchagin, I., 2016. Thermal conditions for geothermal energy exploitation in the Transcarpathian depression and surrounding units. Contrib. Geophys. Geod. 46, 33–49. https://doi.org/10.1515/congeo-2016-0003.

Majorowicz, J., Polkowski, M., Grad, M., 2019. Thermal properties of the crust and the lithosphere–asthenosphere boundary in the area of Poland from the heat flow variability and seismic data. Int. J. Earth Sci. 108, 649–672. https://doi.org/10.1007/s00531-018-01673-8.

Ferrand, T.P., Manea, E.F., 2021. Dehydration-induced earthquakes identified in a subducted oceanic slab beneath Vrancea, Romania. Sci. Rep. 11. https://doi.org/10.1038/s41598-021-89601-w.

Mants, Gy., 1974. Opportunities for the commercialization of natural therapeutic factors in the area of Băile Tuşnad and its immediate surroundings. In: The natural therapeutic factors of Harghita County, The People's Council and the Directorate of Health of Harghita County. In Hungarian, p. 449.

Marcinčáková, Z., Košuth, M., 2015. Characteristics of Xenoliths in the East Slovakian Neogene Volcanites. In: Scientific Annals of the Al.I.Cuza University of Iasi, 57, 1, pp. 7–27.

Marks, L., Ber, A., Gogolek, W., Piotrowska, K., 2006. Geological Map of Poland 1: 500000. Polish Geological Institute.

Martelli, M., Nuccio, P.M., Stuart, F.M., Burgess, R., Ellam, R.M., Italiano, F., 2004. Helium-strontium isotope constraints on mantle evolution beneath the Roman Comagmatic Province. Italy. Earth Planet. Sci. Lett. 224, 295–308. https://doi.org/10.1016/j.epsl.2004.05.025.

Marty, B., Jambon, A., 1987. $C/^3He$ in volatile fluxes from the solid Earth: implications for carbon geodynamics. Earth Planet. Sci. Lett. 83, 16–26.

Marty, B., Tolstikhin, I.N., 1998. CO_2 fluxes from mid-ocean ridges, arcs and plumes 2. Chem. Geol. https://doi.org/10.1016/S0009-2541(97)00145-9.

Marty, B., Jambon, A., Sano, Y., 1989. Helium isotopes and CO_2 in volcanic gases of Japan. Chem. Geol. 76, 25–40. https://doi.org/10.1016/0009-2541(89)90125-3.

Marty, B., O'Nions, R.K., Oxburgh, E.R., Martel, D., Lombardi, S., 1992. Helium isotopes in Alpine regions. Tectonophysics 206, 71–78. https://doi.org/10.1016/0040-1951(92)90368-G.

Marty, B., Almayrac, M., Barry, P.H., Bekaert, D.V., Broadley, M.W., Byrne, D.J., Ballentine, C.J., Caracausi, A., 2020. An evaluation of the C/N ratio of the mantle from natural CO_2-rich gas analysis: geochemical and cosmochemical implications. Earth Planet. Sci. Lett. 551. https://doi.org/10.1016/j.epsl.2020.116574.

Mason, P.R.D., Downes, H., Thirlwall, M.F., Seghedi, I., Szakacs, A., Lowry, D., Mattey, D., 1996. Crustal assimilation as a major petrogenetic process in the East carpathian neogene and quaternary continental Margin Arc, Romania. J. Petrol. 37, 927–959. https://doi.org/10.1093/petrology/37.4.927.

Mason, P.R.D., Seghedi, I., Szákacs, A., Downes, H., 1998. Magmatic constraints on geodynamic models of subduction in the East Carpathians, Romania. Tectonophysics. https://doi.org/10.1016/S0040-1951(98)00167-X.

Mason, E., Edmonds, M., Turchyn, A.V., 2017. Remobilization of crustal carbon may dominate volcanic arc emissions. Science 357 (290–294), 4. https://doi.org/10.1126/science.aan5049.

Matenco, L., Bertotti, G., 2000. Tertiary tectonic evolution of the external East Carpathians (Romania). Tectoniphysics 316, 255–286. https://doi.org/10.1016/S0040-1951(99)00261-9.

Matenco, L., Krézsek, Cs., Merten, S., Schmid, S., Cloething, S., Andriessen, P., 2010. Characteristics of collision orogens. Terra Nova 22 (3), 155–165. https://doi.org/10.1111/j.1365-3121.2010.00931.x.

Matsumoto, T., Kawabata, T., Matsuda, J.I., Yamamoto, K., Mimura, K., 2003. $^{3}He/^{4}He$ ratios in well gases in the Kinki district, SW Japan: surface appearance of slab-derived fluids in a non-volcanic area in Kii Peninsula. Earth Planet. Sci. Lett. 216, 221–230. https://doi.org/10.1016/S0012-821X(03)00479-5.

Melinte-Dobrinescu, M., Jipa, D.C., 2007. Stratigraphy of the Lower Cretaceous Sediments from the Carpathian Bend Area, Romania. Acta Geol. Sin. 81, 949–956. https://doi.org/10.1111/j.1755-6724.2007.tb01018.x.

Michalko, Juraj, 2016. Beginnings of the isotope research of mineral and thermal groundwaters of Slovakia. Slovak Geol. Mag. 2, 27–40.

Milesi, G., Cardoso, C.D., Pik, R., Moreira, M., Charpentier, D., Mercadier, J., 2025. Origin of helium and associated fluid in fault-related hydrothermal systems of the Eastern Pyrenees. Terra Nova 37, 93–102. https://doi.org/10.1111/ter.12753.

Molnár, K., Harangi, S., Lukács, R., Dunkl, I., Schmitt, A.K., Kiss, B., Garamhegyi, T., Seghedi, I., 2018. The onset of the volcanism in the Ciomadul Volcanic Dome Complex (Eastern Carpathians): eruption chronology and magma type variation. J. Volcanol. Geotherm. Res. 354, 39–56. https://doi.org/10.1016/j.jvolgeores.2018.01.025.

Molnár, K., Lukács, R., Dunkl, I., Schmitt, A.K., Kiss, B., Seghedi, I., Szepesi, J., Harangi, S., 2019. Episodes of dormancy and eruption of the Late Pleistocene Ciomadul volcanic complex (Eastern Carpathians, Romania) constrained by zircon geochronology. J. Volcanol. Geotherm. Res. 373, 133–147. https://doi.org/10.1016/j.jvolgeores.2019.01.025.

Molnár, K., Czuppon, G., Palcsu, L., Benkó, Z., Lukács, R., Kis, B.M., Németh, B., Harangi, S., 2021. Noble gas geochemistry of phenocrysts from the Ciomadul volcanic dome field (Eastern Carpathians). Lithos 394–395. https://doi.org/10.1016/j.lithos.2021.106152.

Moriya, I., Okuno, M., Nakamura, T., Szakács, A., Seghedi, I., 1995. Last eruption and its 14C age of Ciomadul volcano. In: Summaries of Researches Using AMS at Nagoya University, 6, pp. 82–90.

Moriya, I., Okuno, M., Nakamura, T., Ono, K., Szakács, A., Seghedi, I., 1996. Radiocarbon ages of charcoal fragments from the pumice flow deposit of the last eruption of Ciomadul volcano, Romania. In: Summaries of Researches using AMS at Nagoya University, p. 7.

Mörner, N.-A., Etiope, G., 2002. Carbon degassing from the lithosphere. Glob. Planet. Change 33, 185–203. https://doi.org/10.1016/S0921-8181(02)00070-X.

Muirhead, J.D., Fischer, T.P., Oliva, S.J., Laizer, A., van Wijk, J., Currie, A.C., Lee, H., Kazimoto, E., Sano, Y., Takahata, N., Tiberi, C., Foley, S.F., Dufek, J., Reiss, M.C., Ebinger, C.J., 2020. Displaced cratonic mantle concentrates deep carbon during continental rifting. Nature 582, 67–72. https://doi.org/10.1038/s41586-020-2328-3.

Murgeanu, G., Mirauta, O., Joia, T., Mirauta, E., Alexandrescu, G., 1968. Geological Map 1:200 000, No.13 Piatra Neamț. Geological Institute of Romania, In Romanian.

Murgeanu, G., Dumitrescu, I., Mirăuță, O., Săndulescu, M., Ștefănescu, M., Bandrabur, T., 1962. Geological Map 1:200 000. Springer Berlin Heidelberg.

Murgeanu, G., Dumitrescu, I., Sandulescu, M., Bandrabur, T., Sandulescu, J., 1970. Geological Map 1:200 000, No.29 Covasna. Geological Institute of Romania, Bucharest.

Nakapelyukh, M., Bubniak, I., Bubniak, A., Jonckheere, R., Ratschbacher, L., 2018. Cenozoic structural evolution, thermal history, and erosion of the Ukrainian Carpathians fold-thrust belt. Tectonophysics 722, 197–209. https://doi.org/10.1016/j.tecto.2017.11.009.

Necea, D., Juez-Larré, J., Matenco, L, Andriesse, P.A.M., Dinu, C., 2021. Foreland migration of orogenic exhumation during nappe stacking: Inferences from a high-resolution thermochronological profile over the Southeast Carpathians. Global and Planetary Change 200, 103457. https://doi.org/10.1016/j.gloplacha.2021.103457.

Neska, A., 2016. Conductivity Anomalies in Central Europe. Surv. Geophys. https://doi.org/10.1007/s10712-015-9349-8.

Newell, D.L., Jessup, M.J., Cottle, J.M., Hilton, D.R., Sharp, Z.D., Fischer, T.P., 2008. Aqueous and isotope geochemistry of mineral springs along the southern margin of the Tibetan plateau: implications for fluid sources and regional degassing of CO2. Geochem. Geophys. Geosyst. 9 (8), Q08014. https://doi.org/10.1029/2008GC002021.

Newell, D.L., Jessup, M.J., Hilton, D.R., Shaw, C.A., Hughes, C.A., 2015. Mantle-derived helium in hot springs of the Cordillera Blanca, Peru: implications for mantle-to-crust fluid transfer in a flat-slab subduction setting. Chem. Geol. 417, 200–209. https://doi.org/10.1016/j.chemgeo.2015.10.003.

Olson, P.L., Sharp, Z.D., 2022. Primordial helium-3 exchange between Earth's core and mantle. Geochem. Geophys. Geosyst. 23. https://doi.org/10.1029/2021GC009985.

O'Nions, R.K., Oxburgh, E.R., 1988. Helium, volatile fluxes and the development of continental crust. Earth Planet. Sci. Lett. 90, 331–347. https://doi.org/10.1016/0012-821X(88)90134-3.

Oszczypko, N., 2004. The structural position and tectonosedimentary evolution of the Polish Outer Carpathians. Przeglad Geol. 52, 780–791.

Oszczypko, N., Zuber, A., 2002. Geological and isotopic evidence of diagenetic waters in the Polish Flysch Carpathians. Geol. Carpathica 53, 257–268.

Oszczypko, N., Zuchiewicz, W., 2007. Geology of Krynica Spa, Western Outern Carpathians, Poland. Ann. Soc. Geol. Poloniae 77, 69–92.

Oszczypko, N., Krzywiec, P., Popadyuk, I., Peryt, T., 2007. Carpathian Foredeep Basin (Poland and Ukraine): Its Sedimentary, Structural, and Geodynamic Evolution. In: Golonka, J., Picha, F.J. (Eds.), The Carpathians and Their Foreland, Geology and Hydrocarbon Resources: AAPG Memoir, vol. 84, pp. 293–350. https://doi.org/10.1306/985612m843072.

Oszczypko, N., Ślączka, A., Oszczypko-Clowes, M., Olszewska, B., 2015. Where was the Magura Ocean? Acta Geol. Polonica 65, 319–344. https://doi.org/10.1515/agp-2015-0014.

Oszczypko, N., Wójcik-Tabol, P., Oszczypko-Clowes, M., 2018. The genesis of the carbon dioxide in the Polish Outer Carpathians – Szczawa tectonic window case study – new insight. Acta Geol. Polonica 68, 181–206. https://doi.org/10.1515/agp-2018-0001.

Palcsu, L., Vető, I., Futó, I., Vodila, G., Papp, L., Major, Z., 2014. In-reservoir mixing of mantle-derived CO_2 and metasedimentary CH_4-N_2 fluids - noble gas and stable isotope study of two multistacked fields (Pannonian Basin System, W-Hungary). Mar. Pet. Geol. 54, 216–227. https://doi.org/10.1016/j.marpetgeo.2014.03.013.

Palcsu, L., Koltai, G., Horváth, A., Baran, I., Baran, A., Hałas, S., 2017. Stable isotope and noble gas constraints on the genesis of therapeutic waters in southeast Poland. Carpathian J. Earth Environ. Sci. 12, 225–233.

Parello, F., Allard, P., D'Alessandro, W., Federico, C., Jean-Baptiste, P., Catani, O., 2000. Isotope geochemistry of Pantelleria volcanic fluids, Sicily Channel rift: a mantle volatile end-member for volcanism in southern Europe. Earth Planet. Sci. Lett. 180, 325–339. https://doi.org/10.1016/S0012-821X(00)00183-7.

Patrulius, D., Dimitrescu, R., Dessila-Codarcea, M., 1968. Geological Map 1:200 000, No.28 Brasov. Geological Institute of Romania, Bucharest.

Pavlyuk, M., Shlapinsky, V., Savchak, O., Ternavskyi, M., 2019a. Geology of fossil fuels-perspectives of oil and gas industry in the north-western part of the internal flysch nappe of the Ukrainian Carpathians. In: Geology and Geochemistry of Fossil Fuels, p. 2.

Pavlyuk, M., Shlapinsky, V., Savchak, O., Ternavskyi, M., 2019b. Perspectives of oil and gas industry in nort-western part of the internal flysch on the Ukrainian Carpathians. In: Geology and Geochemistry of Fossil Fuels, 2, pp. 5–27.

Pawlewicz, M., 2006. Total petroleum systems of the North Carpathian Province of Poland, Ukraine, Czech Republic, and Austria. USGS Bull. 32.

Pawlewicz, M., 2007. Total petroleum systems of the Carpathian – Balkanian Basin Province of Romania and Bulgaria. Bulletin 2204-F, 19.

Peacock, S.A., 1990. Fluid processes in subduction zones. Science 248 (4953), 329–337. https://doi.org/10.1126/science.248.4953.329.

Pécskay, Z., Lexa, J., Szakács, A., Seghedi, I., Balogh, K., Konečný, V., Zelenka, T., Kovacs, M., Póka, T., Fülöp, A., Márton, E., Panaiotu, C., Cvetković, V., 2006. Geochronology of Neogene magmatism in the Carpathian arc and intra-Carpathian area. Geol. Carpath. 57, 511–530.

Pécskay, Z., Gméling, K., Molnár, F., Benkó, Z., 2015. Neogene calc-alkaline intrusive magmatism of post-collisional origin along the Outer Carpathians: a comparative study of the Pieniny Mountains and adjacent areas. Ann. Soc. Geol. Poloniae 85, 77–89. https://doi.org/10.14241/asgp.2014.006.

Péter, E., Makfalvi, Z., 1977. Apele termominerale de la extremitatea sudica a Masivului Harghita. Acta Siculica 181–191.

Pinna, E., Soare, A., Stănică, D., Stănică, M., 1992. Carpathian conductivity anomaly and its relaton to deep structure of the substratum. Acta Geod. Geoph. Mont. Hung. 27, 35–45.

Plank, T., Manning, C.E., 2019. Subducting carbon. Nature 574, 343–352. https://doi.org/10.1038/s41586-019-1643-z.

Polyak, B.G., Tolstikhin, I.N., Kamensky, I.L., Yakovlev, L.E., Marty, B., Cheshko, A.L., 2000. Helium isotopes, tectonics and heat flow in the Northern Caucasus. Geochim. Cosmochim. Acta 64 (11), 1925–1944. https://doi.org/10.1016/S0016-7037(00)00342-2.

Polyak, B.G., Lavrushin, B.Y., Inguaggiato, S., Kikvadze, O.E., 2011. Helium isotopes in gases of Mineral Waters in the western Caucasus. In: Lithology and Mineral Resources, 46, pp. 495–506. https://doi.org/10.1134/S0024490211060113.

Polyak, B.G., Cheshko, A.L., Kikvadze, O.E., Kamensky, I.L., Prasolov, E.M., 2018. Isotope-geochemical features and genesis of gases in the East Carpathian Region. Lithol. Miner. Resour. 53, 380–393. https://doi.org/10.1134/S0024490218050085.

Popa, M., Radulian, M., Szakács, A., Seghedi, I., Zaharia, B., 2012. New seismic and tomography data in the southern part of the Harghita Mountains (Romania, Southeastern Carpathians): connection with recent volcanic activity. Pure Appl. Geophys. 169, 1557–1573. https://doi.org/10.1007/s00024-011-0428-6.

Pradhan, S., Sen, I.S., 2024. Metamorphic CO_2 fluxes offset the net geological carbon sink in the Himalayan-Tibetan orogen. Earth Planet. Sci. Lett. 647. https://doi.org/10.1016/j.epsl.2024.119018.

Radulian, M., Popa, M., Dinescu, R., 2023. What we know and what we don't know about the earthquakes in the Vrancea region (Romania). Ann. Acad. Romanian Sci. Ser. Phys. Chem. 8, 58–92. https://doi.org/10.56082/annalsarsciphyschem.2023.1.58.

Răileanu, G., Radulescu, D., Marinescu, F., Peltz, S., 1967. Geological Map 1:200 000, No.11 Bistrita.pdf. Geological Institute of Romania.

Răileanu, G., Marinescu, F., Popescu, A., 1968. Geological Map 1:200 000, No.19 Targu Mures.pdf. Geological Institute of Romania.

Randazzo, P., Caracausi, A., Aiuppa, A., Cardellini, C., Chiodini, G., D'Alessandro, W., Li Vigni, L., Papic, P., Marinkovic, G., Ionescu, A., 2021. Active degassing of deeply sourced fluids in Central Europe: new evidences from a geochemical study in Serbia. Geochem. Geophys. Geosyst. 22. https://doi.org/10.1029/2021GC010017.

Randazzo, P., Caracausi, A., Aiuppa, A., Cardellini, C., Chiodini, G., Apollaro, C., Paternoster, M., Rosiello, A., Vespasiano, G., 2022. Active degassing of crustal CO_2 in areas of tectonic collision: a case study from the Pollino and Calabria sectors (Southern Italy). Front. Earth Sci. (Lausanne) 10. https://doi.org/10.3389/feart.2022.946707.

Randazzo, P., Aiuppa, A., Borović, S., Buttitta, D., Cardellini, C., Chiodini, G., Ionescu, A., Tamburello, G., Caracausi, A., 2025. Degassing of deep fluids in the Pannonian basin and adjacent areas. Earth Sci. Rev. https://doi.org/10.1016/j.earscirev.2025.105168.

Ratschbacher, L., Frisch, W., Linzer, H.-G., Merle, O., 1991a. Lateral extrusion in the Eastern Alps, part 2: structural analysis. Tectonics 10, 257–271. https://doi.org/10.1029/90TC02623.
Ratschbacher, L., Merle, O., Davy, P., Cobbold, P., 1991b. Lateral extrusion in the Eastern Alps, part 1: boundary conditions and experiments scaled for gravity. Tectonics 10, 245–256. https://doi.org/10.1029/90TC02622.
Ratschbacher, B.C., Paterson, S.R., Fischer, T.P., 2019. Spatial and depth-dependent variations in magma volume addition and addition rates to continental arcs: application to global CO2 fluxes since 750 Ma. Geochem. Geophys. Geosyst. 20, 2997–3018. https://doi.org/10.1029/2018GC008031.
Raymo, M.E., Riddiman, W.F., Froelich, P.N., 1988. Influence of late Cenozoic Mountain building on ocean geochemical cycles. Geology 16, 649–653.
Rizzo, A.L., Pelorosso, B., Coltorti, M., Ntaflos, T., Bonadiman, C., Matusiak-Małek, M., Italiano, F., Bergonzoni, G., 2018. Geochemistry of noble gases and co2 in fluid inclusions from lithospheric mantle beneath Wilcza Góra (Lower silesia, southwest Poland). Front. Earth Sci. (Lausanne) 6. https://doi.org/10.3389/feart.2018.00215.
Rokityansky, I.I., Ingerov, A.I., 1999. Conductive structure of Ukrainian Carpathians from EM observations. Phys. Chem. Earth A 24, 849–852.
Rolfo, F., Groppo, C., Mosca, P., 2017. Metamorphic CO_2 production in calc-silicate rocks from the eastern Himalaya. Ital. J. Geosci. 136, 28–38. https://doi.org/10.3301/IJG.2015.36.
Royden, L., Horváth, F., Nagymarosy, A., Stegena, L., 1983. Evolution of the Pannonian Basin System. 2. Subsidence and thermal hystory. Tectonics 2 (1), 91–137.
Săndulescu, M., 1984. Geotectonics of Romania (Geotectonica României). Technical Publishing House, Bucharest. In Romanian.
Bucher, K., Frey, M., 2002. Petrogenesis of Metamorphic Rocks, Petrogenesis of Metamorphic Rocks. Springer Berlin Heidelberg. https://doi.org/10.1007/978-3-662-04914-3.
Sano, Y., 2018. Helium isotopes. In: White, W.M. (Ed.), Encyclopedia of Geochemistry. Encyclopedia of Earth Sciences. Springer. https://doi.org/10.1007/978-3-319-39312-4_205.
Sano, Y., Marty, B., 1995. Origin of carbon in fumarolic gas from island arcs. Chem. Geol. 119, 265–274. https://doi.org/10.1016/0009-2541(94)00097-R.
Sano, Y., Wakita, H., 1985. Geographical distribution of 3He / He ratios in Japan: implications for arc tectonics and incipient magmatism. J. Geochem. Res. 90, 8729–8741. https://doi.org/10.1029/JB090iB10p08729.
Saulea, E., Popescu, I., Mirauta, E., 1967. Geological Map 1:200 000, No.06 Suceava. Geological Institute of Romania. In Romanian.
Sano, Y., Williams, S., 1996. Fluxes of mantle and subducted carbon along convergent plate boundaries. Geophysical Research Letters 20 (23), 2749–2752. https://doi.org/10.1029/96GL02260.
Saulea, E., Ghenea, C., Bandrabur, T., Ghenea, A., 1968. Geological Map 1:200 000, No.30 Focsani. Geological Institute of Romania. In Romanian.
Schmid, S.M., Fügenschuh, B., Kounov, A., Matenco, L., Nievergelt, P., Oberhänsli, R., Pleuger, J., Schefer, S., Schuster, R., Tomljenović, B., Ustaszewski, K., van Hinsbergen, D.J.J., 2020. Tectonic units of the Alpine collision zone between Eastern Alps and western Turkey. Gondw. Res. https://doi.org/10.1016/j.gr.2019.07.005.
Schoell, M., 1983. Genetic characterization of natural gases. Am. Assoc. Pet. Geol. Bull. 67, 2225–2238.
Seghedi, I., Downes, H., 2011. Geochemistry and tectonic development of Cenozoic magmatism in the Carpathian-Pannonian region. Gondw. Res. 20, 655–672. https://doi.org/10.1016/j.gr.2011.06.009.
Seghedi, I., Downes, H., Szakács, A., Mason, P.R.D., Thirlwall, M.F., Ros, E., Pécskay, Z., Márton, E., Panaiotu, C., 2004. Neogene – quaternary magmatism and geodynamics in the Carpathian – Pannonian region: a synthesis. Lithos 72, 117–146. https://doi.org/10.1016/j.lithos.2003.08.006.
Seghedi, I., Matenco, L., Downes, H., Mason, P.R.D., Szakács, A., Pécskay, Z., 2011. Tectonic significance of changes in post-subduction Pliocene-Quaternary magmatism in the south east part of the Carpathian-Pannonian Region. Tectonophysics 502, 146–157. https://doi.org/10.1016/j.tecto.2009.12.003.
Seghedi, I., Besutiu, L., Mirea, V., Zlagnean, L., Popa, R.-G., Szakács, A., Atanasiu, L., Pomeran, M., Visan, M., 2019. Tectono-magmatic characteristics of post-collisional magmatism: case study East Carpathians, Călimani-Gurghiu-Harghita volcanic range. Phys. Earth Planet. In. 293, 106270. https://doi.org/10.1016/j.pepi.2019.106270.
Seghedi, I., Lukács, R., Soós, I., Guillong, M., Bachmann, O., Cserép, B., Harangi, S., 2023. Magma evolution in a complex geodynamic setting, South Harghita volcanic area, East-Central Europe: constraints from magma compositions and zircon petrochronology. Lithos 442–443. https://doi.org/10.1016/j.lithos.2023.107059.
Sherwood Lollar, B., Ballentine, C.J., O'Nions, R.K., 1997. The Fate of Mantle-Derived Carbon in a Continental Sedimentary Basin: Integration of C/he Relationships and Stable Isotope Signatures. Pergamon Geochimica et Cosmochimica Acta.
Shinohara, H., 2013. Volatile flux from subduction zone volcanoes: Insights from a detailed evaluation of the fluxes from volcanoes in Japan. Journal of Volcanology and Geothermal Research 268 (1), 46–63. https://doi.org/10.1016/j.jvolgeores.2013.10.007.
Skelton, A., 2013. Is orogenesis a net sink or source of atmospheric CO_2? Geol. Today 29 (3), 102–107.
Ślączka, A., Krugłov, S., Golonka, J., Oszczypko, N., Popadyuk, I., 2006. Geology and hydrocarbon resources of the outer Carpathians, Poland, Slovakia, and Ukraine: general geology. In: Golonka, J., Picha, F.J. (Eds.), The Carpathians and Their Foreland, Geology and Hydrocarbon Resources: AAPG Memoir, vol. 84, pp. 221–258. https://doi.org/10.1306/985610m843070.
Sleep, N.H., Zahnle, K., 2001. Carbon dioxide cycling and implications for climate on ancient Journ. Geophys. Res. 106 (1), 1373–1399. https://doi.org/10.1029/2000JE001247.
Solcanu, M., 2015. Stratigraphic and tectonic data on the Cretaceous flysch in the Northern Ciuc Mountains (Eastern Carpathians, Romania). Acta Papaeontol. Roman. 11, 9–24.
Sperner, B., Ioane, D., Lillie, R.J., 2004. Slab behaviour and its surface expression: new insights from gravity modelling in the SE-Carpathians. Tectonophysics 382, 51–84. https://doi.org/10.1016/j.tecto.2003.12.008.
Stănică, D., Stănică, M., 1993. An electrical resistivity lithospheric model in the Carpathian Orogen from Romania. Phys. Earth Planet. In. 81, 99–105.
Ștefănescu, M., Dicea, O., Butac, A., Ciulavu, D., 2007. Hydrocarbon geology of the Romanian Carpathians, their foreland, and the Transylvanian Basin. In: The Carpathians and Their Foreland: Geology and Hydrocarbon Researces: AAPG Memoir 84, 84. The American Association of Petroleum Geologists Memoir, pp. 521–567. https://doi.org/10.1306/985619m843077.
Stewart, E.M., Ague, J.J., 2020. Pervasive subduction zone devolatilization recycles CO2 into the forearc. Nat. Commun. 11, 1–8. https://doi.org/10.1038/s41467-020-19993-2.
Stewart, E.M., Ague, J.J., Ferry, J.M., Schiffries, C.M., Tao, R.-B., Isson, T.T., Planavsky, N.J., 2019. Carbonation and decarbonation reactions: implications for planetary habitability. Am. Mineral. 104, 1369–1380. https://doi.org/10.2138/am-2019-6884.
Svensen, H., Jamtveit, B., 2010. Metamorphic fluids and global environmental changes. Elements 6, 179–182. https://doi.org/10.2113/gselements.6.3.179.
Szabó, C., Harangi, S., Csontos, L., 1992. Review of neogene and quaternary volcanism of the Carpathian-Pannonian region. Tectonophysics 208, 243–256. https://doi.org/10.1016/0040-1951(92)90347-9.
Szakács, A., Seghedi, I., 1995. The Calimani-Gurghiu-Harghita Volcanic Chain, East Carpathians, Romania: Volcanological features. Acta Vulcanologica.
Szakács, A., Seghedi, I., Pécskay, Z., Mirea, V., 2015. Eruptive history of a low-frequency and low-output rate Pleistocene volcano, Ciomadul, South Harghita Mts., Romania. Bull. Volcanol. 77. https://doi.org/10.1007/s00445-014-0894-7.
Szalay, R., Kis, B.-M., 2023. Development of a Low-cost Tool for the Compositional Measurement of Gases Derived From Mineral Water Wells From the Eastern Carpathians, 64. Studia Universitatis Babes-Bolyai, Seria Geologia, pp. 1–7. https://doi.org/10.5038/1937-8602.64.1.1307.
Tamang, Shashi, Groppo, C., Girault, F., Perrier, F., Rolfo, F., 2024. Metamorphism of dolomitic and magnesitic rocks in collisional orogens and implications for orogenic CO_2 degassing. J. Petrol. 65. https://doi.org/10.1093/petrology/egae021.
Tamburello, G., Pondrelli, S., Chiodini, G., Rouwet, D., 2018. Global-scale control of extensional tectonics on CO_2 earth degassing. Nat. Commun. 9. https://doi.org/10.1038/s41467-018-07087-z.
Tari, G., Horváth, F., Rumpler, J., 1992. Styles of extension in the Pannonian Basin. Tectonophysics 208, 203–219. https://doi.org/10.1016/0040-1951(92)90345-7.
Tassi, F., Capecchiacci, F., Cabassi, J., Calabrese, S., Vaselli, O., Rouwet, D., Pecoraino, G., Chiodini, G., 2012a. Geogenic and atmospheric sources for volatile organic compounds in fumarolic emissions from Mt. Etna and Vulcano Island (Sicily, Italy). J. Geophys. Res. Atmos. 117. https://doi.org/10.1029/2012JD017642.
Tassi, F., Fiebig, J., Vaselli, O., Nocentini, M., 2012b. Origins of methane discharging from volcanic-hydrothermal, geothermal and cold emissions in Italy. Chem. Geol. 310–311, 36–48. https://doi.org/10.1016/j.chemgeo.2012.03.018.
Tiliță, M., Lenkey, L., Matenco, L., Horváth, F., Surányi, G., Cloetingh, S., 2018. Heat flow modelling in the Transylvanian basin: implications for the evolution of the intra-Carpathians area. Glob. Planet. Change 171, 148–166. https://doi.org/10.1016/j.gloplacha.2018.07.007.
Torgersen, T., 1993. Defining the role of magmatism in extensional tectonics: 3helium fluxes in extensional basins. J. Geophys. Res. 98, 16257–16269. https://doi.org/10.1029/93JB00891.
Trua, T., Serri, G., Birkenmajer, K., Pécskay, Z., 2006. Geochemical and Sr – Nd – Pb isotopic compositions of Mts Pieniny dykes and sills (West Carpathians): evidence for melting in the lithospheric mantle. Lithos 90, 57–76. https://doi.org/10.1016/j.lithos.2006.01.001.
Umeda, K., Ogawa, Y., Asamori, K., Oikawa, T., 2006. Aqueous fluids derived from a subducting slab: observed high ^{3}He emanation and conductive anomaly in a non-volcanic region, Kii Peninsula southwest Japan. J. Volcanol. Geotherm. Res. 149, 47–61. https://doi.org/10.1016/j.jvolgeores.2005.06.005.
Varekamp, J.C., Kreulen, R., Poorte, R.P.E., Van Bergen, M.J., 1992. Carbon sources in arc volcanism, with implications for the carbon cycle. Terra Nova 4, 363–373. https://doi.org/10.1111/j.1365-3121.1992.tb00825.x.
Vaselli, O., Minissale, A., Tassi, F., Magro, G., Seghedi, I., Ioane, D., Szakács, A., 2002. A geochemical traverse across the Eastern Carpathians Romania: constraints on the origin and evolution of the mineral water and gas discharges. Chem. Geol. 182, 637–654. https://doi.org/10.1016/S0009-2541(01)00348-5.
Wenzel, F., Lorenz, F.P., Oncescu, M.C., 1999. Seismotectonics of the Romanian Vrancea area. In: Wenzel, F., Lungu, D., Novak, O. (Eds.), Vrancea Earthquakes: Tectonics, Hazard and Risk Mitigation. Springer Science Business Media, pp. 15–25. https://doi.org/10.1007/978-94-011-4748-4_2.
Werner, C., Fischer, T.P., Aiuppa, A., Edmonds, M., Cardellini, C., Carn, S., Chiodini, G., Cottrell, E., Burton, M., Shinohara, H., Allard, P., 2019. Carbon dioxide emissions from subaerial volcanic regions: two decades in review. In: Orcutt, B., Alvarez, D., Dasgupta, R. (Eds.), Deep Carbon: Past to Present, vol. 8, pp. 188–236. https://doi.org/10.1017/9781108677950.008.
Wexsteen, P., Jaffé, F.C., Mazor, E., 1988. Geochemistry of cold CO_2-rich springs of the Scuol-Tarasp region, Lower Engadine, Swiss Alps. J. Hydrol. (Amst.) 104 (1–4), 77–92. https://doi.org/10.1016/0022-1694(88)90158-8.
Whitley, S., Gertisser, R., Halama, R., Preece, K., Troll, V.R., Deegan, F.M., 2019. Crustal CO 2 Contribution to Subduction Zone Degassing Recorded through Calc-silicate Xenoliths in Arc Lavas, pp. 1–11. https://doi.org/10.1038/s41598-019-44929-2.

Wong, K., Mason, E., Brune, S., East, M., Edmonds, M., Zahirovic, S., 2019. Deep carbon cycling over the past 200 million years: a review of fluxes in different tectonic settings. Front. Earth Sci. 7, 263. https://doi.org/10.3389/feart.2019.00263.

Wortel, M.J.R., Spakman, W., 2000. Subduction and slab detachment in the Mediterranean-Carpathian region. Science (1979) 290, 1910–1917. https://doi.org/10.1126/science.290.5498.1910.

Wycherley, H., Fleet, A., Shaw, H., 1999. Some observations on the origins of large volumes of carbon dioxide accumulations in sedimentary basins. Mar. Pet. Geol. 16 (6), 489–494. https://doi.org/10.1016/S0264-8172(99)00047-1.

Zeyen, H., Dérerová, J., Bielik, M., 2002. Determination of the continental lithospheric thermal structure in the Western Carpathians: Integrated modelling of surface heat flow, gravity anomalies and topography. Phys. Earth Planet. In. 134, 89–104. https://doi.org/10.1016/S0031-9201(02)00155-3.

Zhang, L., Guo, Z., Sano, Y., Zhang, M., Sun, Y., Cheng, Z., Yang, T.F., 2017a. Flux and genesis of CO_2 degassing from the volcanic-geothermal fields of Gulu-Yadong rift in the Lhasa terrane, South Tibet: constraints on characteristics of deep carbon cycle in the India-Asia continent subduction zone. J. Asian Earth Sci. 149, 110–123. https://doi.org/10.1016/j.jseaes.2017.05.036.

Zhang, M., Guo, Z., Zhang, L., Sun, Y., Cheng, Z., 2017b. Geochemical constraints on origin of hydrothermal volatiles from southern Tibet and the Himalayas: Understanding the degassing systems in the India-Asia continental subduction zone. Chem. Geol. 469, 19–33. https://doi.org/10.1016/j.chemgeo.2017.02.023.

Zhang, M., Xu, S., Sano, Y., 2024. Deep carbon recycling viewed from global plate tectonics. Natl. Sci. Rev. https://doi.org/10.1093/nsr/nwae089.

Zhao, W., Guo, Z., Li, J., Ma, L., Liu, J., 2022. Fluxes and genesis of deep carbon emissions from southern Tibetan Plateau and its adjacent regions. Acta Petrol. Sin. 38, 1541–1556. https://doi.org/10.18654/1000-0569/2022.05.17.

Żytko, K., 1997. Electrical conductivity anomaly of the Northern Carpathians and the deep structure of the origen. Ann. Soc. Geol. Pol. 67, 25–43.